UNIFORMED SERVICES UNIVERSITY OF THE HEALTH SCIENCES

4301 JONES BRIDGE ROAD

BETHESDA, MARYLAND 20814-4799

MAY 2008

Title of Thesis: "Neutron Fading Characteristics of Copper-Doped Lithium Fluoride (LiF: MCP) Thermoluminescent Dosimeters (TLDs)"

Name of Candidate: LT Jeffrey A. Delzer
Master of Science in Public Health
Department of Preventive Medicine and Biometrics

Thesis and Abstract Approval:

Tomoko I. Hooper — 21 May 2008
Chairman: Tomoko Hooper, MD, MPH — Date

21 May 2008
Research Advisor: — Date
CDR Luis Benevides, PhD, MSC, USN

21 May 2008
CDR, Russell Lawry, MS, MSC, USN — Date

21 May 2008
Alex Romanyuka, PhD. — Date

The author hereby certifies that the use of any copyrighted material in the thesis manuscript entitled:

Neutron Fading Characteristics of Copper-Doped Lithium Fluoride Thermoluminescent Dosimeters

beyond brief excerpts is with the permission of the copyright owner, and will save and hold harmless the Uniformed Services University of the Health Sciences, Department of the Navy, and Department of Defense from any damage, which may arise from such copyright violations.

Jeffrey A Delzer
LT, MSC, USN
Department of Preventive Medicine and Biometrics
Uniformed Services University of the Health Sciences

ABSTRACT

Title of Thesis: "Neutron Fading Characteristics of Copper-Doped Lithium Fluoride (LiF: MCP) Thermoluminescent Dosimeters (TLDs)"

Author: Jeffrey Alan Delzer, degree candidate, Master of Science in Public Health, 2008

Thesis directed by: Luis Benevides, PhD
Adjunct Professor
Department of Preventive Medicine and Biometrics

LiF thermoluminescent dosimeters (TLDs) are used by the United States Navy to record radiation exposure of personnel. The DT-648 has been used for many years and has undergone extensive testing to identify its pre-irradiation and post-irradiation fade operating characteristics. Studies have shown that the addition of copper increases the thermoluminesence sensitivity of the TLD for improved low-level radiation monitoring, which prompted the introduction of the DT-702/PD LiF: MCP TLD as a replacement for the DT-648/PD LiF: MT TLD.[4] Using current equipment for processing of TLDs and calibrating to National Institute of Standards and Technology (NIST) standards, this study evaluated the various neutron fading characteristics of the copper-doped dosimeter. The 34 week study took place at the Naval Dosimetry Center (NDC), Bethesda, Maryland. The TLDs were stored for pre-specified lengths of time according to a 34 week schedule to account for realistic fading effects. The TLDs were irradiated to a Plutonium-Beryllium radiation source before and after storing the TLDs. After the storing requirements were satisfied, the TLDs were then

processed using current procedures used by the Naval Dosimetry Center. The resulting data were compared to the calibrated exposure. The change in signal (fade) was then evaluated. Results show that the DT-702/PD TLD has no significant change in sensitivity or signal response with up to 34 weeks of pre-exposure, post-exposure, or combination of pre-exposure and post-exposure time. The data obtained from this study indicate that an evaluation of extending the issue periods beyond the current limits is warranted. In so doing, the extended issue periods can increase the flexibility associated with time dependence from shipping procedures, reduce workload requirements, and provide a cost savings for dosimetry processing.

NEUTRON FADING CHARACTERISTICS

OF COPPER-DOPED LITHIUM FLUORIDE (LIF: MCP)

THERMOLUMINESCENT DOSIMETERS (TLDS)

by

Jeffrey Alan Delzer

Thesis/dissertation submitted to the Faculty
Department of Preventive Medicine and Biometrics
F. Edward Hébert School of Medicine
Uniformed Services University of the Health Sciences in partial fulfillment of the
Requirements for the degree of
Master of Science in Public Health May 2008

UNIFORMED SERVICES UNIVERSITY OF THE HEALTH SCIENCES
4301 JONES BRIDGE ROAD
BETHESDA, MARYLAND 20814-4799

ACKNOWLEDGMENT

I wish to express sincere appreciation to my research advisor, CDR Luis Benevides, whose critical eye, and enlightened mentoring were instrumental and inspiring. I wish to convey my gratitude to CDR Russell Lawry, who spent valuable time performing endless reviews and provided encouraging feedback in the creation of this thesis. Additionally, sincere thanks are necessary to Dr. Tomoko Hooper, Committee Chair. She ensured that all of the thesis requirements were met and kept me focused through this trying time. I also would like to thank Dr. Romanyukha and Faculty members of the Preventive Medicine and Biometrics Department for their valuable input and encouragement.

This study was supported by the Naval Dosimetry Center.

DEDICATION

To my wife, Donna, and my two sons Trevor and Noah, for the sacrifices you have made during my nineteen-year Naval career and the last two years of study. You are my love and inspiration and I dedicate this thesis to you.

TABLE OF CONTENTS

LIST OF FIGURES

LIST OF TABLES

LIST OF EQUATIONS

CHAPTER ONE: INTRODUCTION

Statement of the Problem

Since the inception of the United States Navy's Radiation Safety Program in 1946, the primary objective has always been to provide the best technology available for monitoring personnel, through the use of dosimetry, to occupational exposure to ionizing radiation. Current statutes are based on the principal that exposure to ionizing radiation, regardless of how small, involves some risk. Therefore, personnel dosimetry can provide the foundation for medical, epidemiological and legal interpretations of that risk. Today, the Navy uses Thermoluminescent Dosimeters (TLD) for monitoring radiation exposure. The Navy's primary dosimeter is the DT-702/PD Lithium Fluoride with Magnesium, Copper and Phosphor impurites (LiF: MCP).

The legal significance of the dosimetric record is such that it requires the best precision and accuracy in documenting radiation dose for personnel who are monitored with TLDs. There are several external factors that can influence the signal response from the TLD and these affect the proper interpretation of the readings. These factors include energy, dose response, thermal treatment, optical light, heat, humidity, sensitivity fade and signal fade. Fading is defined as a change of TL signal associated with the time from the initial exposure. Prior to this study, the DT-702/PD fading characteristics for neutron radiation had only been characterized by one published study. [5] That study, conducted by Jones et al., had some limitations that included statistical methodology, number of data points used, and the period of observation only lasting 24 weeks.

In this study, the design and methods were selected to improve on the limitations identified by Jones et al. as well as numerous other photon studies. Some of the improvements in study design included increased sample size, to ensure statistical power, and the use of control TLDs to account for background radiation. In addition, statistical tests performed were described in detail, and pre, post and combined fade were assessed.

The Navy's current issue period for DT-702/PD is limited to eight weeks due to many factors that include the fading characteristics and lowest limit of detection (LLD). The short issue periods can result in unnecessary processing and shipping issues that can contribute to additional uncertainty of assigned dose and also increased program costs. The data presented in this study will evaluate the long-term fading characteristics of the DT-702/PD which can be used to evaluate the appropriate issue period.

Research Goal

The goal of this research was to evaluate LiF: MCP TLD for signal resulting from neutron exposure over an extended period of observation.

Research Question

This study determined if the neutron fading characteristics of the DT-702/PD remained within acceptable limits over an extended period of time. Specifically, that the signal response of LiF: MCP will vary significantly from the initial exposure. The null hypothesis was that the signal response showed no difference over the study period. The alternative hypothesis was that there was a difference over time. The test for significant differences was set at an alpha level

of 0.05 (α=0.05), for a 95% confidence level.

Specific Aims

The specific aims of this study were to:

1. Measure and evaluate if LiF: MCP neutron fade, to include both change of sensitivity (Pre-Irradiation fade) and change of signal (Post-Irradiation fade), was significant over a 34 week period and that they are within acceptable limits required for personal monitoring.
2. Compare fade results with previously published data performed on this dosimeter with shorter observation times to evaluate its impact on issue periods.
3. Evaluate if a difference exists between neutron and photon fade characteristics.

CHAPTER TWO: BACKGROUND AND SIGNIFICANCE

In the late 1800's, a discovery occurred that transformed science and brought on the dawn of the Nuclear Age. The discovery was made by Wilhelm Conrad Roentgen in 1895 when he discovered an unknown ray that he called the "x-ray". Soon after Roentgen's discovery came the discovery of radioactivity by Henri Becquerel, and radium by Marie and Pierre Curie. By 1896, the deleterious effects of radiation were evident. X-rays caused skin damage, a prelude to systematic cancers, which resulted in x-ray safety. In 1904, Clarence Madison Dally became the first documented death attributed to cumulative over exposure to x-rays.[6]

As a result of this danger, an increase in concern for radiation protection was realized, and measures were taken to define the danger and minimize its effects. Throughout the first half of the 20th century, researchers concentrated on time, distance to the source, and shielding as their three main focal areas to limit personnel exposure to radiation. The result of their efforts led to the implementation of the first dedicated protective measures for exposure reduction and included crude measuring devices used to determine environmental levels of radiation, as well as rudimentary personal protective equipment, the installation of shielding around the source, and the implementation of minimum distances to the radiation source. The concept of time, distance and shielding became the fundamental basis for exposure reduction.

Along with the early efforts to minimize personnel exposure, there remained the concern to be able to accurately monitor and measure a person's exposure to radiation. "In 1907 Rome Vernon Wagner reported that in an effort to control his personal exposures, he started to carry a photographic plate in his pocket which he later

developed to determine if he had been exposed. This was the precursor of the film badge and the establishment of personnel monitoring for radiation. "[6] It would be nearly two decades later that the use of a film badge would be adopted and used as an accepted method to monitor personnel radiation exposure. Film badges remained the mainstay of exposure monitoring for the better part of half a century and are still in use today by numerous organizations.

The United States Navy made use of film badge technology from 1946 to 1968 as a whole body dosimeter (Figure 1) to ensure recommended exposure limits were not exceeded.

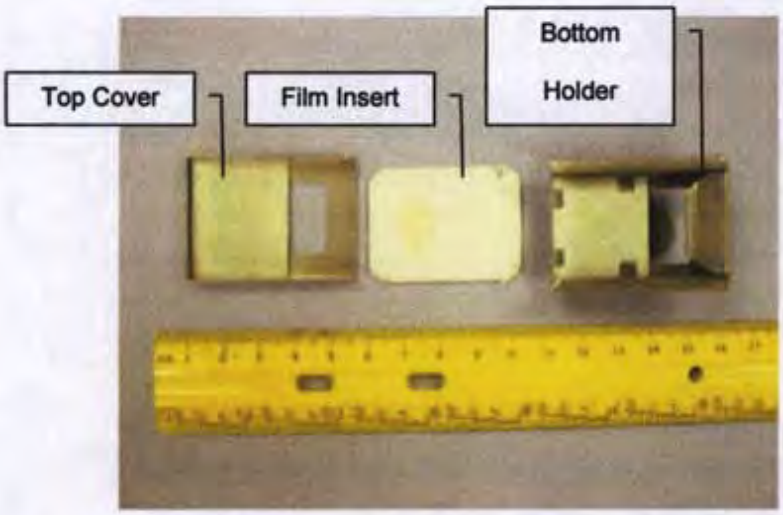

Figure 1. The image shows a picture of US Navy's film badge and holder.[1]

The dosimeter was issued and processed at individual commands. The dosimeter relied on film calibration curves that were provided by the Navy Bureau of Medicine and Surgery (BUMED). Although the lifespan of the film badge was impressive, spanning 27 years, the dosimeter had several disadvantages. The film used was sensitive to

temperature and humidity, which in turn affected its optical density and accuracy. The energy response was poor and required the use of filtration to overcome the over response to low energy photons. The processing of the dosimeter was also costly, cumbersome and was labor intensive as it required manual evaluation. Additionally, the lower limit of detection (LLD), which is the lowest dose that can be reliably detected above background dose, with a specified confidence level (typically 95%), was limited to 30 mrem.[7] This LLD was considered too high to effectively control an individual's exposure and prevent exceeding federal limits of 500 mrem per year. Having a low LLD is a key factor in personnel dosimetry, and it must be distinguished from the variability of background dose arising from different monitoring cycles, geographic locations, and administrative controls. As a result of the film badge limitations, the Navy began evaluating other materials to measure exposure to ionizing radiation.

The Navy established a dosimetry research facility at the Naval Research Laboratory (NRL). One of the research groups at NRL, lead by James Schulman, was the first to study silver-activated phosphate glass as a radiation dosimeter. [8] This research led to the development of a new accident dosimeter, known as the DT-60/PD. This dosimeter was based on the phenomenon of radiophotoluminescence, which occurs when a stable photoluminescent center is formed in a material exposed to ionizing radiation. After being exposed to a light of the proper wavelength, usually near-ultraviolet, the material will fluoresce, or produce light, under a fixed intensity of excitation. The light produced is proportional to the radiation dosage.

Unfortunately, the DT-60/PD, designed as a battlefield dosimeter, was not well suited for whole body personnel monitoring because it lacked the required sensitivity

and accuracy.[8] The minimum dose it could accurately measure was 10 rad, which is well above normal occupational levels that average only 35 mrad/year.[8] Since this dosimeter had significant limitations it couldn't satisfy the requirements for a whole body monitoring device and drove efforts to develop newer technologies. One of those newer technologies explored was in the area of thermoluminescence.

Thermoluminescence (TL) or thermally stimulated luminescence is the emission of light during the heating of a solid material (insulator or semiconductor), previously excited by ionizing radiation.[9] Ionizing radiation striking a solid state crystal can transfer some of its energy to the solid's electrons, raising them to higher energy levels where they can get trapped in a metastable state. Subsequently, electrons can be induced to return from the metastable state to their normal state upon sufficient heating. This change in the electrons state is accompanied by the release of radiation in the form of light. By quantifying the light released as a function of temperature a resulting graph, known as a glow curve, can be constructed. (Figure 2) An in-depth review of

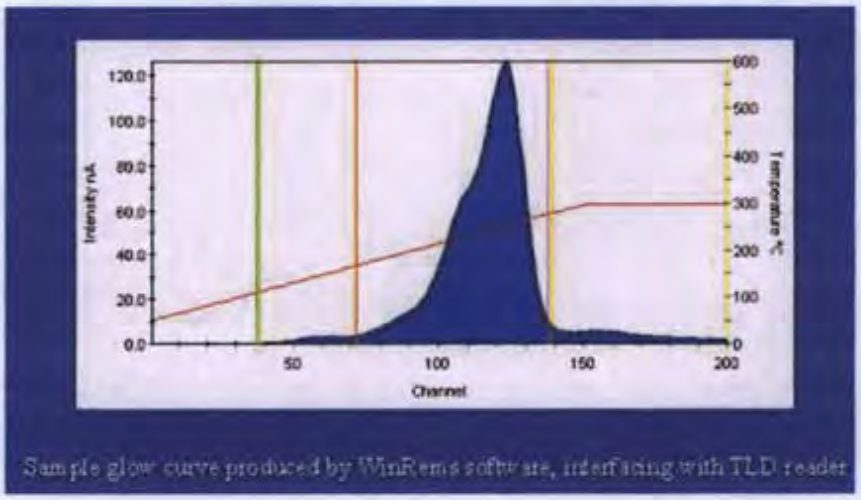

Figure 2. The graph shows a diagram of a thermoluminescent glow curve (LiF: MCP).

luminescence and, specifically, thermoluminescence can be found in Appendix A.

To interpret the glow curve, the amount of light released is determined by taking the integrated area under the curve, which proportionally represents the amount of energy deposited in a medium by ionizing radiation. This in turn can be converted into an absorbed dose (D_R) through the use of calibration correction factors. It is important to understand this term and explain how it relates to biological equivalence. Absorbed dose is equal to the energy deposited per unit mass of medium and is measured in Joules per kilogram (J/kg) and has been adopted as the International System of Units (SI) unit Gray (Gy) or traditional unit rad. The Gy is not an indicator of biological effect since it does not take into account the amount of biological damage imparted by the type of radiation. In order to account for biological damage, the equivalent dose (H_T) is used.

Equivalent dose uses a weighting factor to account for the relative biological damage due to a particular type of radiation and has the SI units of Sieverts (Sv) or traditional units of Röentgen Equivalent Man (rem). It is calculated by multiplying the absorbed dose to an organ or tissue (D_T) with the radiation weighting factor, w_R (Equation 1). The w_R is based on the type and energy of the radiation that is incident on the tissue and is weighted according to the amount of damage the radiation will cause. For example, the w_R for gamma rays and beta particles is 1 where more damaging radiation, such as neutrons or alpha particles can be as much as 20 times higher.[10-12]

$$H_{T,R} = w_R \times D_{T,R}$$

Equation 1. Equation used to calculate Equivalent Dose.

Where:

$H_{T,R}$ = equivalent dose to tissue *T* from radiation *R (Sv)*

w_R = radiation weighting factor (unitless)

$D_{T,R}$ = absorbed dose *D* (in grays) to tissue *T* from radiation *R (Gy)*

The first attempt to practically apply thermoluminescence and improve upon current radiation monitoring methods was attempted by a team led by Farrington Daniels.[13] Since Daniels first proposed thermoluminescence for radiation dosimetry, there has been significant effort across the world to unearth the perfect material exhibiting the best thermoluminescent characteristics for various applications of radiation monitoring including personal, environmental and clinical dosimetry.

The characteristics of an "ideal" dosimeter are linear dose response, flat energy response, no angular dependence, high sensitivity, low LLD, tissue equivalence, low fade, low price, size, durability, reusability, ease of processing and negligible environmental effects. While some of the characteristics are self-explanatory there are several that require refining and are explained below.

- Dose response - A TLD should respond in a linear manner over a wide range of dose (1 mrad to several thousand). Dose response ideally should have a correspondence of one-to-one for thermoluminescence and energy deposited by the exposure to ionizing radiation.
- Energy response - The relative energy response should not vary over a wide energy range (30 keV to 1300 keV) also referred to as a flat energy response. A flat energy response facilitates the ability to monitor personnel in a variety of

operational environments regardless of the energy spectra.

- Angular dependence- The TLD response should not vary with the angular position of the incident spectra.
- Sensitivity- The sensitivity of a material is defined as the thermoluminescent signal strength per unit of absorbed energy. It is essential for a personnel dosimeter to have a high sensitivity to ensure a reliable, low dose (in the mrem (μSv) range) measurement is obtained.
- LLD- The lower limit of detection is defined as the lowest dose that can be detected at a specified confidence level.
- Tissue equivalence- The TLD material should have the same energy absorption and energy scattering characteristics of the tissue being monitored. Ideally a tissue equivalent dosimeter would be made up of the same chemical composition as the tissue in question.
- Fade- Fading constitutes a change of TL sensitivity or signal response from an exposed dosimeter after some time has elapsed from the time of exposure. It is desirable to have a TLD with no fade.
- Environmental Effects- The TLD should be able to withstand the working conditions that are expected from the user that include temperature, humidity and physical shock.
- Ease of processing- The processing of the TLD should be as reliable and simple as possible.
- Reusability- The ideal dosimeter should be able to be reused after an appropriate annealing protocol without affecting the martial characteristics.

The Navy also had a keen interest in this new technology, and NRL began to focus on the practical applications of thermoluminescence as a dosimeter. Introduced in 1973, one of the Navy's dosimeters to use thermoluminescent technology was the DT-526/PD (Figure 3). This TLD was made of two crystals of Manganese (Mn) doped Calcium Fluoride (CaF_2) affixed to a heating strip by a wire. The assembly was sealed within a glass bulb and placed inside of a shielded plastic case. The case shielding material consisted of lead and tin that shields the non-tissue equivalent CaF_2: Mn from lower energy photons. [14]

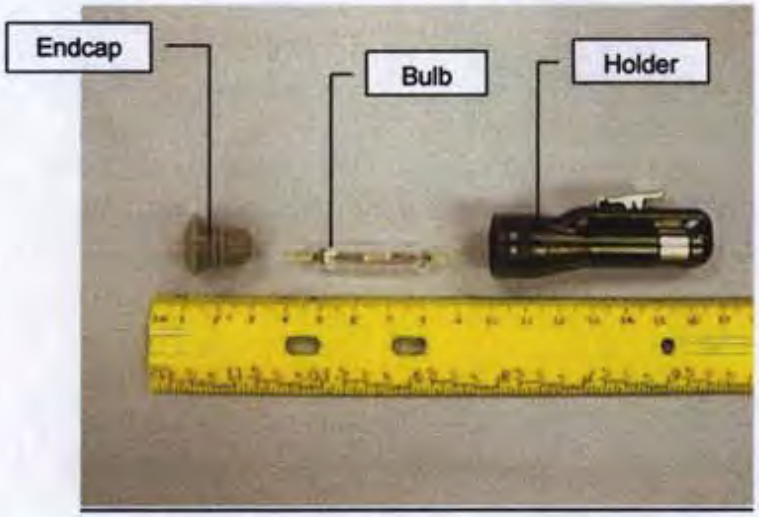

Figure 3. The image shows a picture of US Navy's DT-526/PD TLD. [1]

The DT-518/PD (Figure 4), developed in 1968, was also based on principles of thermoluminescence and was the first accident dosimeter to measure environmental neutron levels. It consisted of activation materials, sulfur and indium, along with Lithium Fluoride (LiF) powder. These dosimeters were used in environments where there was a potential of a nuclear reactor criticality accident. In addition to the DT-518/PD dosimeter, the end cap of the DT-526/PD had been modified to include both indium foil and sulfur pellets, allowing for an assessment of a high level neutron exposure in the

event of a reactor accident. Both the DT-518 and the DT-526/PD with the modified end cap satisfied the need for monitoring high levels of neutron exposure. However, there was still a need for low level neutron monitoring.

Figure 4. The image shows a picture of US Navy's DT-518/PD Accident Dosimeter.[1]

The Navy continued its work to develop an accurate, precise, and reliable personal dosimeter to measure whole body neutron radiation, both for high levels of neutron radiation as previously discussed, and for monitoring low level, occupational neutron exposure. Based on the work of Dr. John Cameron to refine the Lithium Fluoride phosphor doped with magnesium and titanium impurities [15] (LiF: Mg: Ti or LiF: MT), the Harshaw Chemical Company produced a commercial LiF: MT phosphor known as TLD-100 and its isotopic variants, TLD-600, sensitive to thermal neutrons and photons, and TLD-700, sensitive to photons. The LiF:MT phosphor demonstrated good performance characteristics that included a near-tissue-equivalent response, a relative resistance to environmental conditions such as heat and humidity, and a linear dose response at occupational dose levels.[16]

In February 1973, NRL procured these TLDs and based on the results of additional studies, the Navy adopted this dosimeter for occupational monitoring, replacing a portion of the DT-526/PDs in use, and classified it as the DT-583/PD.[17] With the introduction of the DT-583/PD (Figure 5) and its associated automated reader, Harshaw 2271 automated TLD reader (Figure 6), the Navy now had a system that could allow for mass processing and tracking of personnel dose. However, the DT-583/PD had limitations that included a high LLD and the requirement for contact heating to process the TLD. The contact heating process has been shown to heat the material non-uniformly as well as cause and increase in wearing of the TLD. [1, 18-21]

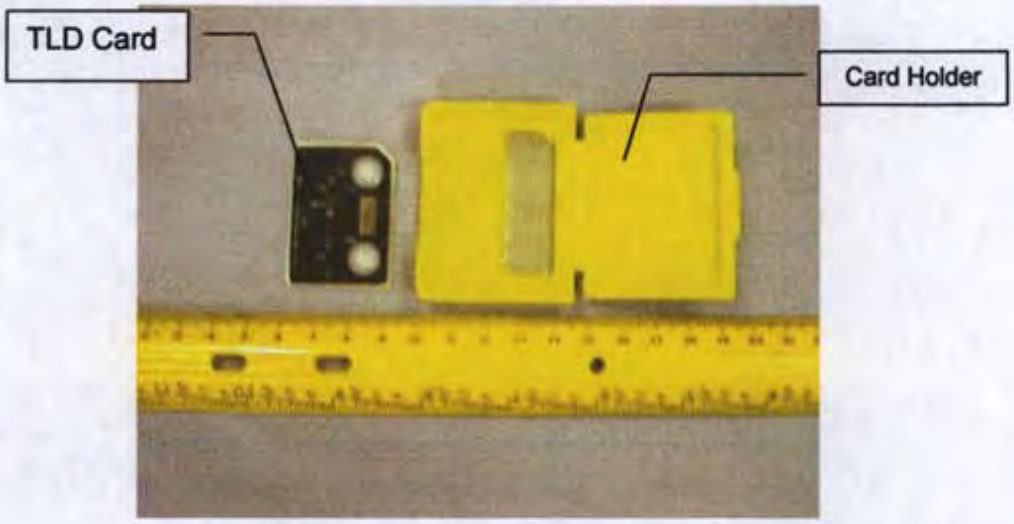

Figure 5. The image shows a picture of US Navy's DT-583/PD (Card & Holder).[1]

Figure 6. The image shows a picture of US Navy's Harshaw 2271 TLD Reader.[1]

Continued studies to improve on TLD effectiveness culminated in the development of the DT-648/PD (Figure 7), which was eventually fielded as the replacement to the DT-583/PD in 1988.[18] This new four element dosimeter was able to monitor all types of radiation the Navy was interested in; photons (x-ray and gammas), beta and neutron. Additionally, it employed a new gas reader, the Harshaw model 8800 that used a heated stream of nitrogen to heat the TLD. By employing gas heating, the TLD exhibited a more uniform heating profile and increased the life expectancy of the TLD. Alongside the DT-526/PD this dosimeter became the workhorse of the Navy for over a decade. Both the DT-526/PD and the DT-648/PD presented limitations that had yet to be addressed.

The DT-526/PD Dosimeter provided a great method for monitoring photon radiation, but failed to address the need to measure neutron radiation for either monitoring personnel exposures during normal operations or the assessment of acute exposures following a reactor accident.[1, 18] The DT-526/PD also suffered from self irradiation, limiting the issue length of the dosimeter to a maximum of 4 weeks.[18, 22, 23]

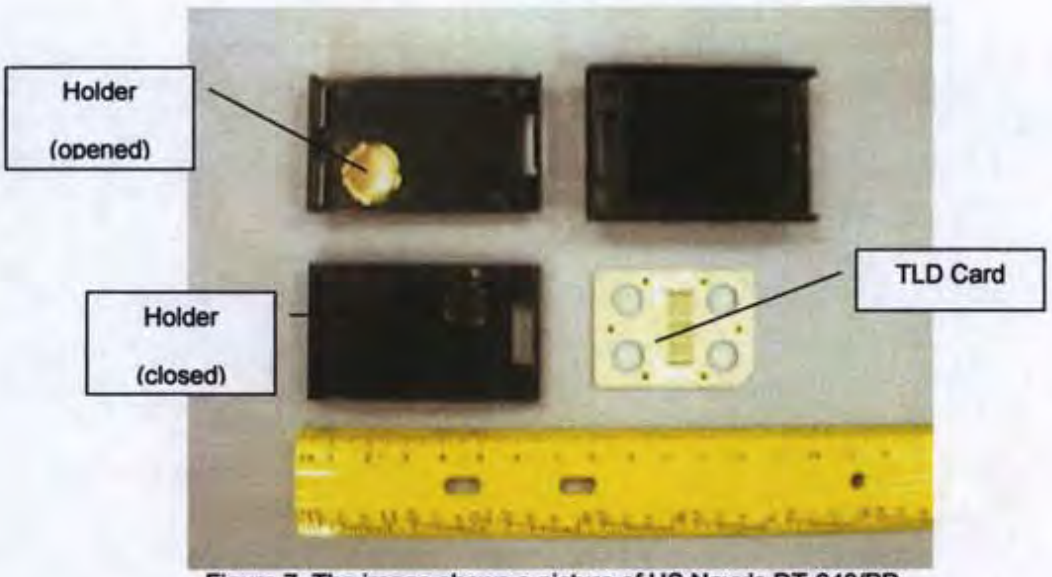

Figure 7. The image shows a picture of US Navy's DT-648/PD Holder and Card. [1]

The DT-648/PD suffered from a reduced ability to accurately determine beta radiation due to the element being too thin and resulting in frequent cracking. Additionally the dosimeter exhibited excessive fade requiring complex algorithms for correction, thereby reducing the accuracy of the measured dose.[1, 7, 22]

After years of development to correct the limitations of the DT-648/PD and DT-526/PD, the DT-702/PD (Figure 8) dosimeter was developed and fielded in 2002. [7] This dosimeter, similar in design to the DT-648/PD, is able to be processed on the same Harshaw 8800 readers, this allowing the Navy to introduce a new dosimeter without incurring significant infrastructure costs. The most important improvement in the DT-702/PD was the increased sensitivity due to the use of a Magnesium Copper Phosphate doped LiF phosphor (LiF: MCP).

This new material was first developed by Nakajima in 1978 [24] and has been commercially available in several forms. Initially, this material was in the form of a powder and demonstrated a TL sensitivity 23 times higher than LiF: MT. In his paper,

Nakajima selected three dopants besides Mg and Cu that were Si, B and P. His research showed that phosphorus should be used as the third dopant, since phosphorus had a higher TL sensitivity than the other two dopants. In 1984, the Solid Dosimetric Detector & Method Lab (Beijing, China) prepared LiF: MCP in a solid form

Figure 8. The image shows a picture of US Navy's DT-702/PD Card and Holder.[1]

that resulted in an even higher sensitivity than the powder form.[25] In order to determine the annealing program for reuse, temperatures between 150° C and 270° C were tested, and experimental results showed that the optimum temperature for reuse was 240° C for 10 minutes. The history and qualities of this phosphor have been extensively described by Moscovitch [26] with an overview provided in appendix A.

The outstanding characteristics of LiF: MCP include high sensitivity as compared to LiF: MT, almost flat photon energy response, linear dose response, and low fading rate.[7] The fading rate of the DT-702/PD, which is the focus of this research, is of particular concern to the Navy, since it is advantageous for a dosimeter to support extended issue periods. This increase in issue periods is desirable since short periods

result in unnecessary processing, shipping, and issuing of TLDs, which can introduce additional uncertainty of assigned dose and also increased costs.

Fading is classified into two distinct categories; Pre-Irradiation Fade and Post-Irradiation Fade. Pre-irradiation fade is a change in sensitivity of the material prior to being exposed to radiation from the time it was annealed, or zeroed. In this case, the materials efficiency in trapping energy from radiation is reduced due to the number of traps available. Post-Irradiation Fade is a change in the signal response of the material after being exposed to radiation. In this case, the traps have the potential of spontaneously releasing the stored energy from their meta-stable state. It should be noted that in each of these cases, fading occurs over time.

Several factors can contribute to the amount of fading including temperature, light, humidity, and time. The most significant cause of TLD fading can be attributed to temperature effects.[2] The simple premise of thermoluminescence explains why this is true. Exposure to heat can impart thermal energy to the electrons and even at slightly elevated temperatures, electrons caught in shallow traps can absorb enough thermal energy to be released back into the conduction band, dropping to a lower energy state and releasing the stored energy. If this occurs before it is intended, a change of signal will result and the reading of the TLD will not accurately correspond to the amount of radiation absorbed.

The thermal treatment used for TLD crystals is an essential process for its re-usability. Studies have shown that LiF: MCP is affected by thermal treatment and the glow curves are strongly dependent on annealing temperatures. Specifically, these studies indicate that if the temperature during annealing for long periods (excess of a

minute) is higher than 240° C, it will affect the glow curve structure and cause a loss of TL sensitivity.[27-29] Typically, through thorough testing, manufacturers recommend an optimal annealing temperature, but even at optimal temperatures, long heating times can cause a decrease in TL sensitivity. It is suggested that if the residual signal is acceptable for a given time temperature profile, the annealing time should be as short as possible.

During the early development of LiF: MCP, annealing temperatures were limited to 240°C. This presented a problem with high residual dose when pre-annealing. Further studies have been done to minimize this residual by heating the TLD to various temperatures.[28, 30, 31] It has been shown that when the TLD is heated to 270° C for 12 seconds, the result is a low residual and almost no loss in sensitivity. Specifically, there was almost no loss in TL sensitivity after 70 cycles of reuse.[26] Therefore, in cases of temperatures above 240° C for short durations, (i.e. - several seconds), there is relatively no loss in sensitivity with good reduction in residual.

The TLDs used in this study used a heating profile, also called a time-temperature profile (TTP) that was designed to maximize the sensitivity and re-usability of the DT-702. The TTP used began with an initial preheat of the TLD to 165°C for 10 seconds to eliminate low temperature traps that are confounding and short lived compared to the main dosimetric peak.[32] This was followed by a 16.67 second acquisition time, where heat increased at a rate of 15°C/sec to a maximum of 260°C. Maximum temperature was limited to 260°C to prevent damage to the material from overheating.[4, 33, 34] It should also be noted, that even though the prescribed maximum temperature for the TTP is 260 °C, the actual material temperature does not

reach this maximum temperature. The TLD was then cooled to ambient temperature before being transferred out of the read station.

Cooling rate is also an important factor in thermal treatment. It can influence the glow curve shape and the TL sensitivity. The cooling rate after annealing should be as fast as possible to avoid any loss of TL sensitivity that has been theorized to be result from thermal damage to carrier traps.[29, 35]

If the material is light sensitive, it can be optically stimulated, causing electron release and a resulting change of signal It has been shown that LiF: MCP does not encounter significant fading from light exposure.[36, 37] However, in a study conducted by Moscovitch et al., they recommended that the TL material be shielded from exposure to light since light can introduce a small amount of error.[4] Yuen et al. also describes the effect of light on LiF: MCP as "moderately sensitive to fluorescent light" and that it is important to "shield the detector in a light tight dosemeter holder".[38].

Although humidity plays less of a role in the effects of fade on the LiF: MCP, it should not be ignored. LiF is a salt and will dissolve in the presence of water. It has been shown that with the absorption of H_2O, adverse effects can result in changes to the shape of the glow curve and the TL properties of the dosimeter due to the formation of OH^{-1}.[39] In that study, it was also identified that the adverse effects can be minimized by storing in a relative humidity of less than 90% and by the use of N^2 gas flow to heat the TL material.[39-41] Even with the best environmental controls and light exposure, fading can still occur. [2]

The reasons behind TL fading are a complex phenomenon to explain. When examining the differences for photons and heavy charged particles (HCP) and neutrons,

it becomes even more complex. Jones et al. performed a study, much like the study performed for this thesis, that concluded there are significant differences in the fading behavior for neutron and photon exposures.[5] However, the authors failed to hypothesize the mechanisms behind the phenomenon.

In Doremus and Higgins study, using LiF: MT, it was hypothesized that fade is greater for thermal neutrons than for photons due to the greater interaction between the higher concentration of charged carrier defects distributed around charged particle tracks. [22] This leads to an increase in the number of thermal escape reactions between defects with trapped charge carriers and possibly by the conversion of peaks into higher energy traps. An in-depth review of micro dosimetric track structure is described in detail by Olko et al. in several articles.[42-46]

Several fade studies have been performed since LiF: MCP TLDs were introduced for personnel monitoring.[5, 7, 25, 47-50] In each of these studies, the goal was to determine the fading characteristics of this material. The duration of those studies ranged from 6 to 26 weeks. It was also noted that photon fade was consistent and ranged from no observed fading up to a maximum of 8% at ambient temperature. There has only been one published study to determine the neutron fading characteristics of LiF: MCP.[5] This study, performed by Jones et al., identified a decreases in sensitivity (pre-exposure time) of 5% after 164 days and no significant change in signal (post-exposure time) was recorded after 164 days at room temperature. Table 1 provides a summary of the fade studies performed and some important features of several studies are reviewed.

A brief discussion of key findings from the fade studies listed in Table 1 is worth

mentioning. The first fade studies were performed during the initial development of LiF: MCP by Nakajima in 1978[24] and by Wu in 1983[25]. These studies were limited in depth and were performed in conjunction with overall characterization of the material. The study performed by Perry et al. was evaluated photon irradiation for three months. The results of the study showed less than 4% fading in 90 days (45 days pre-exposure, 45 days post-exposure), with no pre-heating of the TLD prior to readout. This study did not use a pre-heat even though it has been recommended that pre-heating be used to eliminate low temperature traps that are confounding and short lived compared to the main dosimetric peak.[32, 47, 51] It was noted that if a pre-heat had been used, it would likely have reduced the fading to near zero.

The study conducted by Gilvin et al. used a two element TLD manufactured by Thermo.[48] A total of 75 TLDs were sorted into three groups of 25: aging (pre-exposure time), fading (post-exposure time), and controls. Irradiations occurred immediately after annealing for the fading group and just prior to reading for the aging group. The TLDs were then read using the Harshaw Model 8800 TLD reader and control TLDs accounted for background contribution. Results indicated no change in signal or sensitivity within a ±5% margin of error.

In the study performed by Jones et al., the Harshaw 8841 TLD (DT-702/PD) was used.[5] The study design used by Jones et al. closely resembles the materials and methods used in this study. Pre-exposure and post-exposure time were evaluated separately for both gamma and neutron radiation exposures. The TLDs were irradiated using an Americium Beryllium (AmBe) source to a neutron dose of 2.6 mSv (260 mrem) and a photon dose of 0.83 mSv (83 mrem). The TLDs were irradiated after

annealing to evaluate for post-exposure fade. Irradiation occurred just prior to being read for TLDs evaluated for pre-exposure fade. Control TLDs were also used to account for background radiation accumulation. The results of the Jones et al. study identified a decrease in sensitivity (pre-exposure time) of 5% after 164 days of storage at room temperatures (25±5°C). No significant change in signal (post-exposure time) was recorded after 164 days at room temperature.

The fade studies reviewed have provided valuable data on the unique characteristics of fade for LiF: MCP. Similar methods were used in these studies. Although methodology and resulting data were informative, it should be noted that there were some limitations among these previous studies. Correcting these limitations could have provided better insight into the true fading characteristics.

Some shortfalls noted in many of the studies were that the explanation for statistical analysis used was not clear and the statistical methods or statistical significance of the findings were not explicitly described. For example, it was noted in the Jones et al. study that a unique increase in the response was seen early on and then a decreasing trend over time occurred. Without specific experimental error being presented, it is difficult to interpret the data for statistical significance of any observed differences.

Some other common shortfalls identified were the use of background subtraction, method of irradiation, and assessment of combined fade. In the current study, all of these issues have been addressed and accounted for. Therefore, this study will improve on previous study limitations by increasing the sample size to ensure statistical power to detect a significant difference, include control TLDs for background

subtraction, describe the statistical tests performed, and assess pre, post and combined fade. This in turn should provide a more robust analysis of the neutron fading characteristics of LiF: MCP.

Author	Reference, Year	TLD material	Total TLDs	Source (Rad Type)	Dose Value	Fade Period (days)	Results
T. Nakajima	[24],1978	LiF: MCP	NS	NS	NS	30	Fade indicated a decrease of 5% at 40°C and 50% at 100°C At room temperature, no fade for 63 days
D. Wu	[25],1984	LiF: MCP	NS	Co-60 (Gamma)	0.1 Gy	60	30 days storage at 40°C and 60 days at room temperature were within experimental error 30 days storage at 70°C resulted in 27% fade
L. Duggan T. Kron	[47],1999	LiF: MCP LiF: MT	150	6 MeV photon beam from LINAC	0.5 Gy	180	Fading of LiF: MCP over six months, for a slow and fast cool-down, were 10% and 6% respectively, compared with 10% and 4% for LiF: MT. Sensitivity changes of LiF: MCP over six months, for a slow and fast cooldown, were 3% and 7% respectively, compared with 3% and 19% for LiF: MT
O. R. Perry M. Moscovitch	[49],1999	LiF: MCP	NS	NS	10 mGy	90	Equal time between 'annealing to exposure' (loss of sensitivity) and 'exposure to reading' (loss of signal). less than 4% fading in 90 days
J.C. Sáez Vergara M.Budzanwski	[51],1999	LiF: MCP	150	Cs-137 (Gamma)	4 mGy	90	Storage temperatures from -20°C up to +50°C for GR-200 and MCP-N have stability of main TL peak 4 (1.10 ± 0.10) regardless of storage temperature or regime
J.R. Cassata M. Moscovitch	[7], 2002	LiF: MCP	55	NS	10 mGy	120	Equal time between 'annealing to exposure' (loss of sensitivity) and 'exposure to reading' (loss of signal). Resulted in initial 2% increase then 2% decrease over 120 days
L.A. Jones R.P. Stokes	[5], 2006	LiF: MCP	80	AmBe (Neutron)	2.60 +/- 0.10 mSv	180	Max of 18% (high temp) 8 % for ambient Temp
P.J. Gilvin	[48], 2007	LiF: MCP LiF: MT	150	Sr-90 (Beta)	NS	180	LiF: MT - Pre and Post Fade of ~15% over 6 months LiF: MCP- no effect within ±5%

NS= Not Specified

Table 1. The table provides a summary of fade studies performed.

CHAPTER THREE: MATERIALS AND METHODS

Fade Study Design

This study is designed to measure the neutron fade associated with the DT-702/PD TLD, to include both change of sensitivity (Pre-Irradiation fade), change of signal (Post-Irradiation fade) and combined change of sensitivity/signal over 34 week period. An in-depth review of the Harshaw 8841 Dosimeter (DT-702/PD TLD), Harshaw Model 8800 TLD Reader, and calibration procedures that were used for this study are contained in Appendix C. It should be noted that for the entire study period, the procedure used to process the TLDs and perform the TLD reader calibrations was the Naval Dosimetry Center Standard Organization and Regulations Manual; (NDC SORM).[52] This is the same procedure used by the Naval Dosimetry Center to process their environmental and personnel dosimetry. It was important to use the methodologies described in the NDC SORM because it can provide insight into the Navy's dosimetry program and allow for evaluation of current dosimetry practices.

The methods used for the current study improved upon, as well as adopted ideas from the studies reviewed. Much of the methodology was modeled after the studies performed by Doremus and Higgins[22] and Jones and Stokes[5]. Specifically, this study was designed to analyze the change of sensitivity and signal associated with the issue periods for the Navy, to account for shipping and monitoring periods. In the present study the TLDs were annealed at the beginning of the study and then divided into three sets consisting of pre-irradiation, post-irradiation, and combined pre/post irradiation. Each set was subsequently divided into groups to account for a 34 week period and processed

according to the schedule identified in Table 2.

TLD Preparation

In this study three thousand TLDs, which allowed for a 52 week study, were selected from newly received shipments after they had been evaluated by the Naval Dosimetry Center for their thermoluminescent efficiency and neutron response. The selection criterion was based on establishing realistic operational conditions to ensure that the validity of the results would be applicable to the Navy's dosimetry program. With that in mind, no pre-selection criteria were used to select the study TLDs.

These TLDs were annealed one day prior to the beginning of Day 0 of the study by performing two sequential 2-mrem anneals. The two sets of anneals were performed on the entire set of TLDs to ensure that any residual signal was reduced to the lowest extent possible with the TTP used. [28, 53] In most instances, one anneal would have sufficed and in most cases, the initial anneal process requires at least 2 heats to reduce the signal to less than 2 mrem. A second anneal was added to ensure that the baseline was equal for the entire population.

The TLDs were sorted into several sets according to the irradiation schedule identified in Table 2. Due to the limited number of TLDs available for the study, sets of 15 TLDs were used for the first 13 weeks of the study and for the pure pre- and post- fade sets. Groups of 5 TLDs were used for the other combination pre/post fade sets after the 13 week period. After separation, they were placed into opaque boxes Labeled "PRE-IRRADIATION TLDs", "POST-IRRADIATION TLDs", "CONTROLS", and "WEEK X" where X= the corresponding week of irradiation.

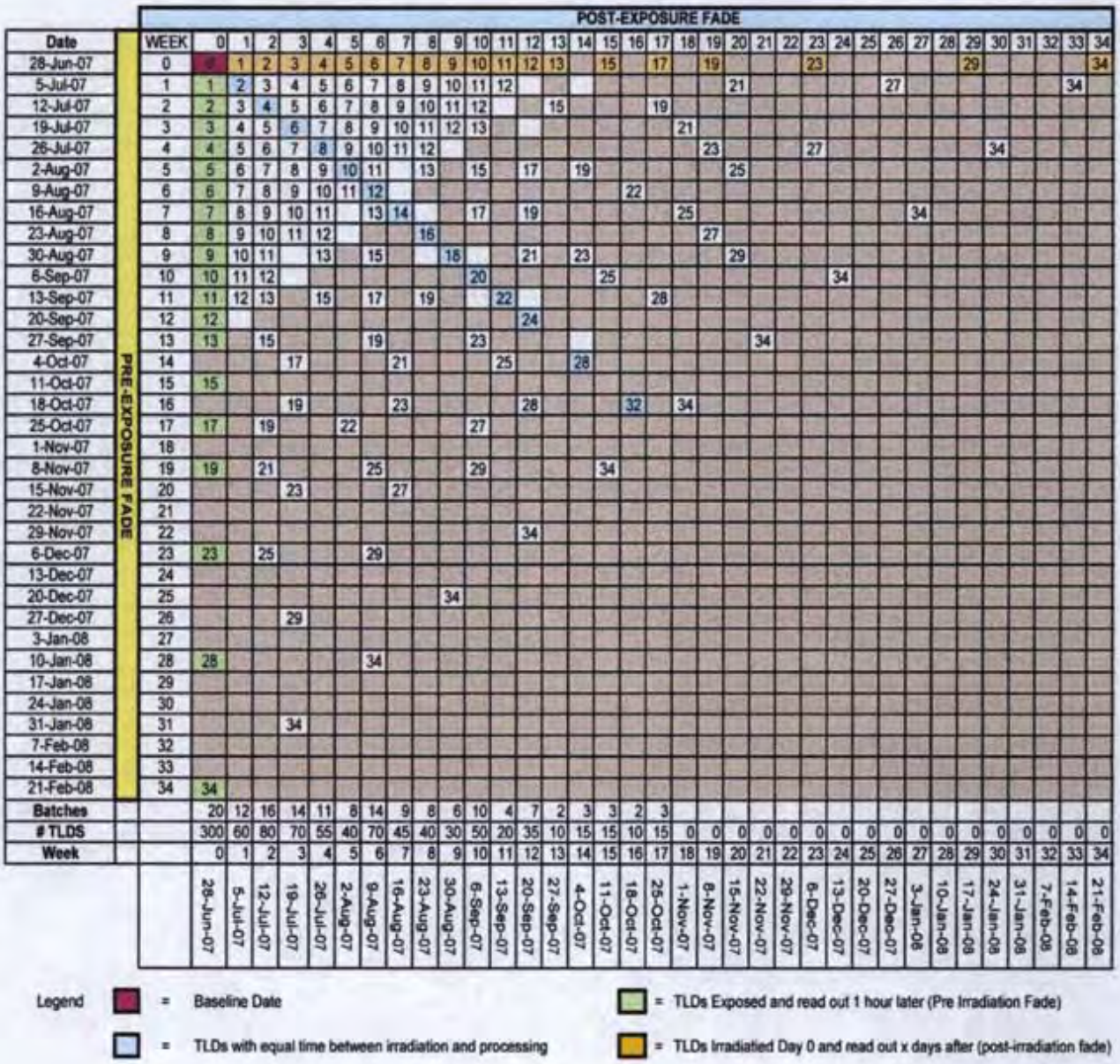

Table 2. The table identifies the 34 week TLD read schedule used for the study.

Irradiation of TLDs

Once the sets of TLDs were established, irradiations were performed in accordance with the established schedule annotated on Table 2. The first TLDs irradiated were the post irradiation set which was done on Day 0. The group of Pre-Irradiation TLDs was irradiated each week per Table 2 prior to processing. Combined Pre/Post Irradiation TLDs were irradiated as indicated in Table 2.

A set of reference TLDs was utilized to account for any machine variance. This set consisted of a group of 15 TLDs and were processed on Day 0. Following Day 0, the reference set was irradiated along with the Pre-Irradiation TLDs and processed with them. Although these TLDs were annealed prior to irradiating, an additional 2 mrem anneal was performed in accordance with NDC SORM. This second anneal was performed for consistency in study design to ensure there was no residual signal on the TLD.

TLD Irradiation was performed utilizing the plutonium beryllium (PuBe) Source and a carousel irradiation method, Appendix D. The neutron source used for this study is an encapsulated plutonium beryllium neutron source manufactured by Monsanto. It consists of 76.37 grams of Plutonium 239 and has a cylindrical shape that measures 1.30 inches (outside diameter) by 3.4 inches high. The source is controlled under a Master Materials License and maintained by the Naval Dosimetry Center.

The PuBe source contains 5 Curies and produces 2.3×10^6 neutrons per cm^2-second per Curie. The source is surrounded by a virgin polyethylene shield to allow for thermalization of neutrons and in order to minimize personnel dose,

borated poly is used to prevent escape of neutrons from the shielding. The delivered dose rate for the irradiation method used was 6.68 mrem per hour. A detailed description of the irradiation method development can be found in Appendix D. Using the carousel irradiator, 100 TLDs were mounted on the carousel and evenly distributed keeping Element 4 of the TLD located on the bottom-inner radius to be irradiated as indicated in Figure 9.

As illustrated in Figure 9, the TLDs were placed in the carousel for irradiation. Prior to irradiation, the carousel was initiated and remained rotation throughout the 1 hr 15 min irradiation. The carousel remained rotating until removed from the PuBe source. The TLDs were removed from the carousel assembly and prepared for processing.

Processing of TLDs

All TLDs were processed on Thursdays based on the processing schedule, Table 2. Prior to reading TLDs, as required by the NDC SORM, the daily reader calibration factor (RCF) was determined and tracked to correct for the day-to-day changes in the reader as discussed in Appendix C. The same set of calibration cards was used for the entire study.

Each week, after performing the calibration of the reader, processing included the following sets of TLDs for that week as indicated on Table 2: Control, Post-Irradiation, Pre-Irradiation and Combined Pre/Post Irradiation TLDs. Consistency in processing was maintained by processing TLDs within one hour after being irradiated.

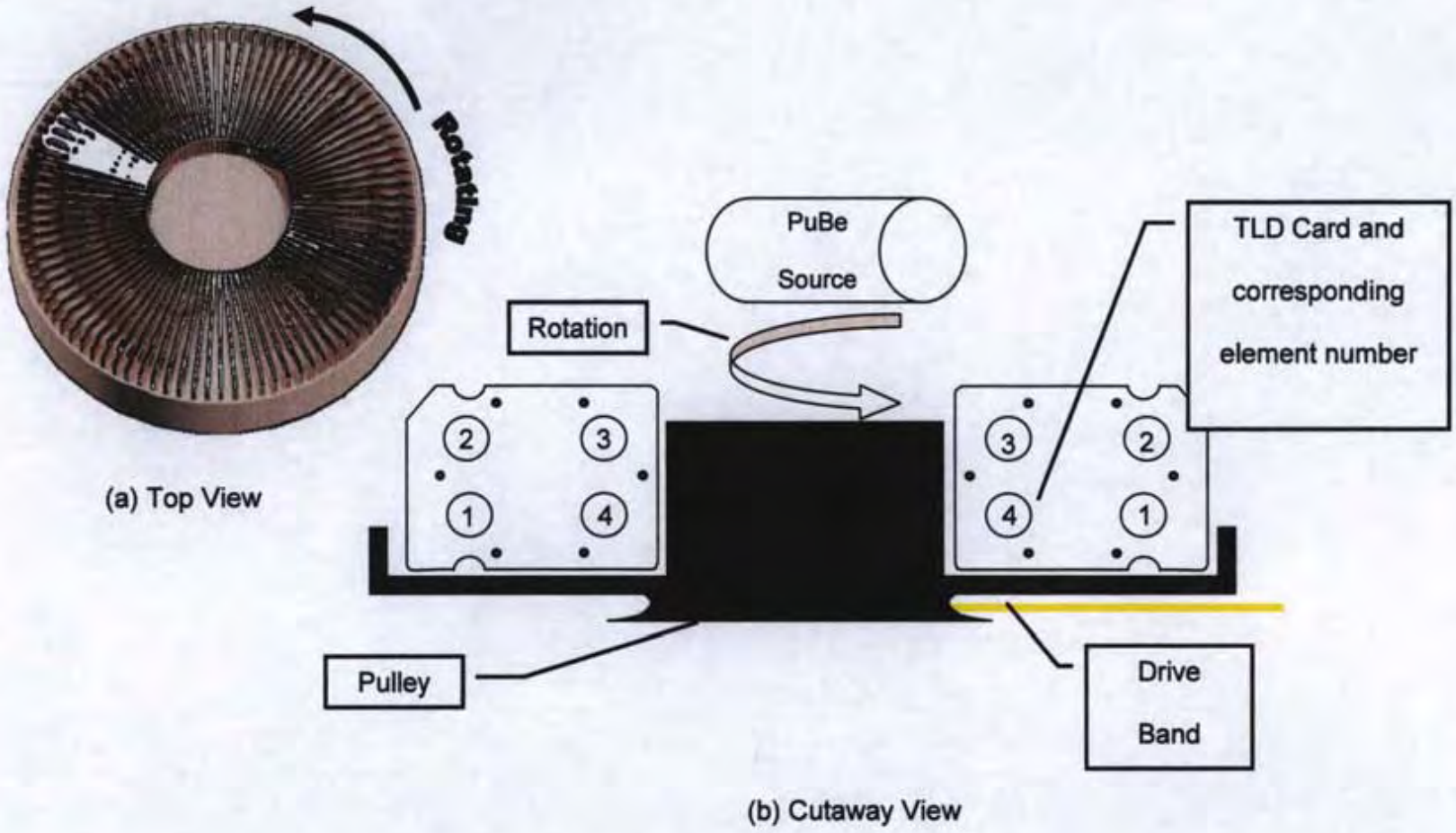

Figure 9. (a) The top view of the carousel used to irradiate the TLDs.

(b) A cut-away view shows the position of the PuBe source in relation to the TLDs cards.

It is important to note that the carousel was placed in motion prior to inserting into source and remained rotating after the irradiation ensuring a homogeneous irradiation.

Storage of TLDs

With the exception of irradiation and processing, all TLDs were stored in the same location for the duration of the study. Upon completion of processing, the TLDs were placed in a separate container labeled processed TLDs. To ensure that the storage areas temperature and humidity remained stable, measurements were taken using an OAKTON Model 35710-10 temperature/humidity meter and tracked on a weekly basis to ensure the storage conditions were maintained between 69 ±9°F and 41 ±17% relative humidity for the duration of the study. Previous studies have shown that this temperature range will not adversely affect the fade response of the TL material and this temperature band represents the operational conditions.[5, 26, 54] Additionally, the TTP used for this study includes a pre-heat thereby minimizing the effect caused by the low temperature peaks. This is an improvement realized from a study concluded by Perry et al.[49] The humidity was also controlled well below the maximum recommended relative humidity level of 90 %.[39]

Data Analysis

Data Discrimination and Error Propagation

Throughout the course of the study, the same evaluation of each group of TLDs was used. The basic process was to determine the average of the group, evaluate for outliers, subtract the contribution of the control TLDs, and then normalize the data to the baseline data determined at the start of the study. It should also be noted that the propagation of error was carried through for the

entire study.

The average dose of each element for each set of DT-702/PD TLD cards was determined for each data point ($\overline{Dose}_{raw}$). The associated standard deviation of each set of data was calculated as the standard error using Equation 2 where $\bar{x}$ is the sample mean, and *N* is the number of cards used for the data point.

$$\sigma_{raw} = \sqrt{\frac{\Sigma(x-\bar{x})^2}{N-1}}$$

Equation 2. The equation identifies the calculation of standard error of the sample mean.

After processing each set of five or fifteen TLDs, the results of each element was evaluated for outliers to identify any statistically spurious data points using Chauvenet's criterion. Chauvenet's criterion allows for the elimination of spurious data points from a set of data based on the probability of obtaining less than $(2N)^{-1}$ deviations away from the mean. [55] Therefore, the removal of outliers was determined by evaluating if the difference between the individual value and the mean was greater than 1.63 (N=5) or 2.13 (N=15) times the standard deviation of the group. This process was performed once for each set of TLDs (both background and fade groups) giving a final mean value ($\overline{Dose}_{raw}$) and standard error (σ_{raw}) for each data point. After evaluating each set of TLDs for outliers, the mean of the control TLDs ($\overline{Dose}_{bkgd}$), was subtracted to give a background corrected reading, ($\overline{Dose}_{net}$) for each element of the TLD using Equation 3.

$$\overline{Dose}_{net} = \overline{Dose}_{raw} - \overline{Dose}_{bkgd}$$

Equation 3. Equation identifies the background corrected dose calculation.

Standard error propagation methods were utilized as described by Knoll.[56] The following paragraphs identify the calculations used to determine the propagated error, normalized response and normalized response error.

The net error (σ_{net}) was propagated using Equation 4.

$$\sigma_{net} = \sqrt{(\sigma_{raw}^2 + \sigma_{bgnd}^2)}$$

Equation 4. The equation identifies the error propagation calculation used to calculate net error.

After correcting each data point for background, the data was normalized against the week 0 TLD results or baseline data, by taking a ratio between Week 0 and Week X. This provided a relative response of signal or sensitivity based on a group of TLDs with no associated pre-exposure or post-exposure fade.

The dose ratio (R_{Dose}) was calculated by dividing by $\overline{Dose}_{net\_week\_X}$ by the $\overline{Dose}_{net\_week\_0}$ (Equation 5).

$$R_{Dose} = \left(\frac{\overline{Dose}_{net\_week\_X}}{\overline{Dose}_{net\_week\_0}} \right)$$

Equation 5. Equation identifies the dose ratio (R_{Dose}) for normalized dose response against baseline data.

The error associated with the Dose Ratio was propagated to account for

the associated errors of each weeks TLD group using Equation 6.[56]

$$\sigma_{Dose} = \left(\frac{\overline{Dose}_{net\_week\_X}}{\overline{Dose}_{net\_week\_0}} \right) * \sqrt{\left(\frac{\sigma_{net\_week\_0}}{\overline{Dose}_{net\_week\_0}} \right)^2 + \left(\frac{\sigma_{net\_week\_X}}{\overline{Dose}_{net\_week\_X}} \right)^2}$$

Equation 6. The equation identifies the error propagation calculation used for determining the error for normalized data

Data Display

Data was plotted using SigmaPlot® for Windows, version 10.0 [57] and Microsoft Excel 2007. All statistical analyses were performed using SigmaStat® for Windows, version 3.11.[58]

Statistical Evaluation

The evaluation of the resulting data focused primarily on the determination of fading over time. Specifically, if a statistical difference existed in the change of signal and sensitivity for pre, post, and combination of fade for the entire 34 week study. In order to perform this evaluation, some assumptions were made on the specific dosimeter characteristics that included the statistical distribution and the expected variations for the TLD. The test for significant differences was set at a 95% confidence interval and performed among sample means (μ) of the independent variable (known signal applied to TLD), and the dependent variable (time).

The statistical single element variation in the DT-702/PD dosimeter has been reported to be 2-4%.[26] In this study, a value of 3.5% was used for reproducibility based on the historical average observed by the Naval Dosimetry Center. The variation was determined by repeated measurements of the same card with the same dose. Given that the distribution of dose is Gaussian

(normal) in nature for the entire population of TLDs, it should be expected that 99% of the readings will fall within three standard deviations (3σ) of the average. Therefore, a maximum 3σ experimental error of about 10.5% would be expected. While this was not mathematically accounted for in this study, it can be assumed that differences of about 10.5% or less are well within the experimental error.

One-way analysis of variance (ANOVA) tests were performed on the results of each element for all variations of storage time. For all ANOVA calculations, an alpha level of 0.05 was used. In the event that a statistical difference was detected by the ANOVA, a multiple comparison test using the Holm-Sidak method was performed.[58] The Holm-Sidak test is a non-parametric test that is more powerful than the standard ANOVA. The test attempts to identify the specific points that are statistically different compared to the control value (no storage time baseline response). [58] When performing the test, the P values of all comparisons are computed and ordered from smallest to largest. Each P value is then compared to a critical level against a 95% significance level, the rank of the P value, and the total number of comparisons made. A P value less than the critical level (0.05) indicates there is a significant difference between the corresponding two groups.

CHAPTER FOUR: RESULTS AND DATA ANALYSIS

Analysis of Background Radiation

Throughout the entire study, control TLDs were used to account for background radiation. Background radiation is present from natural and manmade sources. The contribution of environmental radiation accounts for approximately 100 mrem per year of the total annual effective dose equivalent in the United States of approximately 360 mrem per year.[59] In the case of this study, the TLDs were stored in an area of much lower background resulting in a daily rate of 0.1140 mrem/day or 41.62 mrem/year.

Study TLDs were processed weekly and background radiation levels were subtracted from the study groups. In analyzing the background level, two analyses were performed; determination of a consistent daily background rate, and statistical difference between the different elements for the same groups of TLDs across the entire study period. In theory, the rate should remain constant over time and since the contribution to background is primarily from photons, all four elements should have the same background over time.

To analyze these data points, a simple linear regression was used to evaluate the daily rate and a Pearson Product-Moment Correlation was used to compare the correlation of the first element with the other three.[58] The Pearson Correlation showed no statistical difference between all 4 elements when individual elements were compared against each other. (Table 3)

		Element 2	Element 3	Element 4
Element 1	R^2	0.996	0.998	0.998
	p	2.177E-032	5.159E-036	1.092E-035
	N	31	31	31
Element 2	R^2		0.998	0.998
	p		1.007E-036	8.839E-038
	N		31	31
Element 3	R^2			0.999
	p			3.128E-044
	N			31

Table 3. Table indicates the Pearson Product-Moment Correlation for the background radiation for Elements 1,2,3,4 over 34 week period.

The linear regression for each element resulted in an average R^2 value of 0.998. Figures 10 to 14 show each of the regression plots and their associated equation and R^2 value.

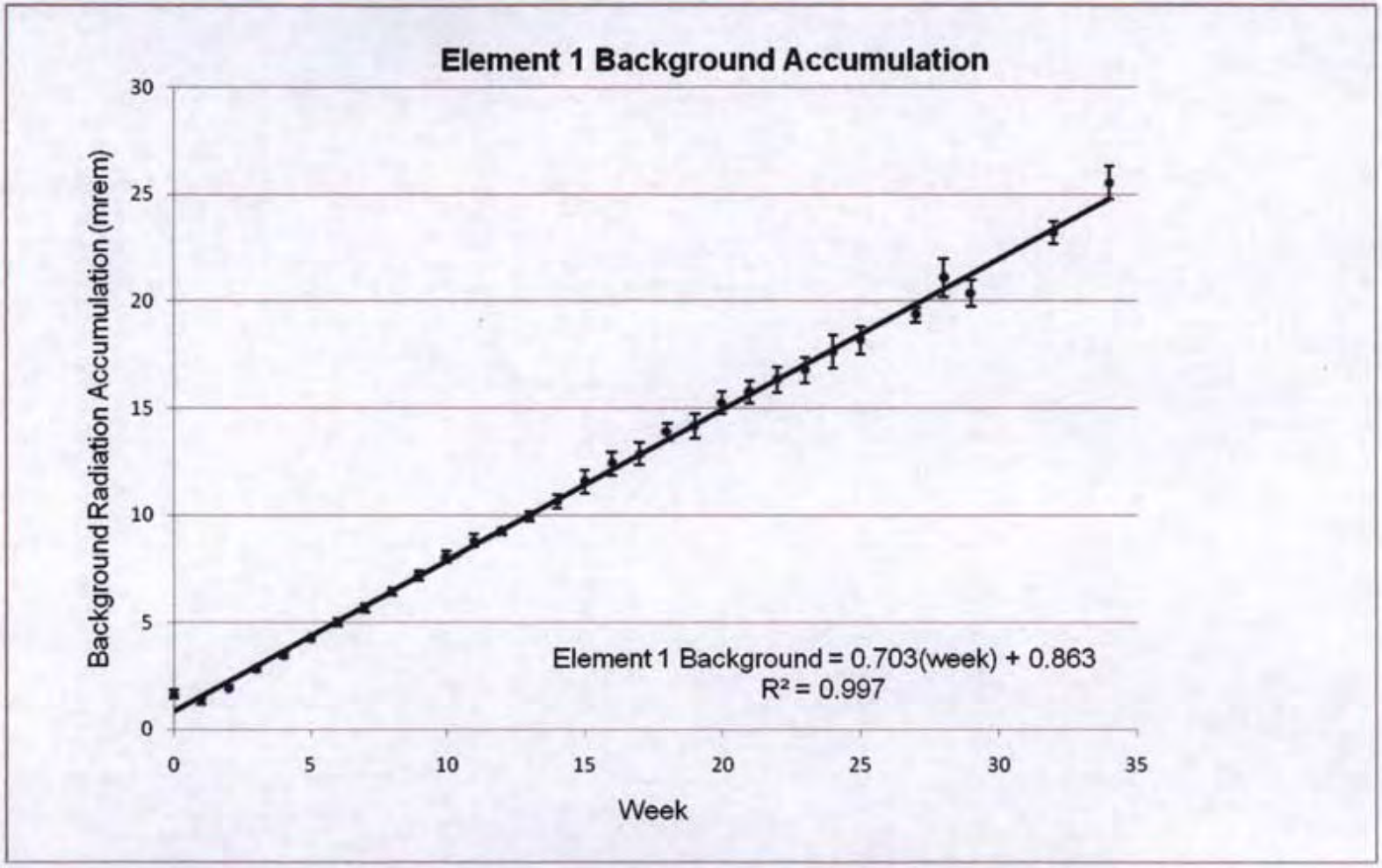

Figure 10. The graph shows Element 1 background radiation accumulation. Linear regression is shown as a solid line through the data points. The error bars indicate the propagated errors for the mathematical manipulation (1σ). Equation of the regression analysis and R^2 value for linear regression fit are listed.

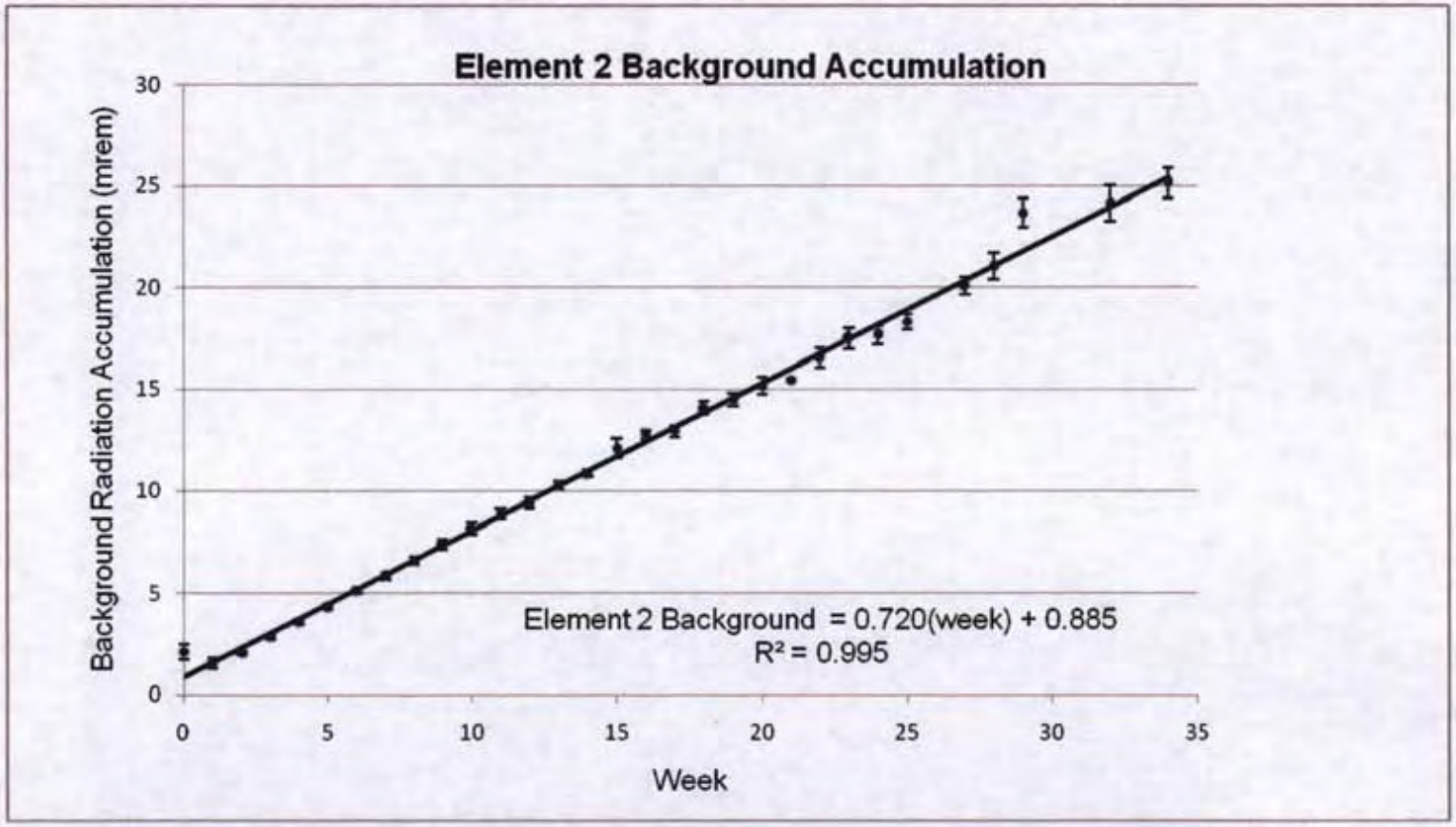

Figure 11. The graph shows Element 2 background radiation accumulation. Linear regression is shown as a solid line through the data points. The error bars indicate the propagated errors for the mathematical manipulation (1σ). Equation of the regression analysis and R^2 value for linear regression fit are listed.

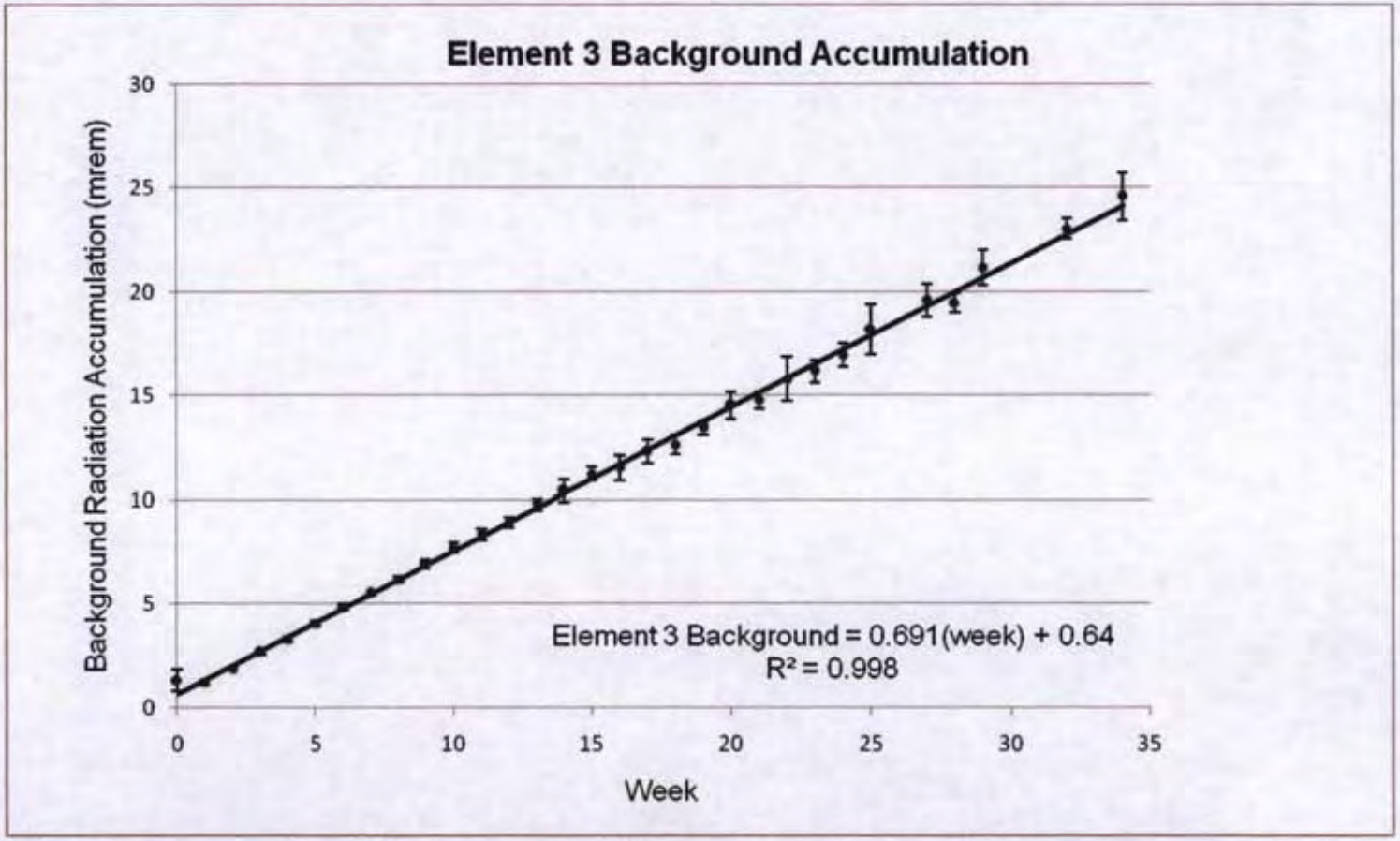

Figure 12. The graph shows Element 3 background radiation accumulation.
Linear regression is shown as a solid line through the data points. The error bars indicate the propagated errors for the mathematical manipulation (1σ). Equation of the regression analysis and R^2 value for linear regression fit are listed.

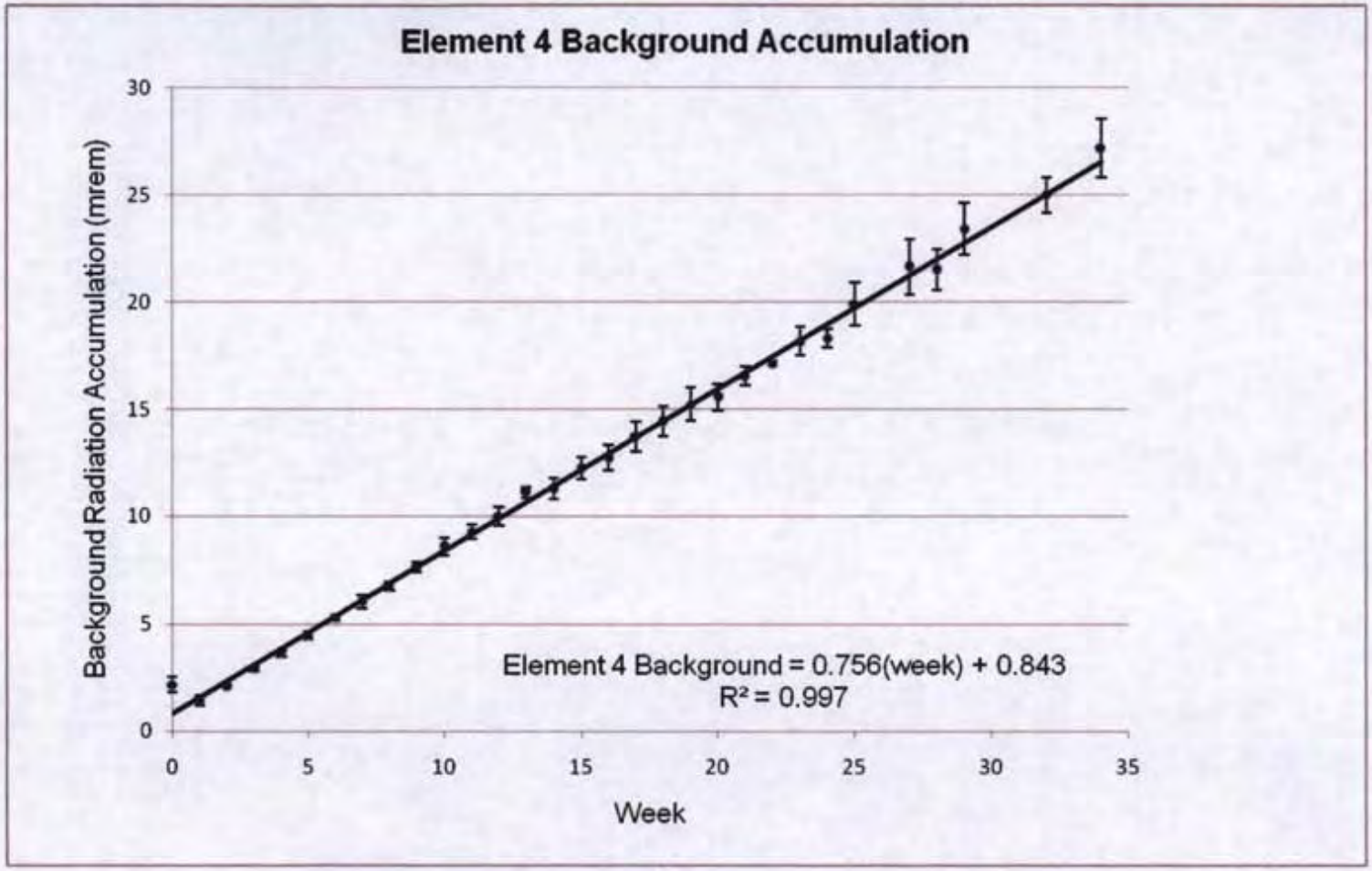

Figure 13. The graph shows Element 4 background radiation accumulation.
Linear regression is shown as a solid line through the data points. The error bars indicate the propagated errors for the mathematical manipulation (1σ). Equation of the regression analysis and R^2 value for linear regression fit are listed.

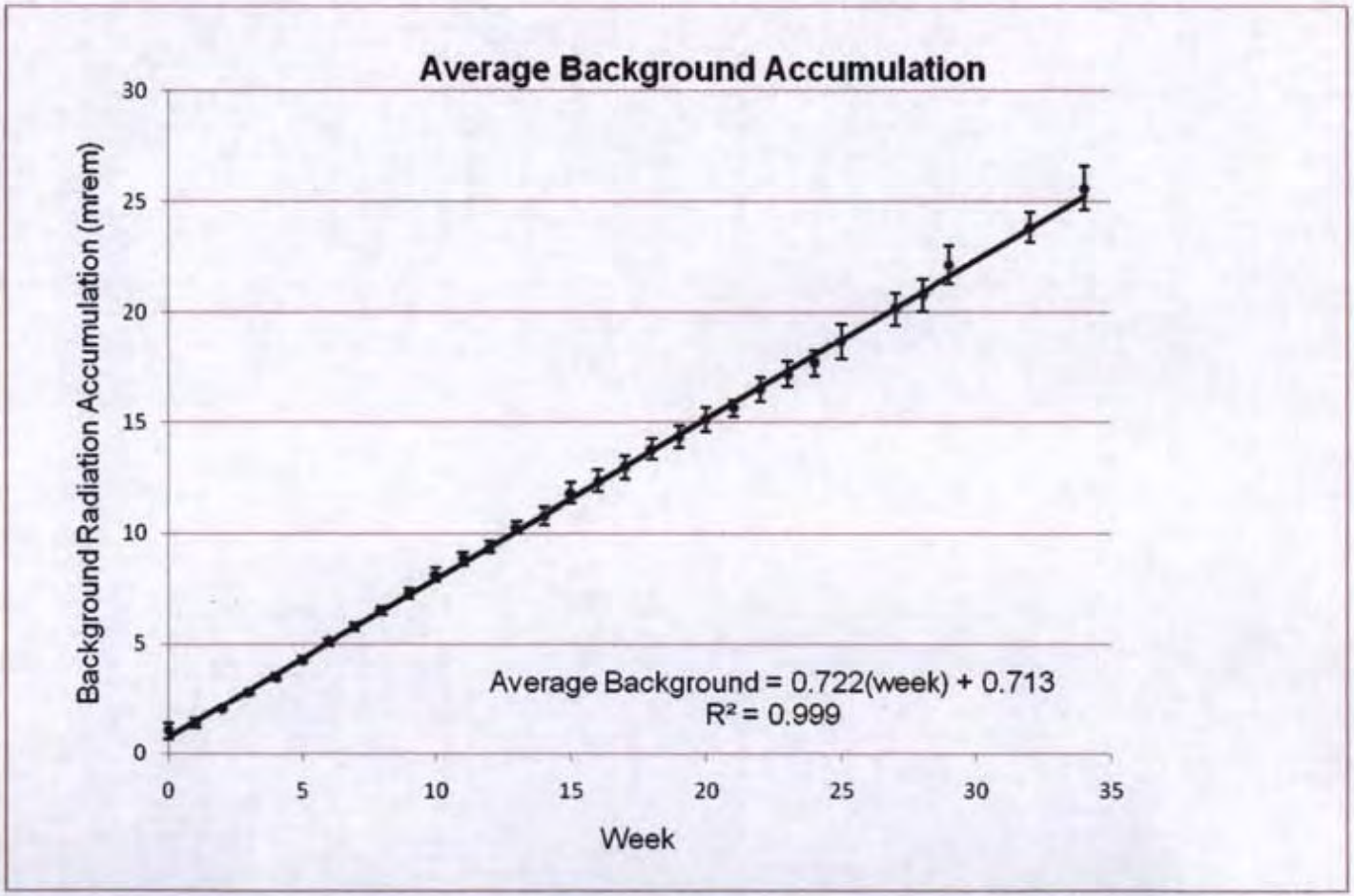

Figure 14. The graph shows the average of all Elements background radiation accumulation. Linear regression is shown as a solid line through the data points. The error bars indicate the propagated errors for the mathematical manipulation (1σ). Equation of the regression analysis and R^2 value for linear regression fit are listed.

Analysis of Pre-Irradiation Fade

For the study, the primary focus was to determine the effects of fading based on neutron irradiation. Element 4 was the primary element for the neutron fade study. A One-way ANOVA test performed on the Pre-Irradiation TLD group for the combined photon and neutron contributions indicated that there was no significant difference between the responses of the elements for the entire 34 week period. (P=0.131). The maximum increase was measured at 5 weeks at 5%. The TLD response for sensitivity appeared to remain consistent for entire study period, with a maximum decreases measured at only 6%. Changes in sensitivity for Element 4 combined photon and neutron is displayed in Figure 15.

To analyze the pure neutron component of pre irradiation fade, the photon component from Element 1 must be subtracted from Element 4. In order to ensure the geometry was consistent, a study was performed to account for the differences in irradiation position. This was performed by rotating the TLD card through all the positions of the carousel and determining the ratio between position 1 and position 4 for pure photon. In each of the Groups, the TLDs were irradiated for the same amount of time. The data obtained in this study are indicated in Figure 16. The two groups used for determining the ratio were Groups 2 and 3. The normal position for Element 4 of all the study groups used a Group 3 geometry therefore Element 1 had to be corrected to this geometry. Consequently, Group 2 geometry had to be compared to Group 3 and a ratio established.

In order to apply a correction factor, it must be determined that there is

truly a significant difference between the two values due to geometry. This was accomplished by performing a t-test for the Element 1 Group 2 and 3 positions.[58] The result of this test identified a significant difference between the two positions ($P \leq 0.001$). Therefore, when calculating a ratio, a difference of 8% due to the geometry differences exists between Element 1 for Groups 2 and 3 (Figure 16). In order to account for this difference, all Element 1 values were adjusted by 8%.

After the correction for Element 1 was determined, it was used to subtract from the contribution of Element 4 value. This methodology was used by Jones et al. in determining the pure neutron effects.[5] The neutron component of the TLD-600H signal, Element 4, was calculated using Equation 7:

$$(CsEDE_{Li\text{-}6} - CsEDE_{Li\text{-}7}) \times CsModCf \times NECF = DDE_n$$

Equation 7. The equation identifies the neutron correction equation used for determination of pure neutron contribution

The Cf-252 equivalent dose equivalent neutron response (CfEDE) for both materials is obtained by subtraction of the Li-7 response from the Li-6 response and multiplying the result by a correction factor (CsModCf) to convert to a moderated Cf-252 calibrated system. The deep dose equivalent (DDE), or the external whole-body exposure dose equivalent at a tissue depth of 1 cm, is then calculated by multiplying the result by a source and neutron energy correction factor (NECF) that is a function of neutron energy, distance between the source

and person, geometry of the surroundings, and the material properties of the surroundings.

The NECF for neutron sources from occupational environments is determined using an unfolding algorithm that uses ratios of measurements from a cylindrical BF_3 gas filled proportional counter, model Army Navy Portable Device RADIAC 70 (ANPDR-70). Ratios are calculated from measurements taken with varying amounts of polyethylene around the BF_3 tube.[7]

After performing the neutron calculation, the effects of fade from pure neutron were analyzed. A One-way ANOVA test performed on the Pre-Irradiation TLD group for the neutron contributions indicated that there was no statistically significant difference between the responses of the elements for the entire 34 week period. (P=0.784). The maximum increase was measured at 5 weeks at 6%, slightly higher than that of the combined photon and neutron fade. The TLD response appeared to remain consistent for entire study period, with a maximum decreases measured at only 6%. Changes in sensitivity for Element 4 for only neutron are displayed in Figure 17. An interesting finding in analyzing both of the curves and data is that there is little difference between pre-irradiation fade for photon and neutron irradiation. This is not surprising, since the contribution from the photon component is only about 4% of the total signal. For that reason, the data provides a minimal insight to the differences of photon and neutron fading characteristics.

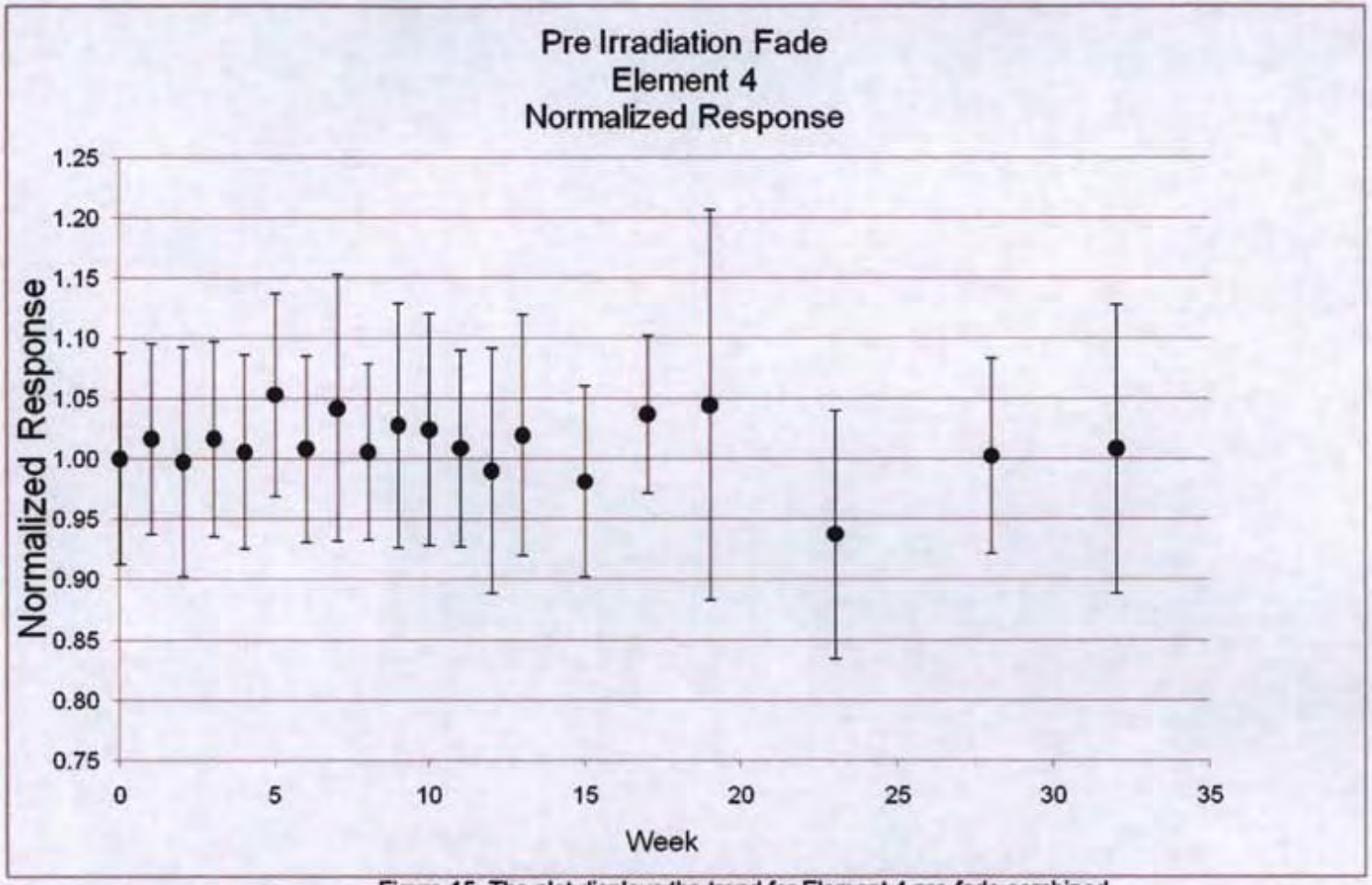

Figure 15. The plot displays the trend for Element 4 pre-fade combined neutron and photon normalized response over a 34 week period. The error bars indicate the propagated errors for the mathematical manipulation (1σ).

	Element 1			Element 2			Element 3			Element 4		
Group	Avg	SD	CV	Avg	SD	CV	Avg	SD	CV	Avg	SD	CV
1	26.60	1.27	4.8%	21.76	0.67	3.1%	17.26	0.53	3.1%	388.24	26.60	6.9%
2	20.59	0.81	3.9%	26.01	1.11	4.3%	20.59	0.54	2.6%	371.55	41.26	11.1%
3	19.00	0.84	4.4%	23.16	0.76	3.3%	25.23	0.55	2.2%	413.99	25.46	6.2%
4	21.37	0.36	1.7%	18.36	0.51	2.8%	19.92	0.70	3.5%	433.39	35.68	8.2%

GROUP 1

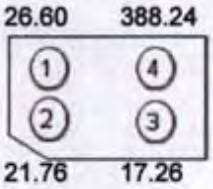

	RATIOS	
1 to 2 1.22		4 to 3 22.49
1 to 4 0.07		2 to 3 1.26
2 to 4 0.06		1 to 3 1.54

GROUP 2

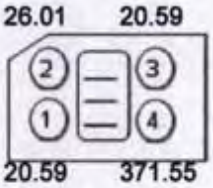

2 to 1 1.26		3 to 4 0.06
2 to 3 1.26		1 to 4 0.06
1 to 3 1		2 to 4 0.07

GROUP 3

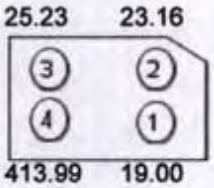

3 to 4 0.06		2 to 1 1.22
3 to 2 1.09		4 to 1 21.8
4 to 2 17.9		3 to 1 1.33

GROUP 4

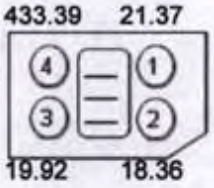

4 to 3 21.75		1 to 2 1.16
4 to 1 20.3		3 to 2 1.08
3 to 1 0.93		4 to 2 23.6

Figure 16. The plot displays the calculations used for the geometry effects during irradiation.

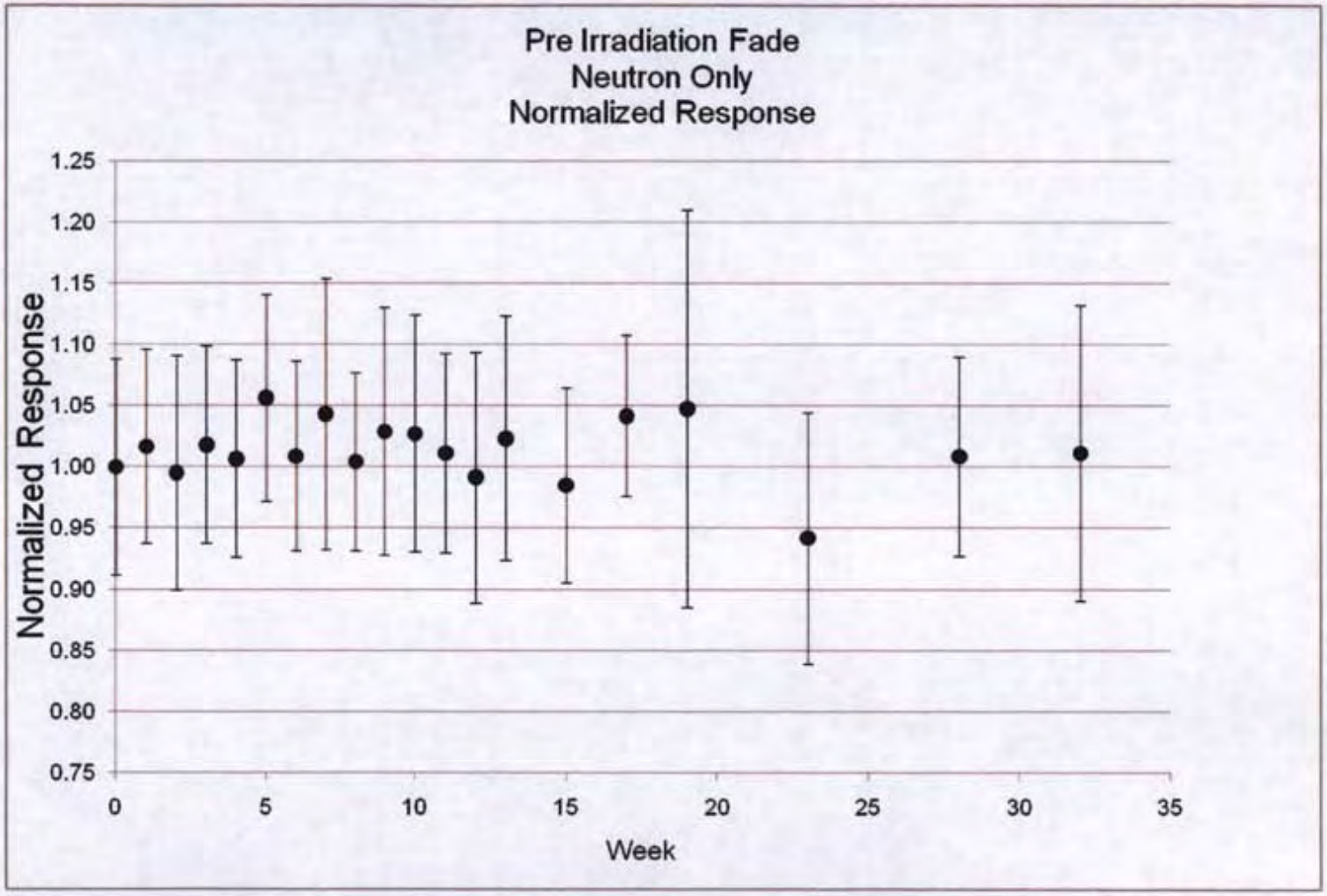

Figure 17. The plot displays the trend for Element 4 pre fade

neutron normalized response over a 34 week period.

The error bars indicate the propagated errors for the mathematical manipulation (1σ).

Analysis of Post Irradiation Fade

Element 4 was analyzed for Post-Irradiation Fade, which is considered a change of signal over time. A One-way ANOVA test performed on the Post-Irradiation TLD group for the combined photon and neutron contributions indicated that there was no significant difference between the responses of the elements for the entire 34 week period. (P=0.523). The maximum increase was measured at 11 weeks at 3%. The TLD response appeared to remain consistent for the entire study, with maximum decreases measured at only 2%. Changes in signal for Element 4 combined photon and neutron is displayed in Figure 18.

After performing the same correction for neutron contribution as used for Pre-Irradiation Fade, the effects of fade from pure neutron were analyzed. A One-way ANOVA test performed on the Post-Irradiation TLD group for the neutron contributions indicated that there was no significant difference between the responses of the elements for the entire 34 week period. (P=0.950). The maximum increase was measured at 34 weeks at 3%. The TLD response appeared to remain consistent for entire study period, with a maximum decreases measured at only 2%. Changes in signal for Element 4 for only neutron are displayed in Figure 19.

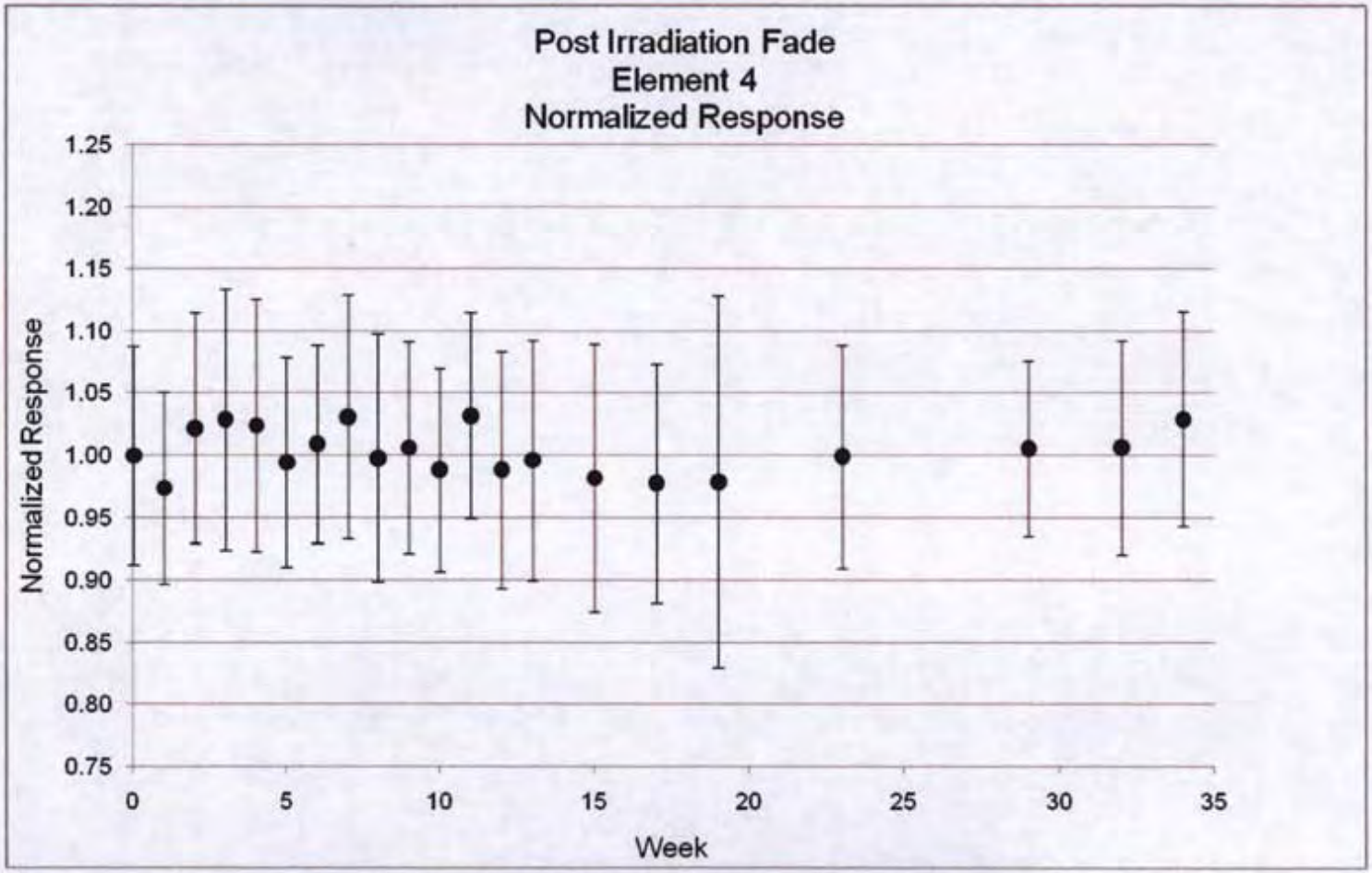

Figure 18. The plot displays the trend for Element 4 post fade combined neutron and photon normalized response over a 34 week period. The error bars indicate the propagated errors for the mathematical manipulation (1σ).

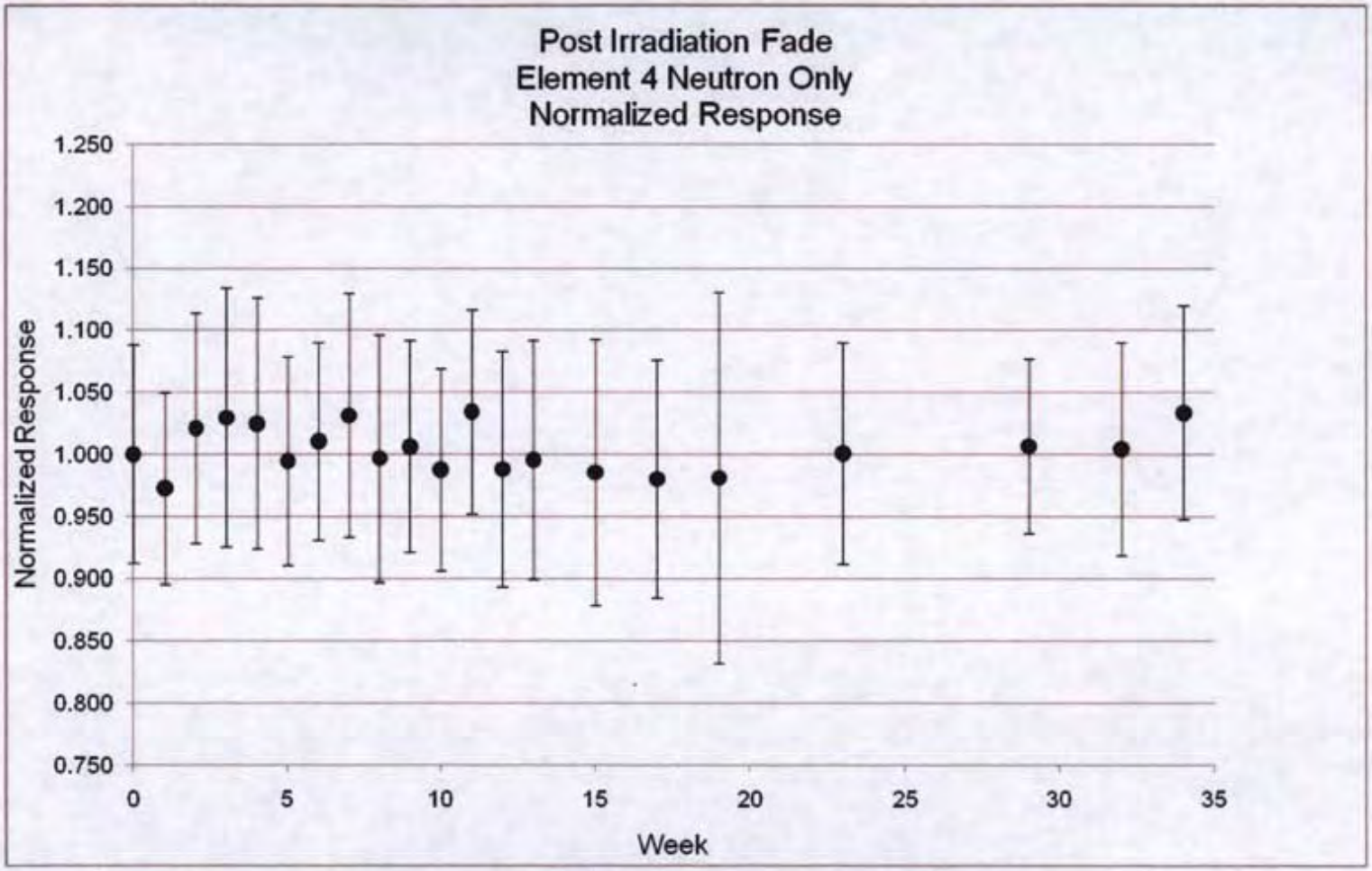

Figure 19. The plot displays the trend for Element 4 post fade neutron normalized response over a 34 week period. The error bars indicate the propagated errors for the mathematical manipulation (1σ).

Analysis of Combined Fade

An analysis was performed on Combined Fade results. Several different combinations are presented with varying results in the data. First, an analysis was done on the combined pure Pre and Post Fade data, then an analysis was performed on equal time between Pre and Post data, and finally an analysis was performed on all of the data.

Analyzing the pure Pre and Post results for combined neutron and photon with one-way ANOVA resulted in no statistically significant difference. (P=0.300) The results can be seen in Figure 20. The combined Pre and Post was also analyzed for only neutron and resulted in no statistical difference (P= 0.970). These results are shown in Figure 21. Once again, it can be seen that the graphs are very similar and no unique trend exists.

The second analysis performed for the combined fade was determining the effects of equal time between pre and post exposure time. This is indicated as the diagonal line on Table 2, which indicates that there was an equal amount of time between the anneal-expose-read periods. One-way ANOVA initially detected a significant difference (P=<0.001), but Holm-Sidak testing determined no point to be statistically significant (P=0.0473). Both the combined neutron/photon and neutron equal pre and post fade results can be seen in Figures 22 and 23, respectively.

Finally, a statistical analysis was performed on the entire population of pre and post exposure fade data. One-way ANOVA initially detected a significant

difference (P=<0.001), but the non-parametric Holm-Sidak testing determined no point to be statistically significant (P=0.00272). This result is quite remarkable considering there are 170 data points, accounting for 1782 TLDs for all the fade groups, over the entire 34 week period. Both the combined neutron/photon and neutron pre and post fade results can be seen in Figures 24 and 25, respectively.

In addition to the Figures 20-25, Table 4 is provided to represent the effects of Pre and Post Fade for both Photon/Neutron on a Pre/Post fade axis. Along with this is a graphical representation of the normalized results (Figure 26).

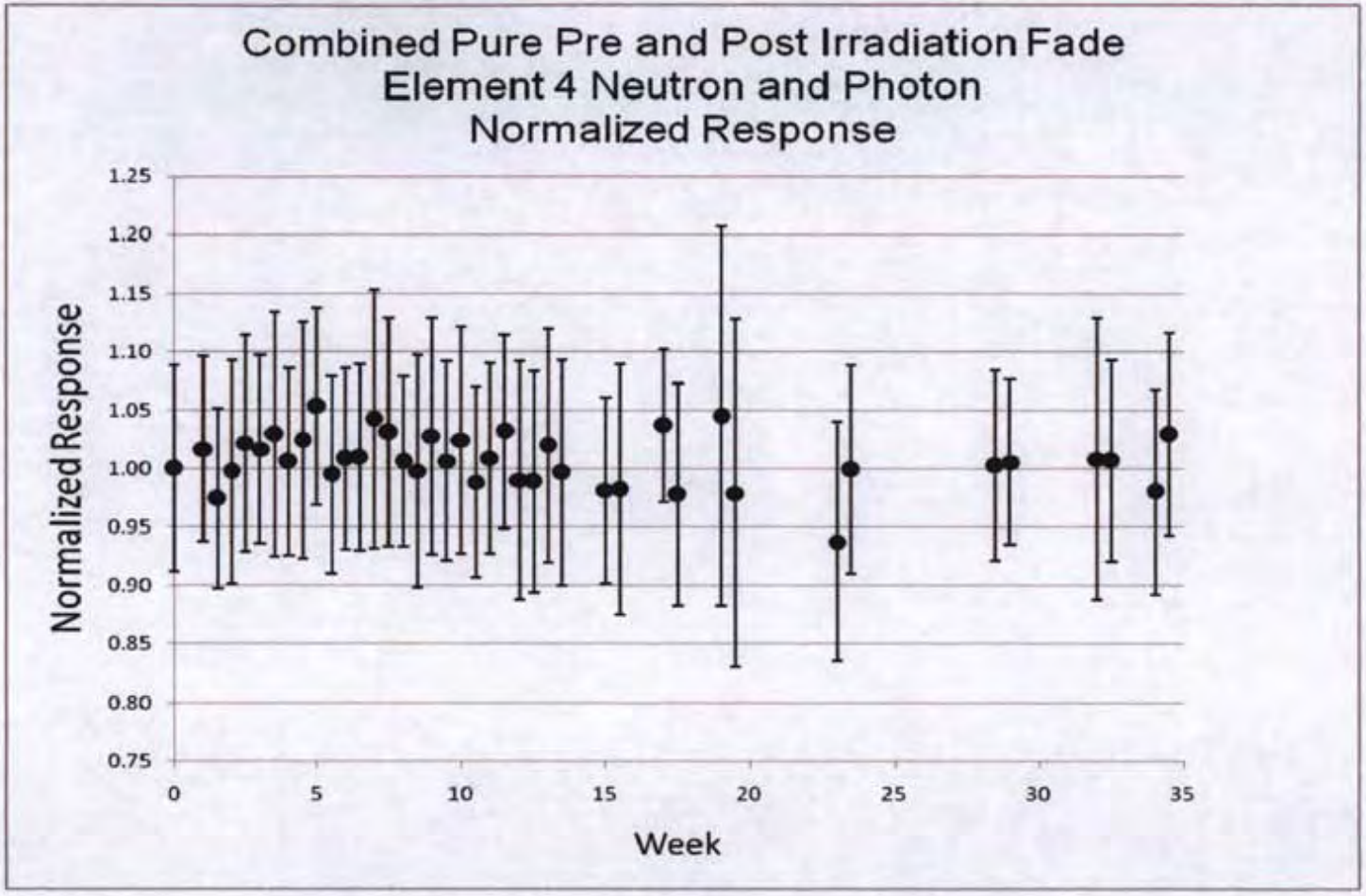

Figure 20. The plot displays the trend for Element 4 pure pre and post neutron and photon normalized response over a 34 week period. The error bars indicate the propagated errors for the mathematical manipulation (1σ).

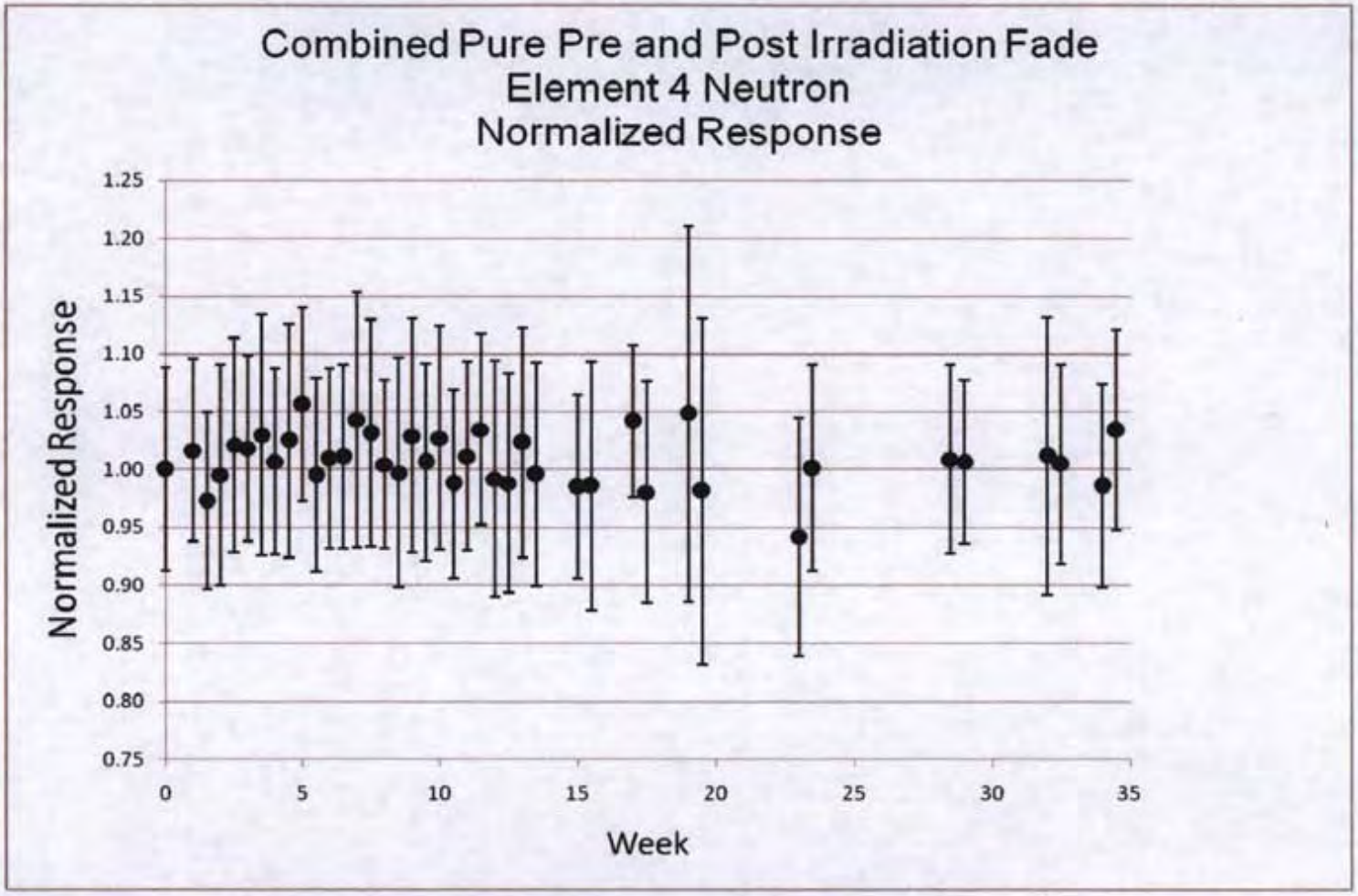

Figure 21. The plot displays the trend for Element 4 pure pre and post neutron normalized response over a 34 week period. The error bars indicate the propagated errors for the mathematical manipulation (1σ).

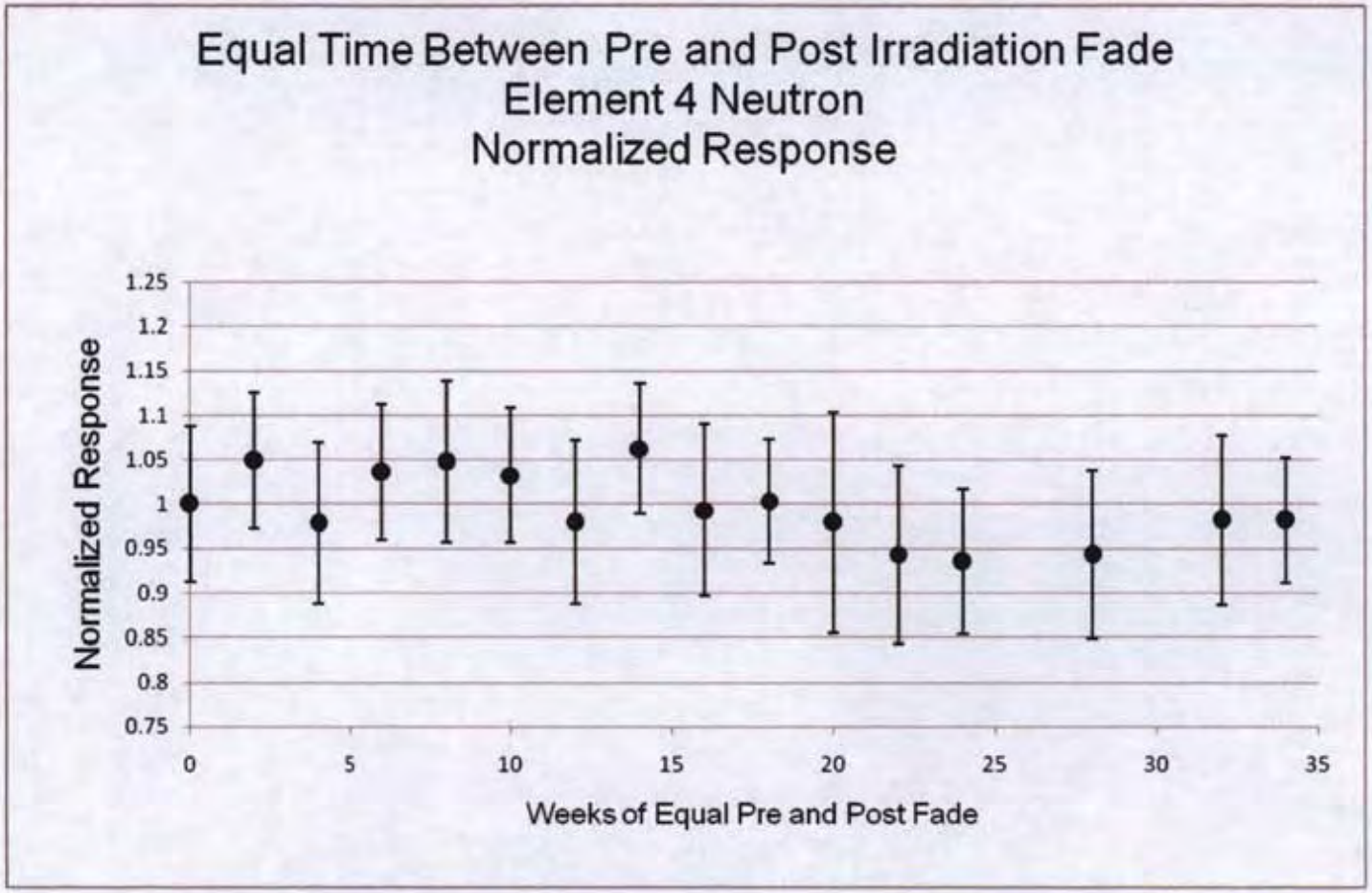

Figure 22. The plot displays the trend for Element 4 equal time between pre and post irradiation fade for neutron and photon normalized response over a 34 week period.

The error bars indicate the propagated errors for the mathematical manipulation (1σ).

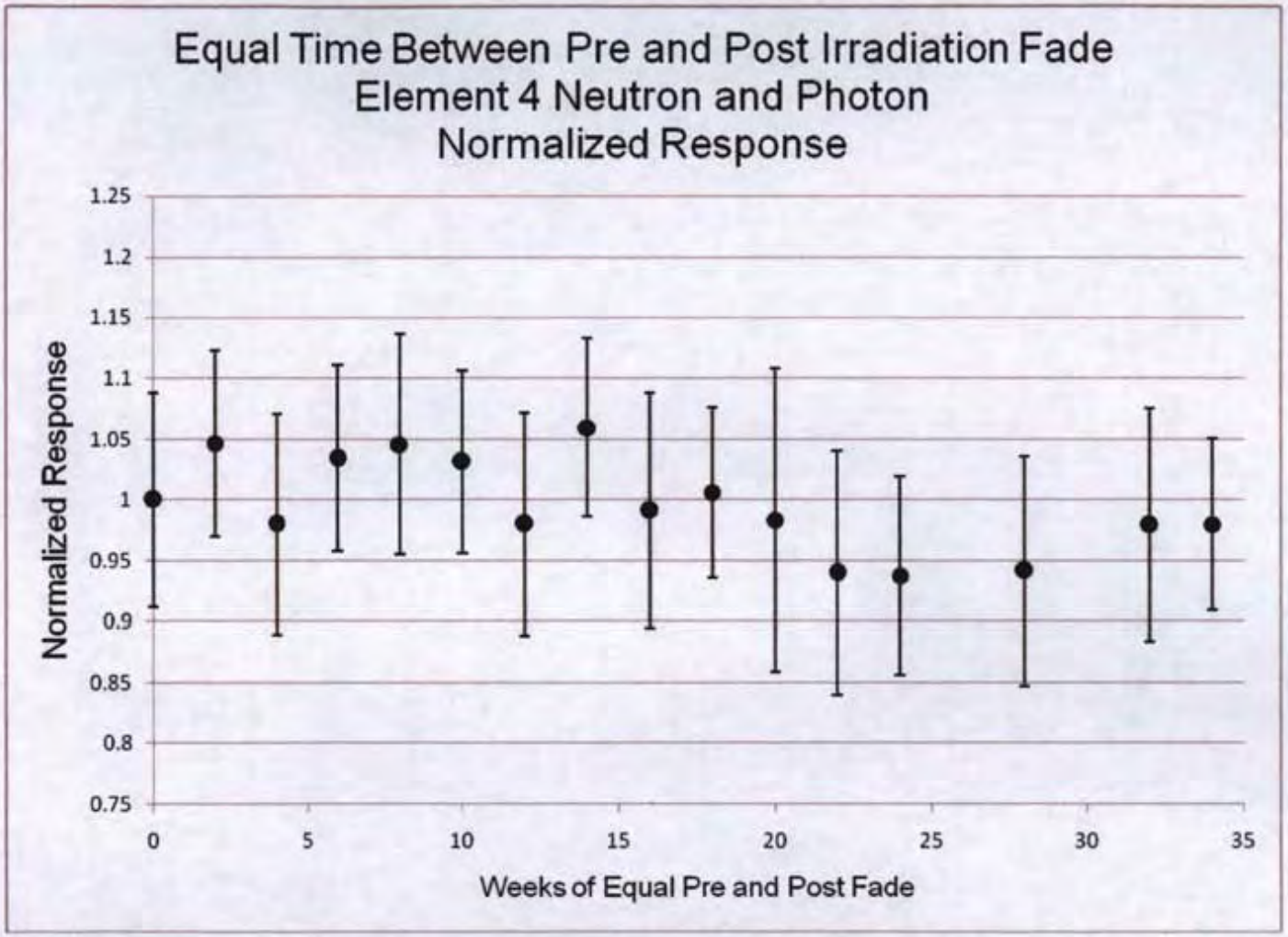

Figure 23. The plot displays the trend for Element 4 Equal time between pre and post irradiation fade for neutron normalized response over a 34 week period.

The error bars indicate the propagated errors for the mathematical manipulation (1σ).

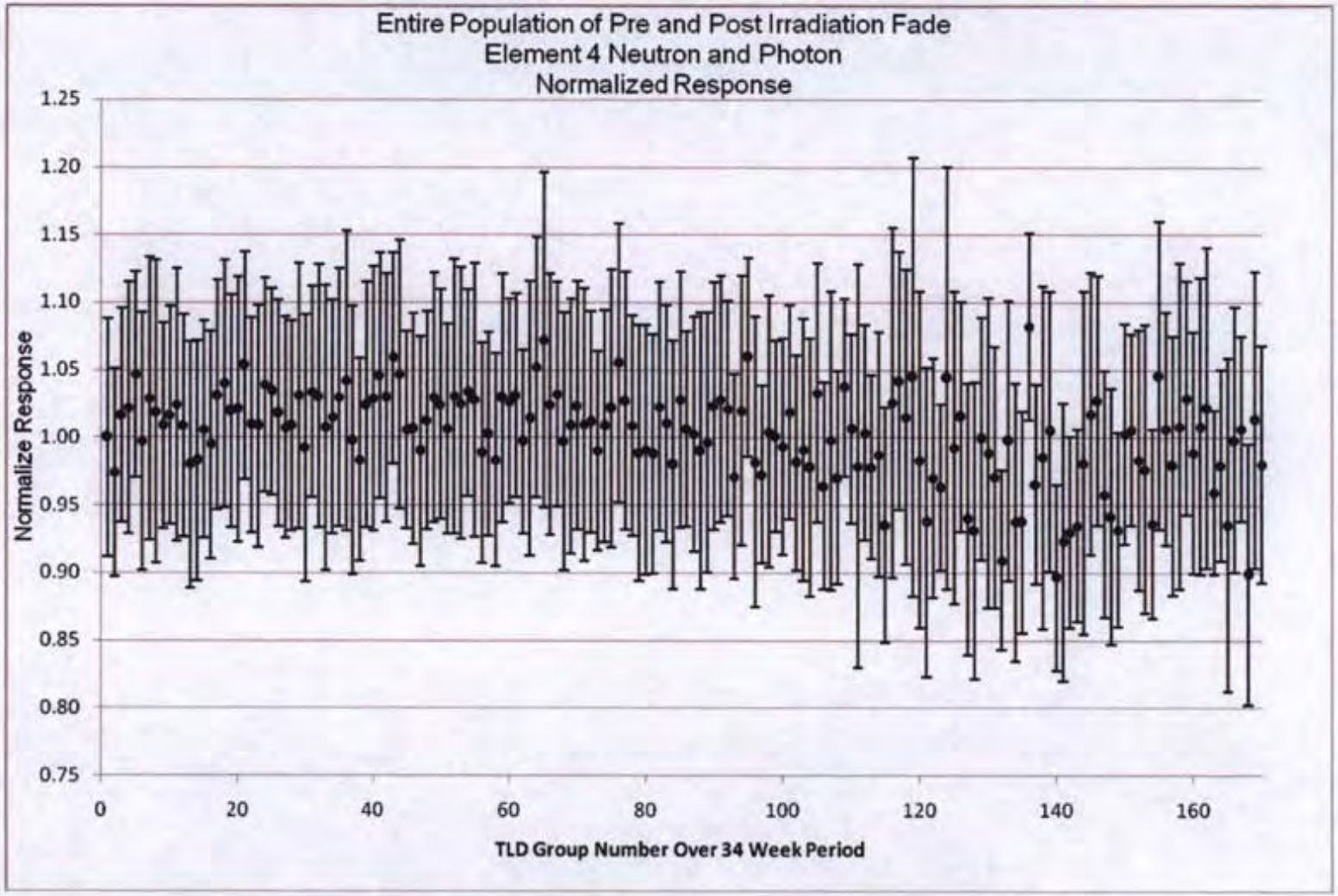

Figure 24. The plot displays the trend for Element 4 entire population of pre and post irradiation fade for neutron and photon normalized response over a 34 week period.

The error bars indicate the propagated errors for the mathematical manipulation (1σ).

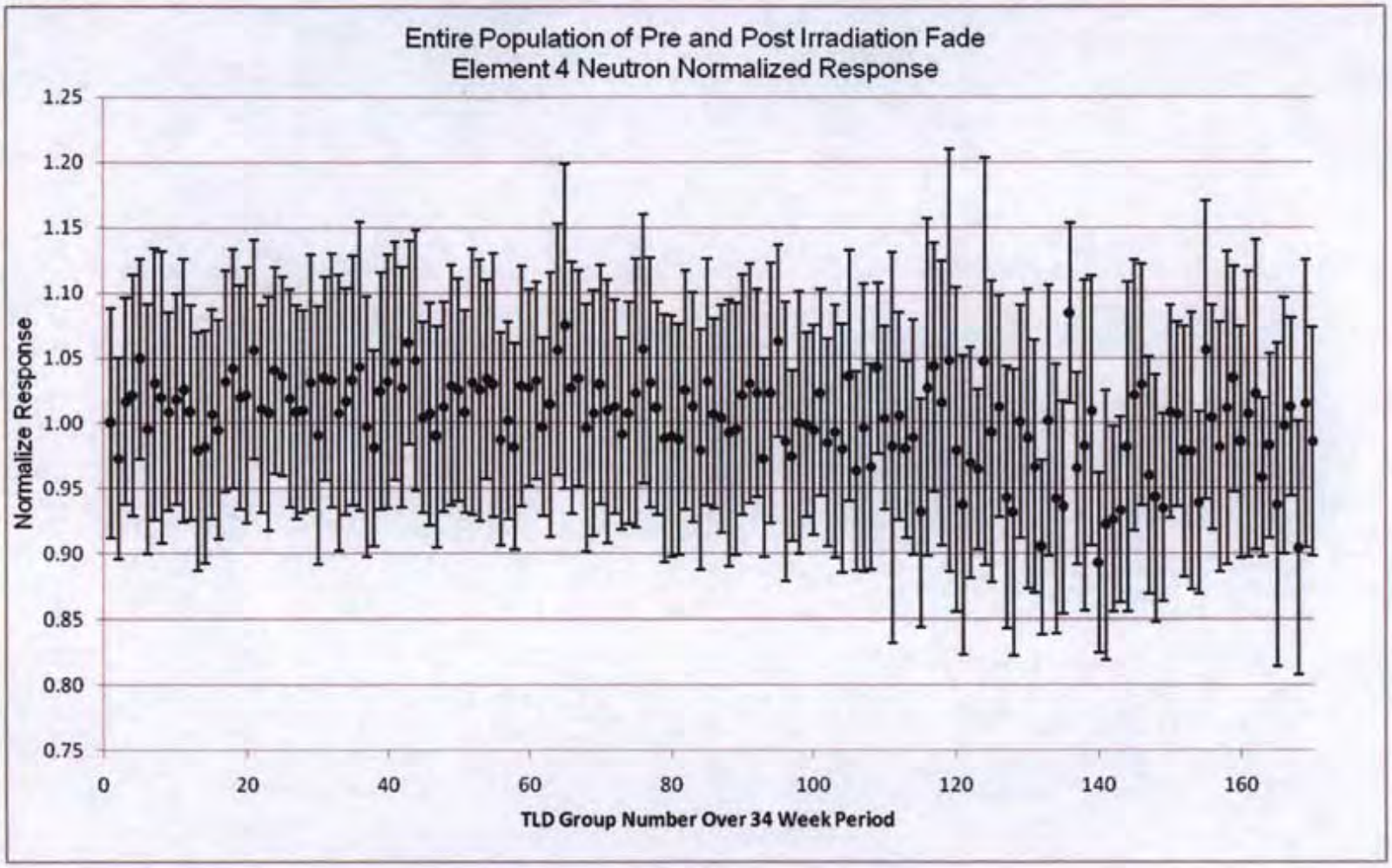

Figure 25. The plot displays the trend for Element 4 entire population of pre and post irradiation fade for neutron normalized response over a 34 week period.

The error bars indicate the propagated errors for the mathematical manipulation (1σ).

PRE-EXPOSURE FADE	POST-EXPOSURE FADE																																						
WEEK	0	1	2	3	4	5	6	7	8	9	10	11	12	13	14	15	16	17	18	19	20	21	22	23	24	25	26	27	28	29	30	31	32	33	34
0	1.03	1.03	0.98	0.97	0.98	1.01	0.99	0.97	1.00	0.99	1.01	0.97	1.01	1.00		1.02		0.96		0.96				1.00						0.99			0.99		0.97
1	0.98	0.96	0.96	0.99	0.97	0.99	1.01	1.02	1.01	1.00	1.00	1.01									1.01						1.03							0.97	
2	1.00	0.99	1.02	0.96	0.96	0.97	0.96	0.99	1.02	0.99	1.01			0.96				0.99																	
3	0.98	1.02	0.96	0.97	0.97	0.97	0.97	0.97	0.98	0.98	0.96								0.96																
4	0.99	0.98	0.96	0.99	0.96	0.98	0.97	0.99		0.98		1.01								1.01				1.07							1.01				
5	0.98	0.99	0.96	0.97	0.99	0.97	0.99	0.99					1.03		0.96						0.92														
6	0.99	0.97	0.94	0.97	1.00	1.01	1.02			1.03																									
7	0.96	0.96	0.96	0.99	0.99			0.94			1.00		0.97						1.04									0.99							
8	0.99	0.97	0.96	0.96	0.97	0.96			0.98											1.02															
9	0.99	0.96	0.97							0.96			1.04		1.03						1.02														
10	0.96	0.97	0.99			1.00					1.02					1.01									0.99									
11	0.99	1.03	1.03				1.04		1.07									1.04																	
12	1.01												1.07																						
13	0.98		1.02				0.98															1.04													
14				0.97				1.03				1.00			1.06																				
15	1.02																																		
16				1.02			1.10						1.07				1.02		1.02																
17	1.02		1.00								0.99																								
18																																			
19	1.02		1.07				1.12				1.02					1.07																			
20																																			
21																																			
22													1.00																						
23	1.07		1.06				1.07																												
24																																			
25										0.99																									
26				0.96																															
27																																			
28	1.00						1.11																												
29																																			
30																																			
31																																			
32	1.03		0.99																																
33																																			
34	1.03																																		

Table 4. The table indicates the normalized results of pre and post exposure fade versus time.

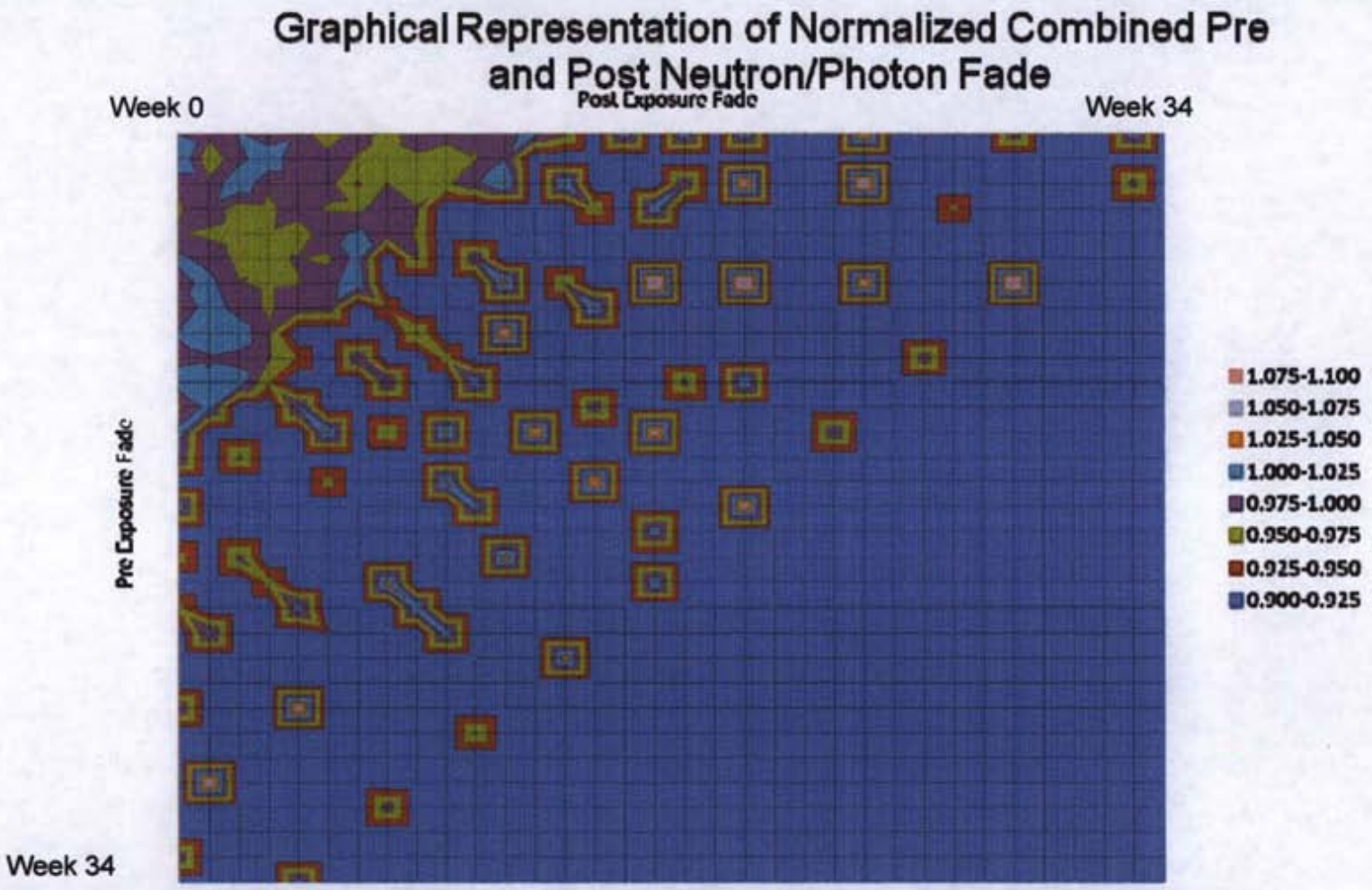

Figure 26. The graph indicates the normalized results of pre and post exposure fade versus time.

CHAPTER FIVE: DISCUSSION AND CONCLUSION

Discussion

The goals and specific aims of this research have been achieved and the data from the study, after a thorough statistical evaluation, provide the fading characteristics as a result of neutron irradiation for the LiF: MCP TLD (DT-702/PD) over a 34 week period of time. It is well established that the photon fade for this material is low, and it comes as no surprise that the results of this study reveal the same findings. Specifically, the results of the study showed no appreciable fade over time and with measurements staying within acceptable limits required for personal monitoring.

Comparison of results to previous studies

Only one other study, performed by Jones et al. [5], has been performed on neutron fading characteristics on the same TLD material for a prolonged period of time. The results of the current study differed in that there was no statistically significant observed fade. The results of the data did identify slight variations over time, although the one-way ANOVA revealed no statistically significant difference over the entire 34-week period.

Other differences between the two studies performed were specific trends in the data. For pre-exposure fade on Element 4, the Jones et al. study showed a significant increase in sensitivity for photon and neutron after 60 days at room temperature (~5%). Additionally, decreases in sensitivity (pre-exposure time) of 5% were seen after 164 days of storage at room temperature and post-exposure signal increases were observed for photon and neutron, with maximum increases of 6-8% for room temperature storage for 30 days. No significant change in

signal was recorded after 164 days at room temperature.

Jones et al. also evaluated neutron information by subtracting the reading of Element 2 (gamma) from the reading for Element 4 (gamma and neutron). A correction factor was also determined and applied to account for the differences in the filter materials for each element in the TLD holder. For the neutron evaluation, the gamma response of Element 4 was assumed to be identical to the gamma response of the TLD-700H material (Element 2). The neutron response of the TLD-600H element did not show the initial increase in sensitivity for pre-exposure storage.

Comparing the results from the current study with those of Jones et al, there was no increase in signal for pre or post fade compared to the increases seen in their study. This may be explained by the larger sample size and frequency of TLD processing that was used in this study. In this study over 170 sets of TLDs were used over the 34 week period compared to only of 6 sets of TLDs over a 24 week period used by Jones et al. Additionally, the number of TLDs in each set was larger for the first 13 weeks of the study and for the pure pre- and post- fade groups, 15 compared to 5, respectively, which also increases the statistical power of the study.

Considering the overall pre and post exposure fade, the findings from this study differed from the data found by Jones et al. since there was no unique trend in the pre or post fade data in this study compared to the one seen in their study. This may also be explained by the sample size and statistical power of this study, further strengthening the fading characterization of the DT-702/PD dosimeter. By increasing the sample size, there is greater statistical power to

detect a true difference if one exists.

Public Health Ramifications

The goal of public health is to ensure conditions are satisfied to keep personnel in our society healthy.[60] The many areas of public health can be grouped into three core functions; assessment, policy development, and assurance. Radiation protection applies to all three core functions and is an essential part of occupational health and safety. Therefore, as a key component of public health, the basic foundation of radiation protection is to ensure that occupational personnel receive as low as reasonably achievable dose from ionizing radiation.

Ionizing radiation can be beneficial to our society in the improvement of health, welfare and productivity if used properly. If radiation is controlled improperly, it can have a detrimental effect to the public's health. The current philosophy of radiation protection is based on the assumption that any radiation dose, no matter how small, may result in human health effects, such as cancer and/or hereditary genetic damage. Consequently, in order to protect against these risks, the bedrock of a radiation monitoring program relies upon precise and accurate measurement methods when assessing an individual's dose.

As discussed in the previous chapters, several factors contribute to the accuracy and precision of radiation dosimetry. The sensitivity, dose and energy response, LLD, and fading characteristics are all examples of key characteristics of dosimeters. It was shown that the fading of the LiF: MCP dosimeter exhibits no neutron fade over a 34 week period and the results of this study provide a better insight into the signal and sensitivity response of the dosimeter. As a

result, by applying this finding to radiation protection as a whole, an improvement in personnel dose monitoring and an overall benefit in the safety of workers can be realized. Finally, the improvement provides a direct impact to public health significance by providing an overall improvement to the safety personnel who are monitored for ionizing radiation.

Military Considerations

It is currently the Navy's policy to maintain personnel radiation exposures as far below Navy radiation protection standards as practicable. Current Navy radiation protection standards are consistent with or more stringent than those of the Environmental Protection Agency, Nuclear Regulatory Commission and the Occupational Safety and Health Administration. The Navy maintains one of the largest radiation monitoring programs in the world. At the forefront of the Navy's radiation monitoring program is the ability to provide the highest confidence in personnel monitoring.

The Naval Dosimetry Center processes approximately 20,000 dosimeters per month. [4] In addition to processing, the Navy maintains a historical database of all personnel monitored. The purpose for such accurate tracking of personnel radiation exposure stems from the legal responsibility associated with radiation protection. In some cases, inquires have been made from the Department of Veterans Affairs concerning potential radiogenic cancer compensation cases. In addition to compensation concerns, the Dosimetry Center is occasionally tasked with providing historical personnel doses to ongoing radio epidemiological studies. Both of these compensation cases and studies require accurate and precise personnel radiation doses. With this strong

radiation monitoring program, the Navy has demonstrated that the majority of cancers appearing in their present and former radiation workers were not caused by occupational exposure to Navy radiation sources.

The importance of having such a program cannot be overstated. Therefore, the Navy is continuously striving to improve its ability to accurately monitor its personnel and with advancing technology, the Navy adopts new methods for an already sound program. The ability to further characterize its current technology also provides the latitude to increase its productivity and provide even more accurate results. This study has identified that for the Navy's current dosimeter, there is no neutron fading over the course of 34 weeks. Along with the potential for improved accuracy, the benefits of this finding also allow for improved cost savings associated with the processing of the TLD as well as better operational flexibility. Once again, by understanding the characteristics of this dosimeter, the findings in this research provide for an overall improvement in the ability to monitor the personnel in the military.

Cost Considerations

Approximately 240 commands in the US Navy ship and receive TLDs every 6 weeks at a cost of approximately $8.00 a shipment (typical domestic shipping, international rates higher). Thus, the Navy spends on average $33,280.00 each year to send and receive TLDs. If six-month issue periods were permitted, this cost would drop to around $6,400, saving the Navy around $26,880 per year. These calculations do not take into account several other factors that include:

- Increased errors associated with documentation of personnel

exposure

- Potential cost incurred from lost or damaged TLDs in shipment
- Cost incurred for additional numbers of TLDs needed to be processed

By having to exchange TLDs every 6 weeks compared to every 24 weeks, for example, you are likely to have 4 times as many errors associated with the transcription of personnel exposure data. This is because accurate exposure data is one of the critical attributes of a sound dosimetry program, reducing the potential for error is an important reason for extending issue periods.

The cost of a one DT-702/PD card is approximately $50.00. Considering even the smallest commands receive at least 10 TLDs, losing a shipment would result in $500.00 in replacement costs. Additionally, this would result in lost personnel exposure history requiring timely and costly investigations to recapture these data. The ability to accurately and reliably measure the dose of personnel exposed to occupational radiation is a key component of the Navy's dosimetry program.

By reducing the total number of TLDs that are being circulated, you would also achieve a reduction in processing cost. This has a far reaching effect as there are many factors involved in processing TLDs. These factors range from reducing the nitrogen consumption, reducing the number of TLD readers required, less wear and tear on the readers, less expensive maintenance contracts, and timelier processing results. Additionally, the number of man-hours required to operate the machines would be significantly reduced providing an overall reduction in operating costs of tens of thousands of dollars.

Conclusion

In conclusion, the DT-702/PD TLD has been shown to have no significant change in sensitivity or signal response with up to 34 weeks of pre-exposure, post-exposure, or combination of pre-exposure and post-exposure time. Currently the DT-702/PD TLDs are normally issued for eight-week periods, with a 12-week maximum for special circumstances. The data presented in this study indicate that an evaluation of extending the issue periods beyond these current limits may be warranted when evaluating issue periods, environmental conditions need to operational conditions should coincide with the ones established by this study design.

CHPATER SIX: FUTURE STUDIES AND LIMITIATIONS

Future Studies and Limitations

The response of the DT-702/PD through 34 weeks has been shown to have no statistically significant change in sensitivity or signal response. Although this study provides significant insight to the unique properties of this material, several improvements in the fade study design were realized that could have made the study even more valuable.

One of the goals of this study was to perform an analysis of the differences in neutron fade characteristics compared to that of photons. Although we saw no statistical differences in the outcome of the data, this analysis could have been improved upon by exposing the TLDs to a photon source, such as Cs-137 or Co-60 to increase the signal contribution from photons.

Although the study period lasted for 34 weeks, which is far longer than any previous study, the study period should be extended until the fade results in a statistically significant difference. This longer observation time would determine how long the TLD could be used before a statistically significant change in sensitivity or signal response can be detected.

Additionally, to effectively apply the results of this study to an operational environment, an extensive study should be conducted on the LLD for the DT-702/PD dosimeter. In order to increase issue periods, further studies are needed to determine if the current LLD (3 mrem for shallow dose, 3 mrem for deep dose, and 5 mrem for neutron dose)[4, 26] will remain accurate with the increased

background reading associated with the longer issue period. The higher the background level, the less likely one will be able to detect a small increase in response from the dosimeter.

APPENDIX A: AN IN-DEPTH LOOK AT LIF: MCP DOSIMETRY

The wide spread use of LiF: MCP has increased over the past two decades as the popularity of this highly sensitive material is becoming the new standard in dosimetry. Although, prior to LiF: MCP, the original LiF: MT, made by the Harshaw Chemical Company before 1954, was the workhorse of personnel dosimetry. LiF, with its low atomic number and simple cubic lattice, as seen in Figure 27, was one of the first phosphors to become commercially available for personnel dosimetry applications. This phosphor has many good performance characteristics including near-tissue-equivalent response, unaffected (relatively) by environmental conditions (i.e., humidity, normal working temperatures, etc.), and linear dose response at occupational dose levels.[16]

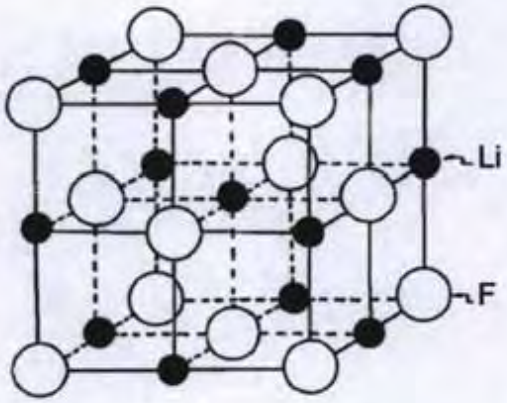

Figure 27. Figure Identifies the Crystal structure of LiF. Used with permission of the publisher [2]

In 1984 Solid Dosimetric Detector & Method Lab (Beijing, China) prepared LiF: MCP in a solid form that produced an even higher sensitivity than the powder form.[25] In order to determine the annealing program for reuse, temperatures between 150° C and 270° C were tested and experimental results showed that the optimum temperature for reuse was 240° C for 10 min.

Types of TL Materials in use

There are many types of TL materials and, for the most part, they can be divided into two categories. One type has good tissue equivalence but relative low TL sensitivity such as LiF: MT (TLD-100). Tissue equivalence is a term used in radiation protection for substances that closely matches biological tissue when comparing its absorbing and scattering properties. It is desirable to have a dosimeter with a close tissue equivalence so direct comparisons of energy deposition can be made without having to perform complex corrections. The other type has high TL sensitivity but poor energy dependence such as $CaSO_4$ and CaF_2. A brief summary of the types of TL materials are listed in Table 5.[3]

The introduction of LiF: MCP has made it possible to have both of these important characteristics, high sensitivity and excellent energy dependence. This

TL Material	Type	Useful Range	Thermal Fading
LiF:Mg,Ti	TLD-100	10μGy-10Gy	5-10% per year
LiF:Mg,Cu,P	TLD-100H	1μGy-20Gy	3% per year
^{6}LiF:Mg,Ti	TLD-600	10μGy-20Gy	Negligible
^{6}LiF:Mg,Cu,P	TLD-600H	Neutron Sensitive 1μGy-20Gy	Negligible
CaF_2:Dy	TLD-200	0.1μGy-10Gy	16% total in 2 weeks
CaF_2:Mn	TLD-400	0.1μGy-100Gy	15% total in 3 months
Al_2O_3:C	TLD-500	0.05μGy-10Gy	3% per year

Table 5. The table displays the various Types of TLD Materials and properties. Used with permission of the publisher. [3]

enables its widespread use in several areas including clinical, personal, and environmental dosimetry.

Composition

LiF: MCP dosimeters are composed of a Lithium (Li) Fluoride (F) crystal structure with Magnesium (Mg), Copper (Cu) and Phosphorous (P) dopants. The Mg dopants play a role in the electron-hole pair trapping action of the crystalline structure, while the P is related to recombination sites in the crystal.[2] The Cu appears to play a role at both the trapping sites and recombination sites; however, the precise TL characteristics of this material are unknown.[61-63] The combination of this TL material and associated dopants give this dosimeter, much like its predecessor LiF: MT, an effective atomic number (Z_{eff}) of approximately 8.14. [2] When Z_{eff} of LiF: MCP is compared to that of soft tissue ($Z_{eff} \approx 7.4$) it has a much closer tissue equivalence than high Z_{eff} dosimeters such as CaF_2: Mn (Z_{eff} 16.3) or $CaSO_4$ (Z_{eff} 14.3), which is an important attribute for dosimetry. (Miljanic, *et al.*, 2002).

LiF: MCP powder has been analyzed with the X-ray diffraction technique.[64] Samples with different dopant concentrations were prepared for the experiments. Experimental results done on testing of the reproducibility of the material showed that the stability of LiF: MCP material depended on the dopant compound, specifically the dopants concentrations in the preparation procedure. The existence of $Li_4\ P_2\ O_7$ influenced the thermal treatment characteristics of the material. The more $Li_4P_2O_7$ that was in the crystal resulted in a greater loss of TL sensitivity after thermal treatment. Additionally repeated testing of the samples changed with different preparation procedures, although the impurity did not change the lattice constants.

It has been seen that the composition of LiF: MCP is very complex and by adjusting the dopant concentrations, there is a direct effect on the dosimeters characteristics. Additionally, the glow curve is dependent upon these concentrations.

Glow Curve Structure

When the LiF: MCP is heated from room temperature to 400° C six peaks exist. [65, 66] A small peak at about 480° C appears only after irradiation to very high doses.[67] Figure 28 provides an example of the six glow curves found in LiF: MCP. [68]

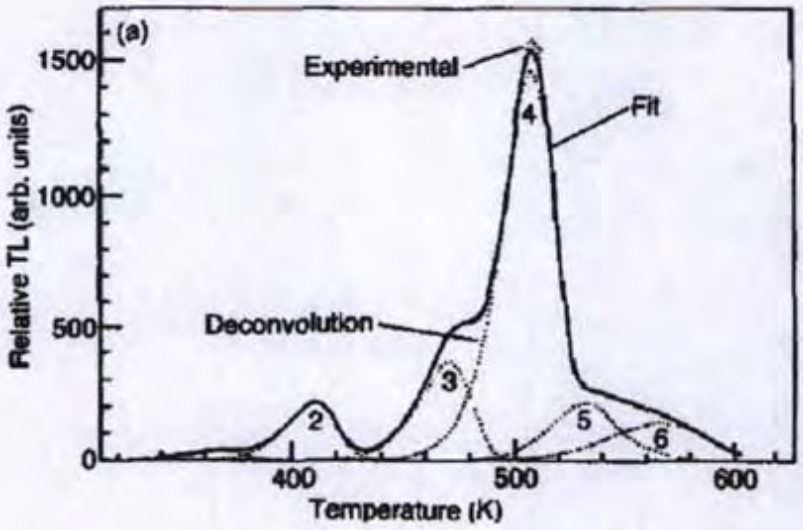

Figure 28. The figure Identifies a GR-200A (LiF: MCP) glow curve Obtained by means of linear heating rate of 2.5 ± 0.1K.s^{-1} for a readout time of 135s from room temperature to 643 K. Used with permission of the publisher. [68]

The glow curve shape of LiF: MCP varies with different dopant concentrations and thermal treatments.[34, 69] For example, with increasing Cu concentration, peaks 2, 3 and 4 increase but peak 5 decreases. [69] The glow curves of LiF: MCP can also be changed by different thermal treatments. Annealing at lower temperatures will result

in glow curves that are different from those annealed with the recommended time temperature profile (TTP) which has an initial preheat of the TLD to 165°C for 10 seconds to followed by a 16.67 second acquisition time, where heat increased at a rate of 15°C/sec to a maximum of 260°C.[34, 69] Research has been done to stabilize the glow curve shape, obtain better repeatability by improving the preparation procedure and develop an annealing program that reduces the relative height of the higher temperature peak.[53] This high temperature peak is responsible for the residual signal and reproducibility.

The specific glow curve structure of the DT-702/PD dosimeter is shown in Figure 29. In this case, a DT-702/PD dosimeter was irradiated to 50 mSv (5 Rem). The

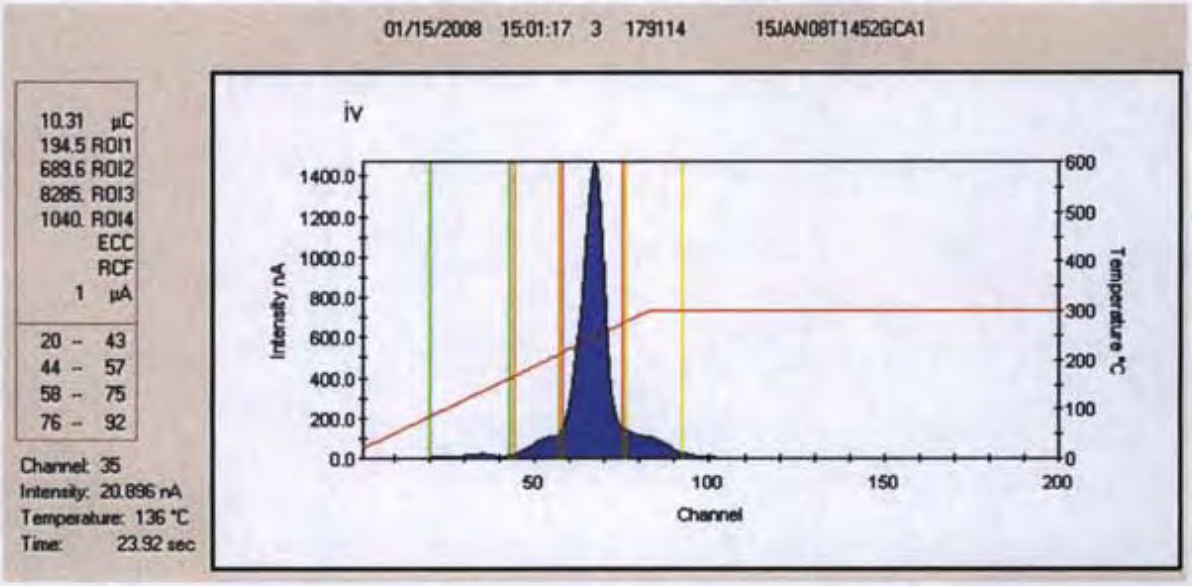

Figure 29. DT-702/PD Dosimeter Example Glow Curve, image was extracted from Thermo-Fisher WinRems operating on a Model 8800 Harshaw TLD Reader.

dosimeter was read as soon as possible after exposing to the Sr/Y-90 source and the heating profile used was 5 °C/sec to 300 °C for 135 s. Peaks 1 and 2 can be clearly seen. Peaks 3 and 4 fall under the main dosimetric peak and peak 5 is visible at the tailing end. Peak 6 is not visible due to the annealing temperature being less than 480°C and the low irradiation value.

Emission Spectra

The emission spectrum for LiF: MCP is shown in isometric form in Figure 30.[2] The main emission appears at about 370 nm with a long, low wavelength tail centered around 410 nm. [2]

Experimental results have shown that the higher temperature peak corresponds to a slightly shorter wavelength than that of dosimetric peak.[70] With varying concentrations of dopants, the TL sensitivity and the glow curve shape can change significantly, but has little effect on the emission spectrum. Additionally, experimental results have shown that with different thermal treatments, the emission spectrum is not affected though changes in the glow curve shape can occur.

Energy Response

LiF: MCP has shown an energy dependence under-response around the 80 keV of about 20%. Over-response of the energy dependence can be filtered to correct the response. In order to correct for an under response you must alter the crystal. In principle this material is tissue-equivalent and needs no correction for X-rays and gamma rays except in some special cases.[26] For beta particles, the energy response is dependent on the grain size of the material.[71]

The distribution of the mean activation energy of LiF: MCP obtained with a fractional glow technique (FGT) has shown that the activation energy at the main dosimetric peak is the deepest one.[72] This result is different from other TL materials. Since the peak responsible for the dosimetric peak is deeper than other traps, it is expected to have a

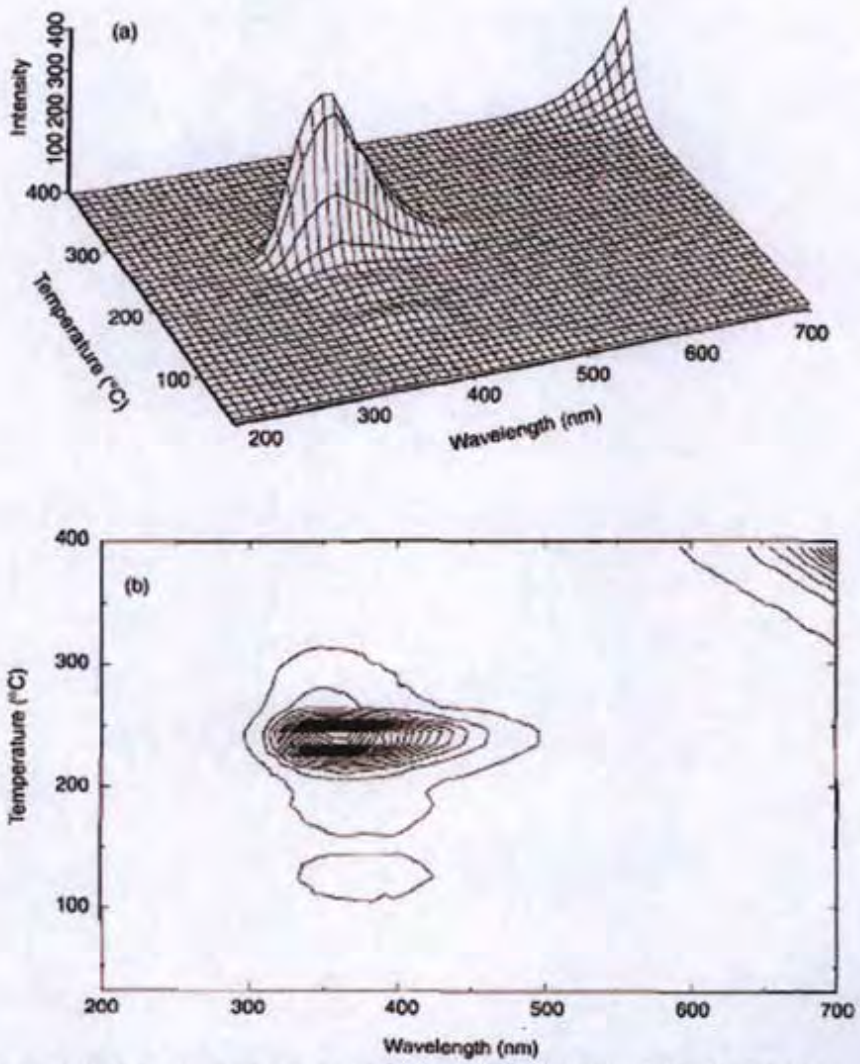

Figure 30. The image displays an isometric plot of the thermoluminescence emission from LiF:Mg,Cu,P Used with permission of the publisher. [2]

better stability. Additionally, the deeper trap has a higher probability of trapping charged carriers, which is one of the reasons why this material has such a high TL sensitivity.

The kinetic parameters have also been studied with various methods. The glow curves were deconvolutioned with a program based on the first order kinetic equation. With this program the behavior of the individual peaks can be analyzed.[20, 50, 73]

Isothermal decay technique has also been applied to analyze the kinetic parameters of LiF: MCP.[74-76] The value of the activation energy of peak 4 is close to the value obtained with fractional glow technique (FGT). The experimental results also showed that for LiF: MCP peak 4 (the dosimetric peak) corresponds to a very stable trap whose structure is not affected by the thermal treatment. This is an important advantage for the use in some dosimetric applications such as environmental monitoring, where the dosimeter is exposed for a long time at uncontrollable ambient temperatures.

The optical absorption and reflection measurement were studied in LiF: MCP powder and the single crystal.[77] The results showed that the absorption band is dependent on the thermal treatments of the material. The absorption from the material after irradiation of powder was similar to the behavior of single crystal. Thermoluminescence emitted from LiF: MCP samples is due to the presence of precipitate phases that also cause the different energies of absorption band of Mg-related defects.[2]

Dose Response

The linear range for LiF: MCP can be up to 10-15 Gy. For doses higher than 10 Gy, the TL response can decrease with the dose, i.e. shows a sublinear response.[78]

The linearity is highly dependent on the dopant concentrations.

For example, the LiF: MCP material produced by the Solid Dosimetric Detector Methods Laboratory SDDML in Beijing, China shows a sub linear response at about 12 Gy.[73] Italian scientists have effectively measured the dose response of GR-200, another form of LiF: MCP, up to a linear range of 18 Gy.[68]

The dose response is dependent on many factors including dopant concentrations, grain size and thermal treatments. Results have shown that LiF with only Mg as the dopant has supralinear dose response. When adding the second dopant, copper, the dose response becomes sublinear.[79] By adjusting the dopants in the same LiF host crystal, you can achieve a different dose response.[65] In another study, four groups of grain sizes of LiF: MCP material was used and the influences of the grain size on the photon dose response were tested in the dose range 0.1-30 Gy of Co-60 gamma -rays. The experimental results showed a dose response dependency on the grain size.

Traditional models used to explain the dose response of TL materials cannot explain the unique sub linear response of LiF: MCP. One explanation that has been proposed is that there exists one non-emission competitive center, which influences the dose response of the TL material.[80] From this model either supralinear or sublinear are the unique cases of the variation of the intrinsic parameters in a certain range. Studies have shown that this theoretical model agrees with the experimental results. [81]

Radiation Damage

As the material is irradiated to doses exceeding 20 Gy the relative TL response

decreases rapidly and has been regarded as radiation damage. Permanent damage can occur if the irradiation dose is significantly high.[62] Damage will result in abnormal glow curves. It is proposed that the damaged carrier traps are similar to that of radiation damage. It has been shown that when annealing at high temperatures that the radiation damage can be recovered.[31]

LiF samples have been irradiated up to one million Gy and when exposed to a very high doses, the color changes, from white to yellow up to brown color.[82] In this case, the self-absorption is severe and the material is badly damaged. For LiF: MCP, the lower temperature peaks are more easily damaged than higher temperature peaks in that case the residual signal cannot be eliminated when annealed. After annealing at 240° C for 10 min the color of the crystal was partially recovered, and after annealing at 400° C the color was recovered to white, the normal color, but the TL sensitivity was very low and unable to be restored with normal annealing program.

It has been well established that at temperatures above 240°C, LiF: MCP TL sensitivity is lost.[26, 29, 54] In an interesting study, it was found that after annealing at 320°C for 10 min that the sensitivity reaches its minimum value and the degradation of sensitivity due to temperatures above 240°C may be reversed partially by re-annealing at 240°C.[33] It was also seen that after annealing at 720°C for 30 min, the TL sensitivity of the material annealed at temperatures above 240°C can be restored completely and the glow curve structure can also be recovered.[83]

Basic Principle of Thermoluminescence

Luminescence is a general term used to explain a process where light is emitted from a material that is not due to incandescence, where incandescence is the emission

of light, both the infrared and visible range, due to its heating to temperatures near the melting point. Luminescence usually occurs at much lower temperatures than incandescence. It should be noted that there are many types of luminescence including;

- chemoluminescence (bioluminescence), which results from a chemical or biological reaction
- crystalloluminescence, which results during crystallization
- electroluminescence (cathodoluminescense), which results in a material emitting light in response to an electrical current passing through it
- mechanoluminescence (triboluminescence, piezoluminescence), which results in light emission resulting from any mechanical action such as stress, sound, or pressure
- photoluminescence (phosphorescence, fluorescence), which results in light emission when a substance absorbs photons and re-radiates them
- radioluminescence, which occurs when a material that luminescent is bombarded by ionizing radiation, such as beta radiation, and gives off light
- sonoluminescence, which occurs when sound waves of sufficient intensity acts upon a gaseous cavity within a liquid to quickly collapse and resulting in light emission.

In each of these cases, a reaction is taking place to induce the light emission. Thermoluminescence (TL) or thermally stimulated luminescence is the emission of light during the heating of a solid sample (insulator or semiconductor), previously excited by ionizing radiation. For this phenomenon to occur, three requirements must be met:[9]

- The material must be an insulator or semiconductor

- The material must have absorbed energy during exposure to ionizing radiation
- The luminescence of the material occurs by heating the material.

TL material absorbs energy during exposure to radiation (ionizing, visible light, UV etc.) and stores this energy until heated. The intensity of the light that is emitted as a function of temperature is known as the thermoluminescence glow curve. Usually the heating rate is constant, and therefore the glow curve is often shown in the literature as the TL intensity as a function of the time of the measurement cycle or the channel number instead of the temperature. In order for a dosimeter to be effective and establish a means to quantify dose, the relationship must be known between the integrated area under the main dosimetric peak of interest between two temperature (channel/time) and the radiation dose.

Although the first theoretical explanation of thermoluminescence was submitted in the middle of the last century, there is no universal theoretical model that includes every dosimeter. The most widespread theoretical explanation of thermoluminescence is based on the electron band theory, which is thoroughly explained by Bos et al. [9] According to the simplest model, the one trap-one center model, in an ideal crystal the electrons occupy the valence bands, which are separated from the conduction band by the so-called forbidden band gap (Figure 31).[2] Crystals can have various defects as a consequence of ionizing radiation or from impurities in the lattice. In both cases the electrons can possess "forbidden" energies.[9]

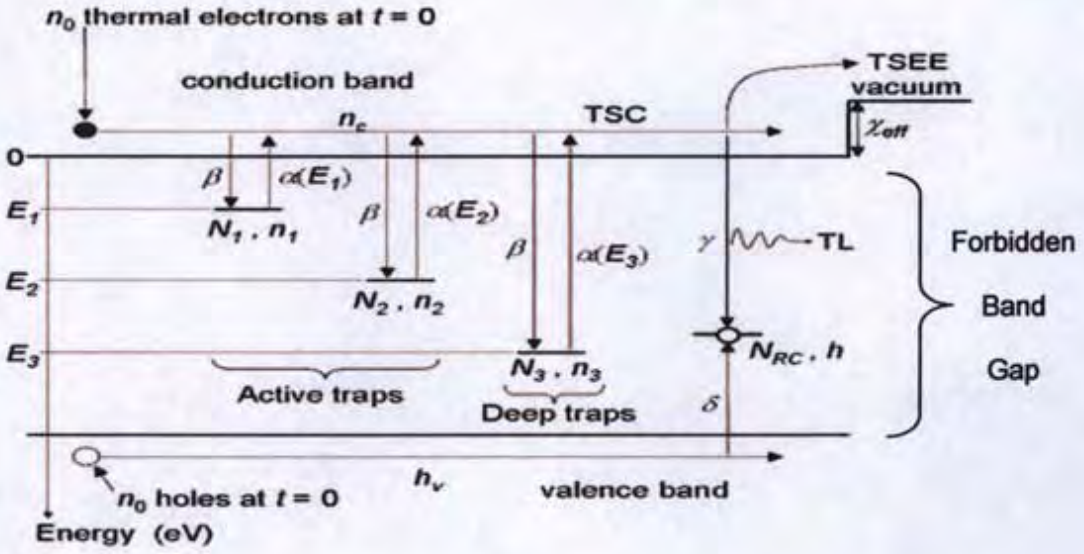

Figure 31. The diagram demonstrates the energy-level properties of the thermoluminescence process. Adapted with permission of the publisher.[84]

The excitation of electrons from the valence band to the conduction band may occur as a result of irradiation, while holes remain in the valence band. Some of the electrons and holes can recombine under emission of light (radioluminescence), while the others will be trapped at the level in the "forbidden" energy gap. The probability of the release of an electron from the forbidden band into the conduction band can be described by the Arrhenius equation. (Equation 4) [9]

$$p = se^{-E/kT}$$

Equation 8. Equation Identifies Arrhenius equation[9]

Where:

p= the probability per unit time (s, seconds)

s= the frequency factor (s^{-1}, $seconds^{-1}$, constant for the simple model)

E =the activation energy (eV, electron volts)

k= Boltzmann's constant (8.617 $\times 10^{-5}$ eV/K)

T= the absolute temperature (K, Kelvin)

Therefore, as the temperature (T) increases the probability (p) of recombination will also increase. The activation energy (E) is related to the energy difference between the trap and the conduction level. As the electron from the conduction level undergoes recombination with the hole in the recombination center that also functions as a luminescent center, causes a recombination accompanied by a light emission, or thermoluminescence (TL). The intensity of the TL (photons) is proportional to the recombination rate, or the concentration of free electrons in the conduction band and holes in the valence band.

The one trap-one center model can describe the shape of the TL glow curve by the intensity of the TL as a function of temperature, as well as the influence of charge concentration, heating rate and trap depth on the glow curve. The more realistic situation is even more complicated and TL can be found only by solving a set of simultaneous differential equations without any simplifying assumptions.[9]

APPENDIX B: AN IN-DEPTH LOOK AT NEUTRON DOSIMETRY

Neutron Dosimetry

Today, neutron radiation exposure exists where personnel are exposed including the nuclear fuel cycle, nuclear power generation, medical accelerators, where radionuclide sources are used and in aircraft and space travel. These neutrons have a large range in energies, from thermal, which is 0.0635 eV, to upwards of several MeV.

Along with these sources are neutrons that reach the earth from cosmic-rays. This is often overlooked and with better technology in neutron measurements, this has been better quantified in recent years. For example, a study performed by Nagaoka et al. used high-sensitive neutron dose equivalent counters with balloons to determine the neutron dose rates with increasing altitude.[85] The results showed a peak in neutron dose at 15 km and very low dose levels at ground level (Figure 32)[85] Doses are approximately 70 times less at sea level compared to those at an altitude of 20 km.[86]

In another recent study performed by Colgan et al. the individual dose to the public from cosmic radiation was evaluated.[86] The study concluded that at sea level, the dose from cosmic radiation varied from 36 nSv h^{-1} during a solar maximum to 44 nSv h^{-1} during a solar minimum and an average of 40 nSv h^{-1}. The contribution from neutrons is 10 nSv h^{-1}. This results in an average dose to the public of 0.0876 mGy/year or 8.76 mrem/year.

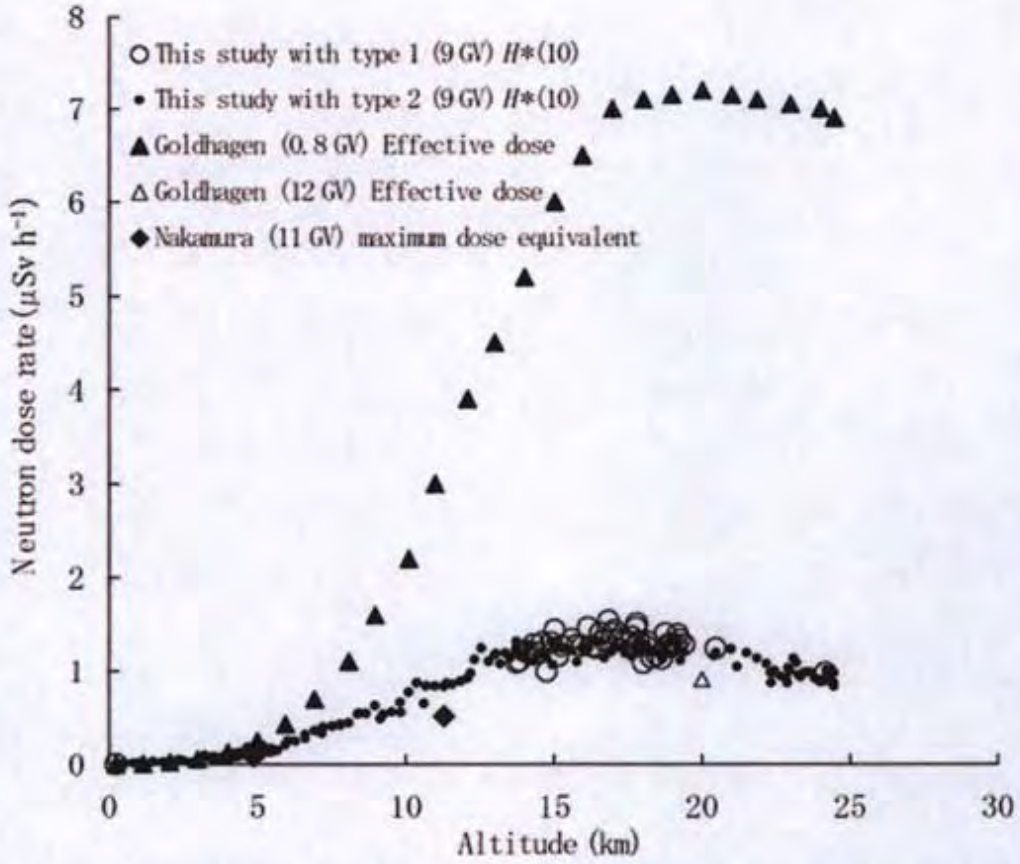

Figure 32. The graph identifies various neutron dose rates at various altitudes. Used with permission of the publisher. [85]

With such a wide range of energies, it is essential to have a dosimeter that can provide an accurate dose that is personal dose equivalent, H_p (10), to the large range of energies. This can prove to be difficult because it is often difficult to distinguish between neutron radiation and various other types of radiation. In this case, various methods must be applied when detecting neutrons.

Neutron Thermalization

All neutrons are born fast, that is at high energy (greater than 0.5 MeV), and they lose their energy by colliding with particles in their environment. A common analogy in

this slowing down process is much like billiard balls colliding and slowing down. Neutrons will slow down to "thermal energies" (.025 eV) that have the same kinetic energy as gas molecules and are indistinguishable from them. Table 6 provides a summary of the classification of energy levels used for neutrons.

Term	Foundation	Energy Range
Thermal	Neutrons that are in thermal equilibrium with the surrounding	Most probable energy at 20°C 0.025 eV Maxwellian distribution of 20°C extends to about 0.1 eV
Epithermal	Neutrons of energy greater than thermal	Energies above about 0.2 eV
Cadmium	Neutrons that are absorbed by cadmium	Energies below about 0.4 eV
Epicadmium	Neutrons that are not absorbed by cadmium	Energies above about 0.6 eV
Slow	Neutrons of energy slightly greater than thermal	Usually means less than 1-10 eV Occasionally means less than 1 keV
Resonance	Refers to neutrons that are captured in the resonance of U-238	A broad range of energies from about 1 eV to about 300 eV
Intermediate	Neutrons between slow and fast	From a few hundred eV to about 0.5 MeV
Fast		Neutrons of energy greater than about 0.5 MeV
Ultra Fast (relativistic)		Neutrons of energy greater than about 20 MeV
Pile	Neutrons over a wide spectrum of energies 'present in nuclear reactors	About 0.001 eV to approximately 15 MeV
Fission	Neutrons produced from fission	About 100 keV to approximately 15 MeV Most probable energy 0.8 MeV Average energy 2.0 MeV

Table 6. The table identifies the various neutron energy terminologies.

Thermalization occurs through collisions and is most effective when neutrons interact with low atomic numbered absorbers such as hydrogen. In a purely head on collision analysis, it can be shown that the energy transferred can be evaluated using Equation 9.

$$E = E_o\left(\frac{M-m}{M+m}\right)^2$$

Where

E_0= energy of the incident neutron (eV),

m= mass of the incident neutron (amu),

M= mass of the scattering nucleus (amu)

Equation 9. The equation identifies the energy transfer from neutron collisions

Therefore, if the masses of the neutron and target are the same (i.e. - hydrogen) you can have a complete transfer of kinetic energy occur. Though, if the target is much heavier, you will only have a fraction of the energy transferred. Collisions typically are not head on with the target; therefore less energy is transferred to the target.

Neutron Detection

It has been generalized that there are three methods used to effectively detect neutrons. [10]

- Have a physical (or chemical or biochemical) effect that has an increased efficiency at higher ionization density with the increase matching the required weighting factor.
- Have a detection system that determines both absorbed dose and an estimation of the weighting factor.
- Have a dosimeter or detector such that the reading (output) matches the neutron 'dose' function in terms of neutron energy.

Current neutron passive personal dosimeters follow the latter two approaches. Examples would be a tissue-equivalent proportional counter such as the Navy's AN/PDR-70 proportional counter, or a neutron etched track detector with a thermal plus

epithermal capture component and a fast recoil proton component.

It has been possible to characterize worker exposure to neutrons during routine operations at nuclear facilities by knowledge of the source, shielding and worker occupancy together with measurements with area survey instruments. Passive devices have worked well in providing reassurance to employers and employees that radiological control measures are adequate.

Neutron Energy Considerations

The main difference for the measurement of neutron 'dose', as opposed to photon or beta 'dose', is that neutron 'dose', involves a weighting factor for the greater radiobiological effectiveness (RBE) due to the densely ionizing radiation produced when neutrons interact with tissue. This densely ionizing radiation consists of protons produced through capture by nitrogen and the recoil protons from elastic scattering with hydrogen. Generally speaking, the absorbed dose, (energy imparted per unit mass), is weighted by a factor of 10. This means that at lower thermal energies, where 15% of the absorbed dose is due to capture protons and 85% is due to capture gamma rays, the overall weighting is about 2.3. A similar weighting factor applies up to about 1 keV for incident neutron energy. At energies above 50 keV or so, the great majority of absorbed dose is from recoil protons, and a factor of about 10 is applied overall. Therefore, the absorbed dose would have to be modified by the weighting factors in order for the device to measure accurately. The problem is, of course, to incorporate similar weightings in the response of a practical dosimeter. Most physical effects in detectors in fact show a lower efficiency at higher ionization densities.

Albedo Dosimetry

TLDs that are used for neutron or neutron-photon personnel dosimetry are albedo dosimeters. The word albedo simply means the proportion of light or radiation reflected by a surface. Albedo techniques were developed in an attempt to overcome the difficulty of TLDs to detect fast neutrons. Neutrons incident on the human body are scattered and moderated by the nuclei of the body, with the most abundant nuclide being H_2, and as a result of these interactions, a fraction, leave the front surface of the body. The spectra of the outgoing neutrons, called albedo neutrons, is shifted towards lower energies with respect to the incident neutrons as a result of the body moderation processes, converting fast into thermal neutrons and permitting their measurement.

Albedo dosimetry measures the neutrons emitted by the body instead of (or in addition to) the incident neutrons. This can be achieved placing the TL detectors behind a thermal neutron absorber, thus eliminating the incident thermal neutrons, but close to the body surface to detect the reflected neutrons. A description of the features of albedo dosimeters can be found in several publications including an all encompassing paper titled "Albedo Neutron Dosimetry" by Piesch and Burgkhardt. [87] Various dosimeter designs using the albedo concept are described in this reference.

A problem of albedo dosimetry is that the fraction of backscattered neutrons depends appreciably on the energy of the incident neutrons, changing from around 0.8 for thermal to 0.2 for 1 MeV. This is an important limitation for determining a reduced energy response.

Types of Albedo Dosimeters

The current method in use for photon dosimetry provides an accurate measurement of very low doses without major difficulty. Neutron individual dosimetry is more complicated and a sufficiently consistent method, covering the whole range of the neutron energies, does not exist. While the dosimetry of thermal and epithermal neutrons is realistic, the dosimetry of fast neutrons remains challenging. This situation is mainly due to the different processes induced by neutrons in tissue for these energy levels and the difficulty of finding adequate tissue replacements for dosimeters.

There have been numerous types of albedo dosimeters developed over the years. Many of them utilize a combination of filters or shields and TLD crystals with high absorption coefficients for neutrons. Capture reactions such as $^{6}Li(n, t)$ or $^{10}B(n, \alpha)$ detect the backscattered field with good efficiency.

LiF is the most common dosimeter that is used. The mechanism in which Li-6 responds is caused by alpha particles released through the Li-6 reaction, $^{6}Li\ (n, \alpha)\ ^{3}H$. Li-6 has a high cross section for thermal neutron absorption.[88] Natural lithium is 7.5% Li-6, 92.5% Li-7. Typically β/γ use TL-detectors that are 99.93% Li-7 and neutron TL-detectors are 95.6% Li-6.

LiF has an additional advantage. The isotope Li-6 has a relatively large capture cross-section (approximately 953 barns) for thermal neutrons, and because this isotope is present in natural lithium (i.e., approximately 7%), LiF makes an excellent detector of thermal neutrons. In contrast, Li-7 has an extremely small capture cross-section (approximately 0.037 barns). Natural lithium can be made more sensitive by enriching it in the isotope Li-6. Likewise, it can be made almost insensitive to thermal neutrons by

depleting the lithium of Li-6. When a radiation worker is irradiated with fast neutrons, there is little probability that the Li-6 in the personnel dosimeter will capture an incident neutron. It is more likely that some fraction of the fast neutrons will be moderated (slowed) by the worker's body, recoil backwards, and be captured by the Li-6 in the TLD. As previously discussed, this "albedo effect" is the basis for neutron dosimetry. When LiF: MCP is exposed to thermal neutron irradiation, there is no obvious change in the glow curve shape. In the case of TLD-100, the higher temperature peak would be raised with thermal neutron irradiation.[30]

For thermal neutrons TL sensitivity is not as high as that of photons.[89] Typically, TL response to thermal neutrons is defined as the equivalent dose from photons. The relative response for LiF: MCP is only about 20% of that of TLD-100. This was measured with the material made of natural LiF. For the pair of dosimeters enriched with Li-7 and Li-6 it was reported that the thermal neutron response of LiF: MCP with Li-6 is about one-third of TLD-600, the neutron response of LiF: MCP with Li-7 is only about 5% of that of TLD-700. TL sensitivities to gamma rays have a difference of 30 times for the two materials. It has been shown that the LiF: MCP with Li-7 is the least sensitive TL material for neutrons; therefore it is the best discriminator for monitoring gamma ray dose in mixed gamma neutron field.

Thermal neutron sensitivity is directly proportional to a self-shielding factor that is based on material type and form. By raising the factor, the TL response to thermal neutron would increase. In one such study, LiF: MCP powder with enriched Li-6 and Li-7 was deposited onto the film to produce thin dosimeters for neutron monitoring. [90] The experimental results showed that the film with enriched Li-6 has thermal neutron

sensitivity 5 times higher than that of the elements. Therefore, LiF: MCP film pair can measure thermal neutron more effectively than elements.

A study performed by the Naval Dosimetry Center examined the neutron response characteristics for the MT and MCP materials for neutron energies from thermal to 14.2 MeV. The data showed that the MCP material produces on average about 3.9 times less light per Sv delivered by neutrons than does the MT material.[7] This behavior may be explained as a microdosimetry effect of the MCP material where the neutron capture with Li-6 results in the high linear energy transfer (LET) particles. This causes saturation along dose tracks causing a decrease in efficiency to produce light per absorbed energy unit. This same effect is responsible for the non-supralinear properties at high dose levels and for the increased tissue equivalence for low energy photons.

Even with this effect, the lower level of detection for pure exposures with moderated Cf-252 was calculated to be 50 μSv for the MCP material. This is because with this spectrum, there still exists a light advantage from neutron exposures as compared with photon exposures. Therefore, the moderated Cf-252 exposures result in 3.33 times more light than Cs-137 photons on a per Sv delivered basis for the MCP material.[7] The different values for the MT material (0.08) and for the MCP material (0.30) reflect the reduced light output that the MCP material experiences. The MT material is approximately 3.9 times more sensitive than the MCP over the entire energy range from thermal to 14.2 MeV neutrons.

<u>High LET Radiation TL response to alpha and neutron particles</u>

The sensitivity of LiF: MCP is about 30 times higher than that of TLD-100 for

photons rays. In comparison for high LET radiation, the sensitivity is not as high for alphas particles, which is roughly 5 times as high.[89] This is primarily due to the LET effect that LiF: MCP undergoes compared to TLD-100. Therefore, LET results in significant variations in TL output for LiF: MCP.

Limitations of Albedo Dosimetry

The energy dependence of albedo dosimetry requires correction factors to account for the large spectrum of neutron energies. There have been several methods employed to flatten out the poor energy response inherent to albedo dosimeters. One method used is by including additional detectors so that incident thermal neutrons are also measured. Information on the neutron spectrum is essential to improve the accuracy of the equivalent dose calculated by albedo techniques by using suitable sensitivity factors. The information on the neutron field characteristics provided by extra TL detectors is limited and the required spectral information should be obtained by independent means, such as actual spectrometric methods. Frequently, the neutron spectrum to be monitored is constant or nearly constant and thus, a field calibration providing measured or calculated correction factors is a practical and suitable procedure. Albedo dosimeters are reasonably well suited for the measurement of stray fields with degraded spectra.[91, 92]

The sensitivity of TL materials for photons is very good, and nearly tissue equivalent materials. For example, LiF: MT has detection limits on the order of 20-50 μSv. LiF: MCP, also with good tissue equivalence, is 30 to 40 times more sensitive to photons than LiF: MT and can thus measure doses even lower than 1 μSv.[93] However, the sensitivity to neutrons for Li-6 enriched varieties of these TL materials is

considerably lower than for photons, with practical detection limits of around 100 μSv in albedo dosimeters.[92] Additionally, ^{6}LiF: MCP has a lower sensitivity to neutrons than ^{6}LiF: MT. The dose dependence of these TL materials is linear for doses well above the usual radioprotection levels, both for photons and neutrons.

Another concern for albedo dosimetry is angular dependence. The angle dependence for the measurement of $H_p(10)$ depends on the particular design of the dosimeter badge, but it is not generally a problem. A paper on the angular dependence reports satisfactory results for an albedo dosimeter, comparing the experimentally determined values for $H_p(10)$, exposing to moderated and unmoderated Cf-252 neutron sources, with the calculated values using an MCNP Monte Carlo code. [94]

APPENDIX C: DT-702/PD DOSIMETER DESIGN AND PROCESSING SYSTEM

Harshaw 8841 Dosimeter (DT-702/PD TLD)

Dosimeter Design

The DT-702/PD Dosimeter consists of pressed pellets sandwiched in thin Teflon coated film and mounted in a standard Harshaw aluminum substrate to form a TLD card. Elements 1 through 3 consist of TLD-700H are photon sensitive with a thermal neutron sensitivity of 0.07% while Element 4 consists of TLD-600H and neutron sensitivity of 95.6%.[26] (Figure 33)

Element one and Element two are 0.381 mm thick and used for the photon deep dose measurement. Element three is 0.254 mm thick and used for beta and shallow dose measurements. Element four is 0.381 mm thick and used for the albedo neutron response.

The TLD pellets are encapsulated in clear thin 10 mg/cm^2 Teflon sheets. While this adversely adds to the filtration for beta measurements, the Teflon protects the TL element from adverse environmental conditions. The Teflon encapsulation also extends the effective life of the TL element in an operational environment. Another benefit of Teflon is that it can be sealed under pressure at temperatures below the desensitizing temperature of the LiF: MCP material.

Element Position	Phosphor Description	Phosphor Dimensions (3.6 mm diameter by indicated thickness)	Filter Material (Primary)	Filter Thickness Total (see note)
1	LiF-700H	0.038 (cm)	ABS/Copper	435 (mg/cm^2)
2	LiF-700H	0.038 (cm)	ABS/Teflon	1016 (mg/cm^2)
3	LiF-700H	0.025 (cm)	Mylar	17 (mg/cm^2)
4	LiF-600H	0.038 (cm)	ABS/Tin (Sn)	1307 (mg/cm^2)

(Filter Thickness (mg/cm^2) = Thickness (cm) x Density (mg/cm^3))

Figure 33. The table and image outline the characteristics of the DT-702/PD holder and card. Adapted with permission of the publisher. [95]

The TLD holder provides filtering of the TLD elements providing different radiation absorption thickness. This allows for an estimation of the various dose components including the shallow, deep, and eye dose. There are four filters in the holder as indicated in Figure 34. The shallow dose estimation is based on the response of element 3. The deep dose estimation is based on the response of element 2. Element 1, shielded by a copper filter, acts as an energy spectrometer for low energy photons by taking advantage of the photon attenuation characteristics of the copper. Additionally, element 4 provides medium energy photon discrimination.

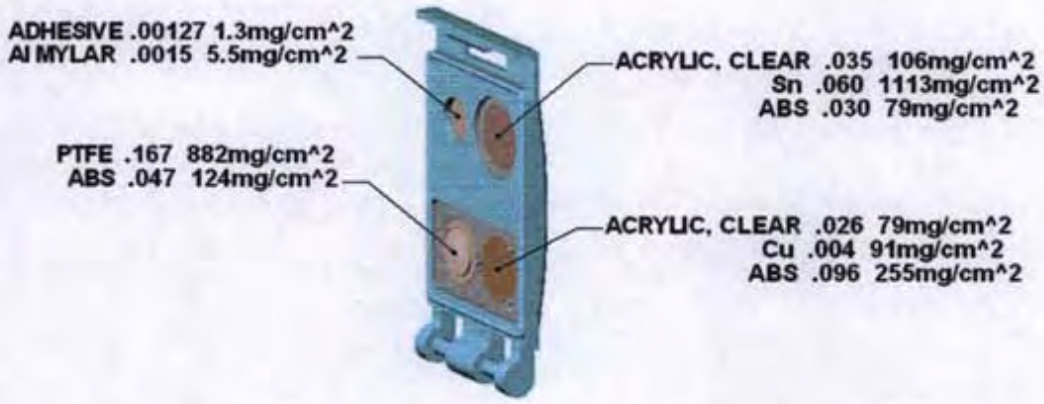

Figure 34. The image provides an example of the TLD holder and its associated filters. Used with permission of the publisher. [7]

Harshaw Model 8800 TLD Reader

General Description

The Harshaw 8800 Workstation is a fully automated reader for thermoluminescence dosimetry (TLD) measurement. It combines high capacity and throughput capabilities with non-contact heating. This is done by utilizing a stream of hot nitrogen gas under precise temperature control to heat the TLD elements. This method greatly increases the life of the TLD cards and provides greater reproducibility of the glow curves.[20] The system consists of two major components: the Card Reader. (Figure 35) and the WinREMS (Windows Radiation Evaluation and Management System) software resident on a personal computer (PC)

Figure 35. The image shows a picture of the Harshaw Model 8800 Reader.[96]

Operation

Up to 1400 cards may be loaded into the Reader for automatic operation. The Reader simultaneously reads up to four TL elements on each card. In addition to the Reader making direct measurements, WinREMS stores, analyzes displays and reports the exposure for each element in. Figure 36 shows the major components of the system. In addition to the processing components, the reader contains an internal Sr-90 irradiator that is used to for calibration purposes.

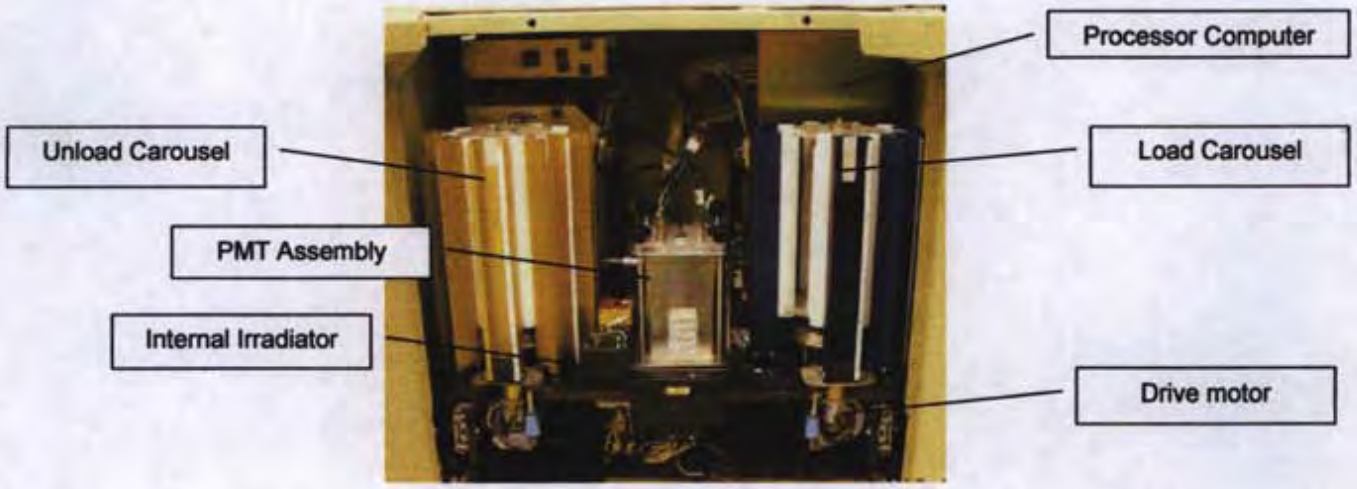

Figure 36. The image identifies the major components of the Harshaw Model 8800 TLD Reader.[96]

The reader provides a dynamic range of reading over seven decades of light output (energy deposited) and can be used to process several different types of TL dosimeters. The internal computer controls the entire TL reader operation and along with the WINREMS software the operator can select and edit the desired time temperature profile (TTP). The TTP is an essential part of the operating parameters of the TL processing system and is directly related to the TL output data results. The TTP for this research is specific for the TLD-100H (LiF: MCP) and is shown in Figure 37.

The use of pre-heat in this TTP is important to remove low temperature peaks that do not contribute useful information to the light output of the dosimeter. The TTP must be selected such that an accurate and reliable output from the TLD-100H (LiF: MCP) is obtained. The temperature must also be limited due to the change of sensitivity of the TLD-100H material when heated above 270° C.[26]

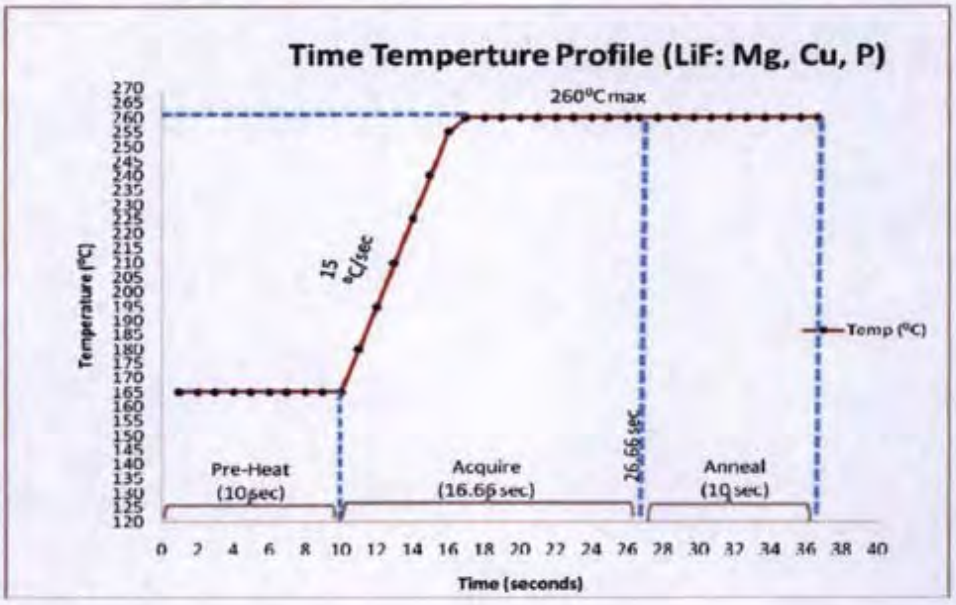

Figure 37. The figure identifies a typical TLD-100H TTP with Hot Gas Pre-Heat.

In addition to the TLD reader, an important component in TLD processing is the supply of Nitrogen (N_2) gas for the heating of the TL material. A liquid nitrogen supply is used and the gas is pulled off the tank to provide 99.995% pure N_2 gas at a pressure of 40 to 90 psi with a flow rate of 400 L h^{-1}. [96]

System Calibration

Generating Calibration Cards

Before a TLD system can be calibrated, it is necessary to establish a set of reference cards that will be used for the purpose of calibrating the reader and calibrating other cards. This set of cards is irradiated and read together as a group. For each element position on the TLD card, the mean light output of all elements in the same position is determined and the output of individual elements in that position compared against this. A sensitivity factor known as an element correction coefficient (ECC) is determined for each element such that the response of the element after correction with the ECC is equivalent to the mean response of all reference elements in the same position on the card. (Figure 38) Thus the ECC corrected responses of all elements in the calibration set are theoretically the same for any given dose [20, 26, 97]

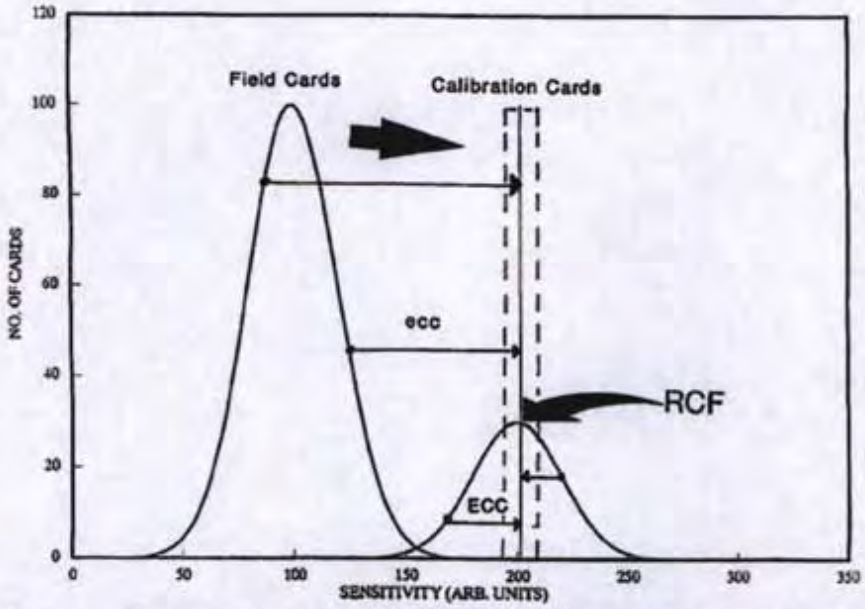

Figure 38. The graph identifies the Element Correction Coefficient determination and application. Used with permission of the publisher. [4]

TLD Reader Calibration

Calibration of each reader was accomplished by exposing a representative sample of reader calibration cards in air without a holder to a known amount of radiation, typically with the internal Sr/Y-90 internal source, and then processed on the reader. The cards used to calibrate the reader were exposed to 100 mR and a RCF, expressed in units of nC/mR, was calculated for each of the four PMT channels using the following method:

$$RCF_i = \frac{\overline{Q}_i}{X} \qquad \overline{Q}_i = \frac{\sum_{j=1}^{k} Q_{ij} * ECC_{ij}}{k}$$

RCF_i = reader calibration factor for i_{th} PMT (nC/mR)

X = exposure value (mR)

Q_{ij} = raw reading for element i of card j (nC)

ECC_{ij} = element correction coefficient for element i of card j (unitless)

k = number of calibration cards used.

Equation 10. Equation Identifies Calculation of the Reader Calibration Factor.

The reader calibration cards used for determining the RCF have been previously calibrated, and the resulting ECC for each element was applied to its raw reading to correct for variations in element sensitivity. This approach allowed for a more precise measurement of PMT sensitivity to be obtained in the reader calibration process with fewer cards. Reader calibration was performed prior to, and as an independent process from, the read-out of personnel cards for dose determination. The RCFs obtained in the reader calibration process were then applied to the subsequent field and QC card readings on a real-time basis as the cards are read. When RCFs were applied, element readings are reported from the reader in units equivalent Cs-137 mR equivalent (in free air).

Card Calibration

The ECC of a given TLD element is a measure of how the element responds to a source of radiation relative to the response of other similar elements in a reference population (calibration card set). The ECC for a given element corrects that element's sensitivity to the mean sensitivity of elements in the same position in the population of cards used to calibrate the reader. The process of card calibration entails calibrating the reader, as previously discussed, with a sample of reader calibration cards exposed to a known amount of radiation and applying the resulting RCFs to subsequent readings of cards being calibrated (that have been exposed to the same source). Therefore, the ECC for each element is determined according to the following relationship (Equation

11):

$$ECC_{ij} = \frac{RCF_i}{Q_{ij}} X$$

ECC_{ij} = element correction coefficient for element i on card j

RCF_i = reader calibration factor for PMT_i (nC/mR)

Q_{ij} = raw reading from element i on card j (nC)

X = delivered exposure value (mR).

Equation 11. Equation Identifies Calculation of the Element Correction Coefficient.

The ECCs are determined for a group of cards by annealing all cards, including "calibration cards," at the same time followed by irradiation as a group and readout on the same day. Subsequent calibrations of the cards are required every two years and a comparison of the old ECC with the new ECC is performed.

APPENDIX D: NEUTRON SOURCE CHARACTERIZATION

In order to accurately measure the fade response of the DT-702/PD dosimeter, a precise method of exposing the dosimeter is required to ensure that same dose is deposited on every TLD. This is especially difficult when you have such a large number of TLDs that need to be irradiated and the source has a non uniform fluency spatial distribution. Through the use of a spinning carousel, it is possible to obtain a homogeneous dose distribution within 2%.

Neutron Source

Characterization of PuBe

The neutron source used for this study, as previously discussed, is an encapsulated plutonium beryllium neutron source manufactured by Monsanto. It consists of 76.37 grams of Plutonium 239 and has a cylindrical shape that measures 1.30 inches (outside diameter) by 3.4 inches high. The source is controlled under a Master Materials License and maintained by the Naval Dosimetry Center.

Neutron Production

There are several methods utilized to produce neutrons including fission, alpha-neutron reactions, and linear accelerators. In small applications, the easiest and most economic means is through the use of a source. Several sources are available and some examples are summarized in Table 7.

Source	Reaction	Half Life	Average Neutron Energy (MeV)	Yield per Ci (neutrons s-1)
Po-Be	α,n	138.4 d	4.2	2.5×10^6
Ra-Be	α,n	1620 y	4.0	1.3×10^7
Pu-Be	α,n	86.4 y	4.5	2.3×10^6
Am-Be	α,n	458 y	4.5	2.2×10^6
Sb-Be	γ,n	60 d	0.024	1.3×10^5
Cf	Spontaneous fission	2.65 y	Fission Spectrum	2.3×10^{12}

Table 7. The table identifies the characteristics of selected radioactive neutron sources. [98]

The main source of neutrons used in this study, as pictured in Figure 39, is from $^{9}Be\ (\alpha, n)^{12}C$ reaction followed by the neutron induced fission in the odd isotopes of Pu.

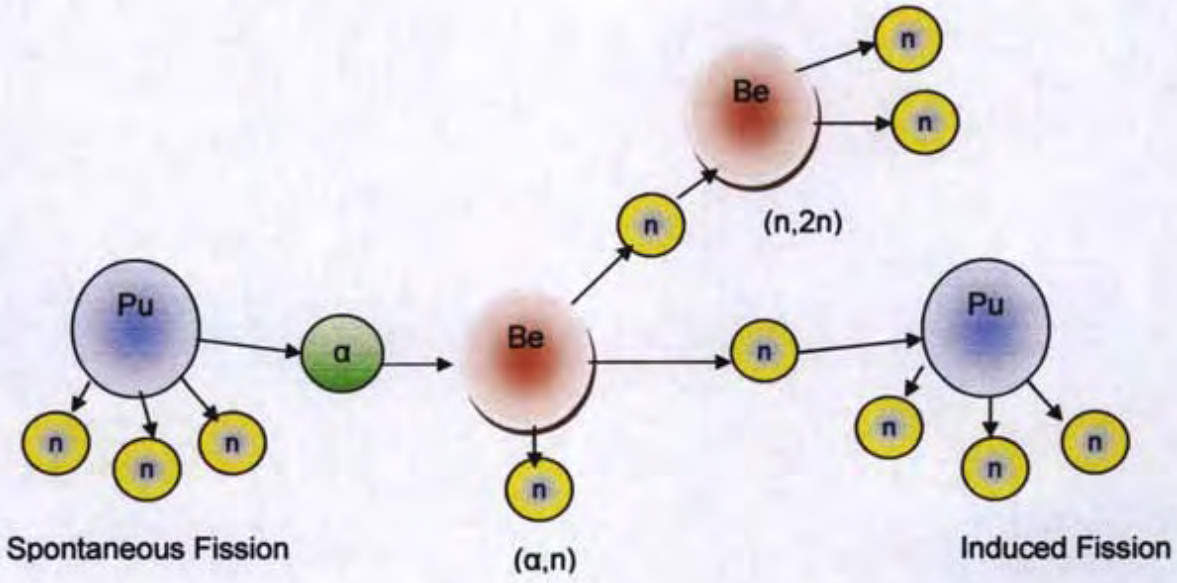

Figure 39. The diagram identifies the various interactions of Pu and Be neutron source.

The PuBe source contains 5 Curies and produces 2.3×10^6 Neutrons per cm^2-second per Curie. The source is surrounded by a virgin polyethylene shield (white) to allow for thermalization of neutrons and in order to minimize personnel dose, borated poly is used (yellow) to prevent escape of neutrons from the shielding. (Figure 40)

Figure 40. The image displays the neutron source configuration with top removed.

Energy Spectrum

The energy spectrum ranges from a few eV to 11 MeV. As indicated in Figure 41 the average energy is approximately 4.5 MeV.

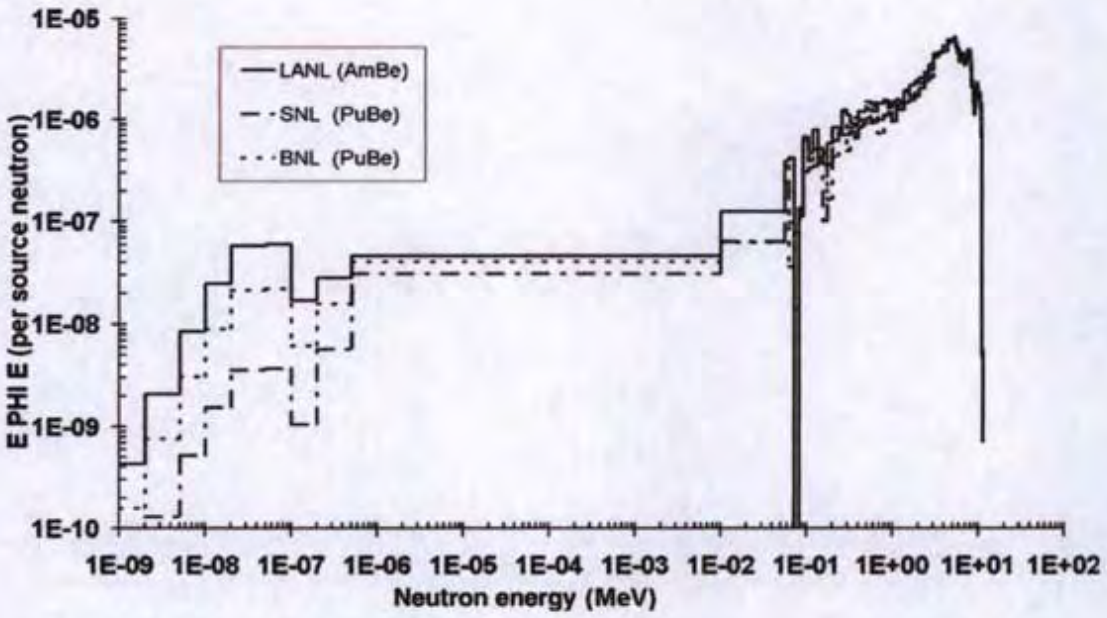

Figure 41. The graph identifies the Pu-α-Be neutron spectrum. Used with permission of the publisher. [99]

Neutron Source Geometry

The neutron source is located in a polyethylene shield shown in Figures 42 and 43. A thermal column measuring approximately 2 inches high by 7 inches wide and 24 inches deep allows for exposing of TLDs. The PuBe source sits encased in virgin poly approximately 3 inches above the thermal column. This geometry proves to be difficult due to the isotropic emission of neutrons from the cylindrical source. Several initial tests were performed in an attempt to evenly expose TLDs without the use of a carousel.

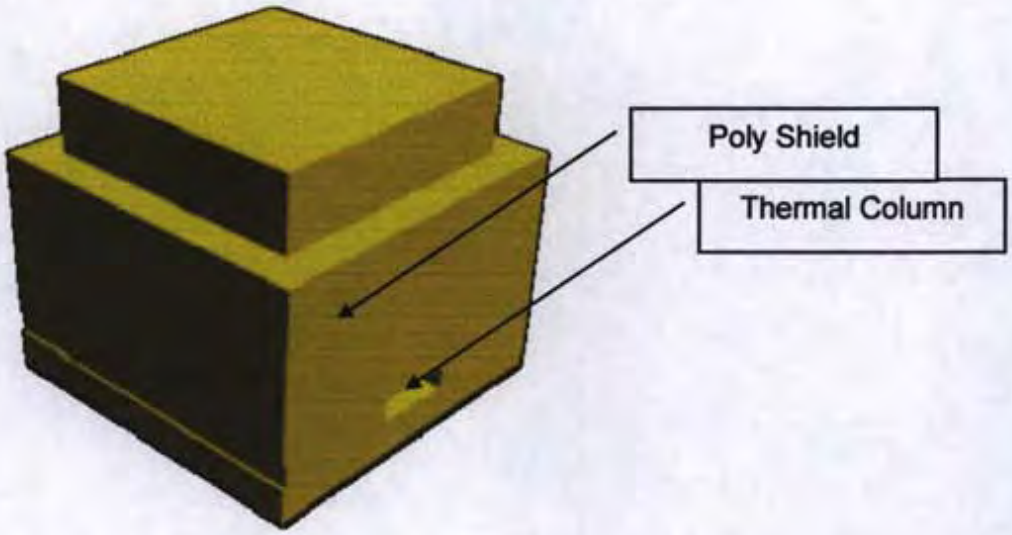

Figure 42. The drawing identifies the polyethylene shield that contains the PuBe Source.

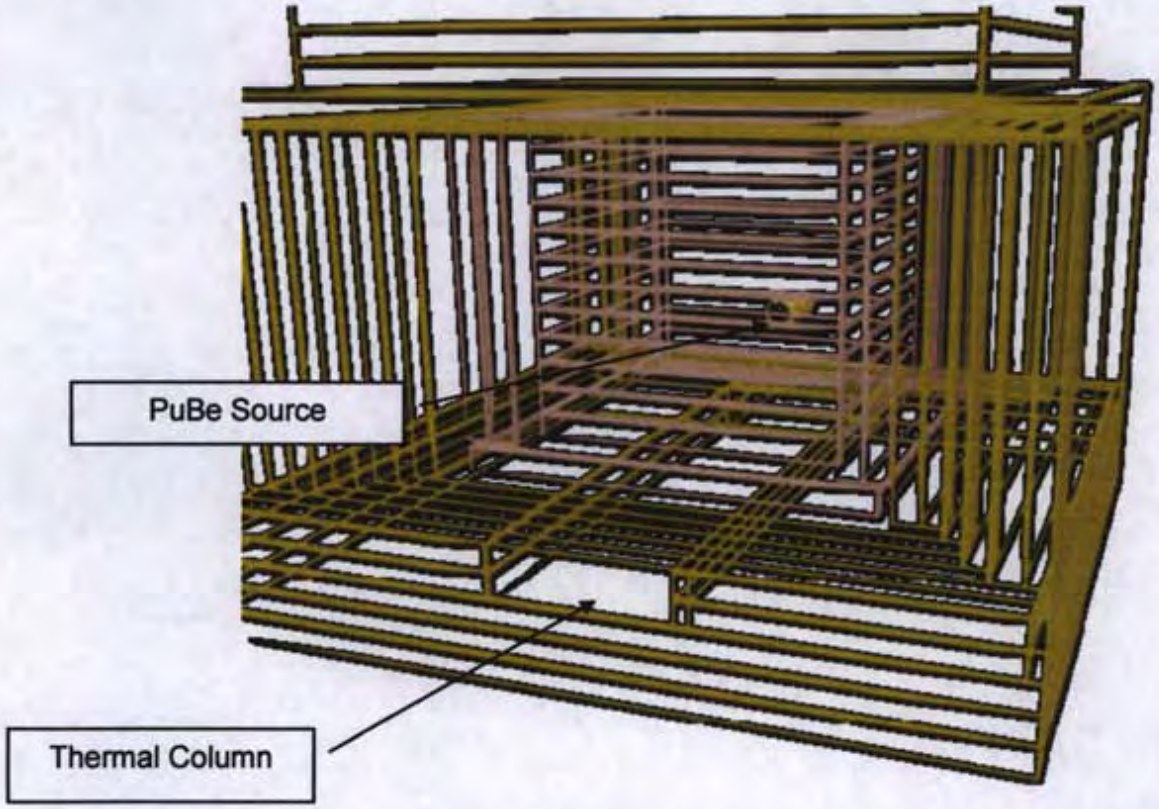

Figure 43. The drawing identifies the relative position of the PuBe source with the thermal column.

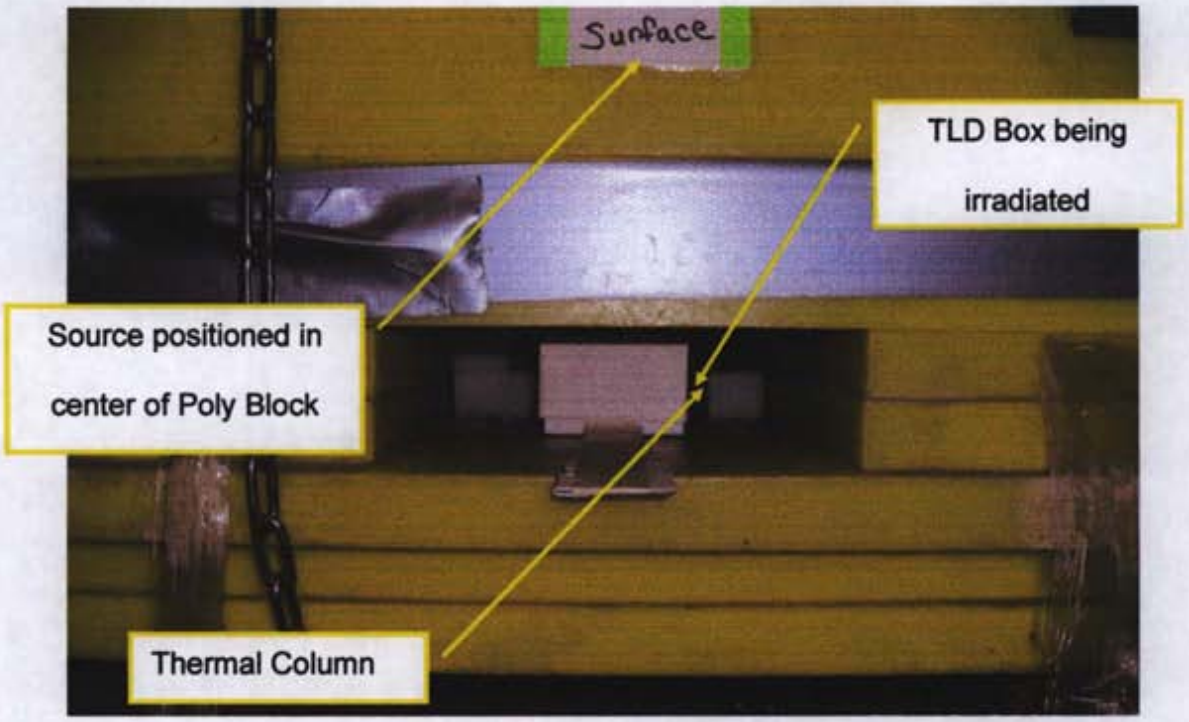

Figure 44. The image identifies the thermal neutron column with box of TLDs being irradiated.

In order to get a better understanding of the fluency spatial distribution a test was performed to determine the source strength related to the geometry of the thermal column. The test consisted of a 5 ×11 matrix of TLDs positioned on a plastic template. (Figure 45)

Figure 45. Image identifies the TLD matrix used for neutron source characterization.

The group of TLDs was inserted into the thermal column, irradiated for one hour, and processed. A graphical representation of the data shows that the source, due to its isotropic emission, is Gaussian in nature. (Figure 46) Therefore, it would be difficult to obtain a precise delivered dose using any type of static means unless a small amount of TLDs were to be used in an exact geometry, such as the TLD exposure drawer.

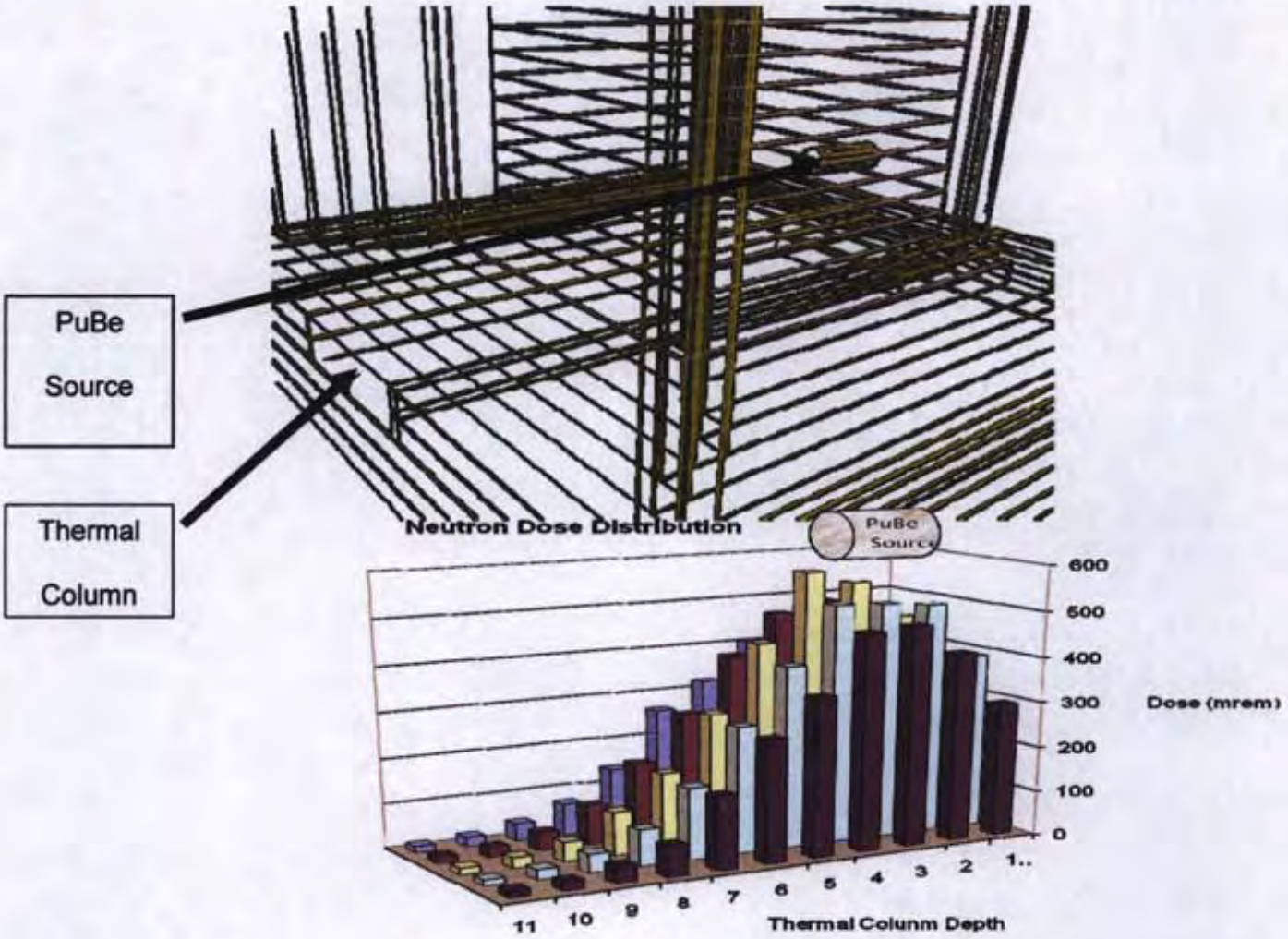

Figure 46. The figure displays the graphical representation of the neutron dose distribution in the thermal column.

Several attempts were made to expose the TLDs in a box and then rotating, rearranging or flipping the TLDs in order to have an even dose distribution. Table 8 summarizes all of the tests performed and the resulting Standard Deviations and Coefficients of Variation obtained.

				Position 1			Position 2			Position 3			Position 4		
Test #	Description	Groups	Number of TLDs	Average	Standard Deviation	Coefficient of Variance	Average	Standard Deviation	Coefficient of Variance	Average	Standard Deviation	Coefficient of Variance	Average	Standard Deviation	Coefficient of Variance
1	Dose Distribution with plastic blocks installed 5 per group	1	25	13.2	2.6	20%	15.8	3.6	23%	14.1	3.2	22%	346.5	108.2	31%
2	Full length Characteristic	1	240	19.4	7.9	41%	16.4	6.1	37%	15.1	5.7	38%	396.4	206.0	52%
3	Wedge on half of width	1	42	17.8	1.3	7%	13.8	1.1	8%	12.7	0.8	6%	419.7	27.1	6%
4	4 groups of 20 tlds stacked	1	20	27.9	2.1	8%	25.0	2.2	9%	22.7	1.7	7%	591.4	65.2	11%
		2	20	44.8	4.9	11%	41.0	4.1	10%	35.2	3.9	11%	939.2	111.2	12%
		3	20	52.7	5.8	11%	51.8	5.4	11%	45.0	5.6	12%	1174.1	133.5	11%
		4	20	43.7	5.2	12%	48.0	5.7	12%	41.3	5.7	14%	937.5	106.7	11%
5	3 rows of 40 TLDs	1	41	8.9	0.6	7%	10.2	0.8	8%	11.6	0.5	4%	220.1	17.2	8%
		2	40	13.2	0.8	6%	11.8	0.6	5%	13.5	0.5	4%	319.0	28.4	9%
		3	41	15.1	0.7	5%	17.2	1.0	6%	19.9	0.7	3%	375.7	32.3	9%
6	Wedge test lengthwise	1	127	28.9	4.9	17%	34.5	6.6	19%	30.9	5.6	18%	634.9	109.5	17%
7	Various set up along width of box	1	40	22.1	1.4	6%	19.8	1.2	6%	22.8	1.2	5%	555.9	50.4	9%
		2	40	27.9	1.5	5%	24.8	1.3	5%	29.8	1.2	4%	723.2	75.2	10%
		3	40	36.3	2.7	7%	34.2	2.3	7%	46.0	2.5	5%	1115.1	89.7	8%
		4	40	38.7	2.3	6%	38.2	2.4	6%	49.5	2.5	5%	1113.2	85.9	8%
		5	40	22.5	1.3	6%	26.4	1.4	5%	29.5	1.5	5%	568.8	39.7	7%
		6	14	12.3	0.5	4%	11.6	0.5	4%	8.4	0.3	3%	103.9	6.4	6%
8	Re Characterize length of Source														
9	2 Rows along width, Flipped length wise for equal time	1	86	29.3	1.9	6%	28.2	1.7	6%	38.0	2.2	6%	819.5	54.5	7%

				Position 1			Position 2						Position 4		
Test #	Description	Groups	Number of TLDs	Average	Standard Deviation	Coefficient of Variance	Average	Standard Deviation	Coefficient of Variance	Average	Standard Deviation	Coefficient of Variance	Average	Standard Deviation	Coefficient of Variance
13	Segregated .5 STDEV of TLDs from test 11	1	54	15.0	0.9	6%	14.2	0.9	6%	19.7	0.7	4%	411.9	12.6	3%
	(non-segregated from 11)	2	23	15.3	0.9	6%	14.3	0.8	5%	19.6	0.7	4%	418.8	33.7	8%
14	Carousel	1	71	10.4	0.5	5%	8.2	0.3	4%	6.7	0.3	4%	172.9	12.1	7%
17	Two rows midline Flipped	Both	121	13.6	0.9	7%	13.1	0.9	7%	17.4	1.0	6%	295.4	19.5	7%
		1	60	13.7	1.0	7%	13.3	1.1	8%	17.6	1.0	6%	298.7	18.5	6%
		2	61	13.5	0.8	6%	12.9	0.7	5%	17.1	0.9	5%	291.4	19.4	7%
18	Stacked TLDs flipped half way	1	30	11.6	0.6	5%	11.8	0.6	5%	10.6	0.5	5%	188.7	20.4	11%
19	Drawer test set of 4 TLDs	1	4	12.5	0.6	5%	13.3	1.0	7%	10.6	0.2	2%	361.4	1.7	0%
20	Drawer test repeat test 19	1	4	20.7	1.6	8%	21.6	1.8	8%	16.6	0.4	2%	763.2	25.7	3%
23	3D source Characterization														
24	2 Rows Lengthwise Re-characterize	1	44	22.6	1.7	7%	21.5	1.7	8%	13.5	0.9	6%	288.9	19.8	7%
		2	44	22.6	1.6	7%	21.4	1.3	6%	13.0	0.7	5%	278.7	15.4	6%
25	2 rows low dose rate	1	110	6.6	0.6	9%	8.1	0.7	9%	7.5	0.6	8%	70.8	5.5	8%
		2	110	5.8	0.3	5%	5.4	0.3	5%	5.7	0.3	5%	48.4	4.4	9%
26	10 TLD flat matrix	1	5	4.2	0.2	5%	4.2	0.2	4%	3.6	0.2	6%	35.5	1.7	5%
27	repeat test 26 10 TLD flat matrix	1	5	3.4	0.2	6%	3.5	0.2	6%	3.2	0.1	4%	22.9	1.8	8%
28	2 Rows width low dose rate	1	110	31.4	1.3	4%	36.8	1.4	4%	35.2	1.7	5%	227.0	20.1	9%
29	One SD segregated from test 28	1	37	5.9	0.2	4%	7.3	0.3	4%	7.2	0.3	4%	52.1	2.6	5%
30	Drawer repeatability	1	20	2.8	0.3	10%	3.1	0.3	11%	2.4	0.3	13%	68.7	3.8	5%
31	Repeat test 30	1	20	2.6	0.3	11%	2.9	0.4	13%	2.4	0.3	12%	68.0	3.9	6%

Table 8. The table provides a summary of neutron source characterization testing.

After several attempts at configuring the various geometries, it was determined that the best method to obtain the most accurate neutron dose would be the drawer, which is located right above the source. This was a problem though; since it only allows 4 TLDs to be irradiated and to obtain a desired dose of 400 mrem for hundreds of TLDs was not feasible for this study.

Further refinement was done on making a better carousel to expose the TLDs. The first prototype consisted of a cooling fan obtained from a Central Processing Unit (CPU). It was modified by adding a plate to hold TLDs that could be mounted and a small DC electrical source could be used to spin the TLDs. This method did not have the required torque to spin enough TLDs for exposure.

The second attempt was a regular cooling fan used in a computer case that was modified by cutting off the blades and a plate attached to hold the TLDs. (Figure 47) This method had the required torque to spin the TLDs though the reliability and durability of the device was questioned for the required study length.

Figure 47. The image shows the TLD carousel loaded with TLDs and rotating.

Finally, it was decided to utilize a high torque motor that would drive a pulley mounted carousel. The carousel could be better designed since the mechanical force required to turn the device would not have to be integrated. This method proved to work exceptionally; therefore two devices were constructed to ensure a backup existed in case the first one failed.

Several tests were performed on the new carousel to ensure that there was sufficient repeatability, precision and accuracy required for the study. In the repeatability test, a group of the same 72 TLDs was irradiated twice by randomly placing on the carousel. Figure 48 shows that the repeat measurements tracked accordingly. A one-way ANOVA was performed on the data and showed no statistical difference between the groups at a 95% confidence interval (α=.05). (Table 9)

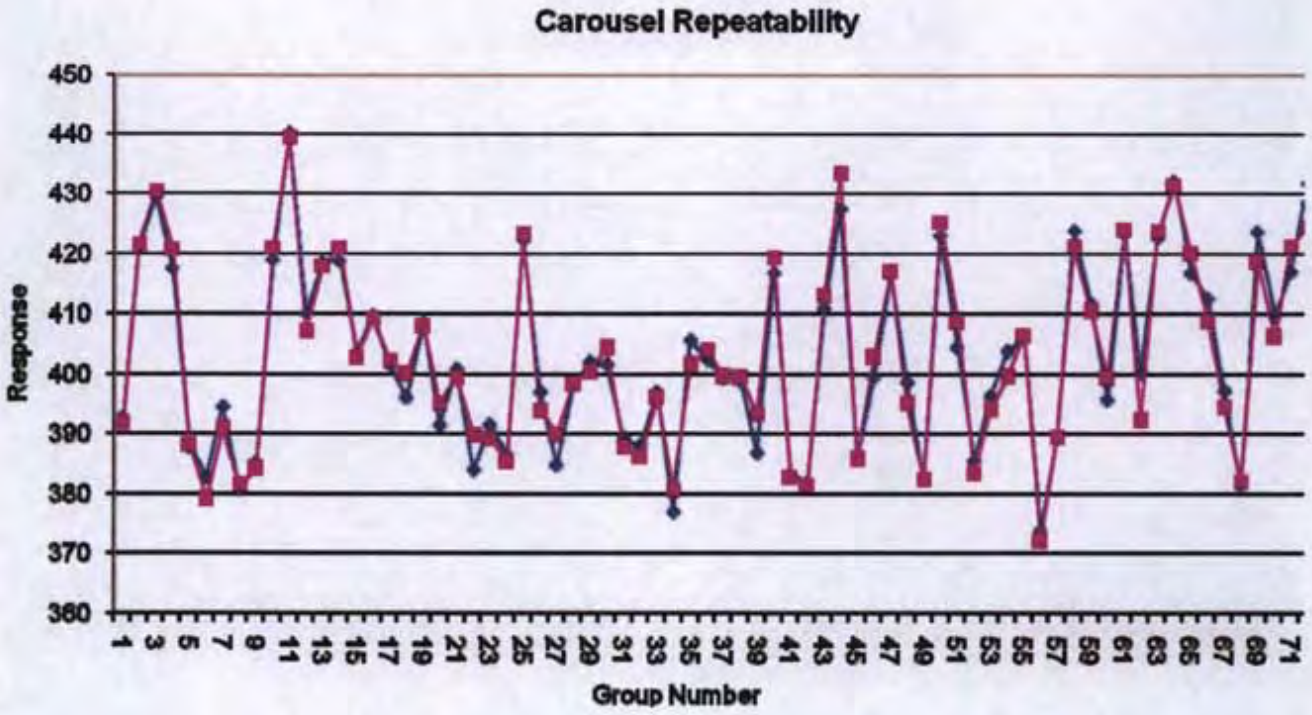

Figure 48. The graph identifies the repeatability test of carousel (Element 4).

ANOVA: Single Factor

SUMMARY				
Groups	*Count*	*Sum*	*Average*	*Variance*
P4 Group 1	40	20250.7	506.2674	1056.523
P4 Group 2	40	20155.65	503.8913	1647.457

ANOVA						
Source of Variation	*Sum of Squares*	*Degrees of freedom*	*Mean Sum of Squares Error*	*F ratio*	*P-value*	*Critical F Value*
Between Groups	112.9133	1	112.9133	0.083516	0.773354	3.963472
Within Groups	105455.2	78	1351.99			
Total	105568.1	79				

Table 9. Table Provides One-Way ANOVA Results for Carousel Repeatability Test

APPENDIX E. DOCUMENTATION OF PERFMISSIONS FOR COPYRIGHT INFORMATION

The following permissions are provided as a reference to the figures and graphs used in this thesis:

OXFORD UNIVERSITY PRESS LICENSE TERMS AND CONDITIONS

May 30, 2008

This is a License Agreement between Jeffrey A Delzer ("You") and Oxford University Press ("Oxford University Press"). The license consists of your order details, the terms and conditions provided by Oxford University Press, and the payment terms and conditions.

License Number	1946830499000
License date	May 12, 2008
Licensed content publisher	Oxford University Press
Licensed content publication	Radiation Protection Dosimetry
Licensed content title	Characterization of neutron reference fields at US department of energy calibration fields
Licensed content author	R. H. Olsher, et. al.
Licensed content date	August 2007
Type of Use	Thesis / Dissertation
Institution name	Uniformed Services University of the Health Sciences
Title of your work	Neutron Fading Characteristics of Copper-Doped Lithium Fluoride (LiF:MCP) Thermoluminescent Dosimeters (TLDs)
Publisher of your work	Uniformed Services University of the Health Sciences

This is a License Agreement between Jeffrey A Delzer ("You") and Elsevier Limited ("Elsevier Limited"). The license consists of your order details, the terms and conditions provided by Elsevier Limited, and the payment terms and conditions.

Supplier	Elsevier Limited The Boulevard,Langford Lane Kidlington,Oxford,OX5 1GB,UK
Registered Company Number	1982084
Customer name	Jeffrey A Delzer
Customer address	801 Crocus Dr. Rockville, , MD 20850
License Number	1946780068891
License date	May 12, 2008
Licensed content publisher	Elsevier Limited
Licensed content publication	Radiation Measurements
Licensed content title	Materials for thermoluminescent dosimetry: Current status and future trends
Licensed content author	V. Kortov
Licensed content date	April-May 2007
Volume number	42
Issue number	4-5
Pages	6
Type of Use	Thesis / Dissertation
Portion	Figures/table/illustration/abstracts
Portion Quantity	1
Format	Electronic
You are an author of the Elsevier article	No
Expected publication date	May 2008
Elsevier VAT number	GB 494 6272 12

OXFORD UNIVERSITY PRESS LICENSE

TERMS AND CONDITIONS

May 30, 2008

This is a License Agreement between Jeffrey A Delzer ("You") and Oxford University Press ("Oxford University Press"). The license consists of your order details, the terms and conditions provided by Oxford University Press, and the payment terms and conditions.

License Number	1946641389984
License date	May 12, 2008
Licensed content publisher	Oxford University Press
Licensed content publication	Radiation Protection Dosimetry
Licensed content title	Technical aspects of the Naval Dosimetry Center quality assurance programme
Licensed content author	T. J. St John, et. al.
Licensed content date	September 2006
Type of Use	Thesis / Dissertation
Institution name	Uniformed Services University of the Health Sciences
Title of your work	Neutron Fading Characteristics of Copper-Doped Lithium Fluoride (LiF:MCP) Thermoluminescent Dosimeters (TLDs)
Publisher of your work	Uniformed Services University of the Health Sciences
Expected publication date	5/30/08
Permissions cost	0.00 USD
Value added tax	0.00 USD
Total	0.00 USD

OXFORD UNIVERSITY PRESS LICENSE TERMS AND CONDITIONS

May 30, 2008

This is a License Agreement between Jeffrey A Delzer ("You") and Oxford University Press ("Oxford University Press"). The license consists of your order details, the terms and conditions provided by Oxford University Press, and the payment terms and conditions.

License Number	1946631107891
License date	May 12, 2008
Licensed content publisher	Oxford University Press
Licensed content publication	Radiation Protection Dosimetry
Licensed content title	A TLD System Based on Gas Heating with Linear Time-Temperature Profile
Licensed content author	M. Moscovitch, et. al.
Licensed content date	December 1, 1990
Type of Use	Thesis / Dissertation
Institution name	Uniformed Services University of the Health Sciences
Title of your work	Neutron Fading Characteristics of Copper-Doped Lithium Fluoride (LiF:MCP) Thermoluminescent Dosimeters (TLDs)
Publisher of your work	Uniformed Services University of the Health Sciences
Expected publication date	5/30/08
Permissions cost	0.00 USD
Value added tax	0.00 USD
Total	0.00 USD

OXFORD UNIVERSITY PRESS LICENSE TERMS AND CONDITIONS

May 30, 2008

This is a License Agreement between Jeffrey A Delzer ("You") and Oxford University Press ("Oxford University Press"). The license consists of your order details, the terms and conditions provided by Oxford University Press, and the payment terms and conditions.

License Number	1946630149484
License date	May 12, 2008
Licensed content publisher	Oxford University Press
Licensed content publication	Radiation Protection Dosimetry
Licensed content title	A New Paradigm in Personal Dosimetry Using LiF:Mg,Cu,P
Licensed content author	J. R. Cassata, et. al.
Licensed content date	August 1, 2002
Type of Use	Thesis / Dissertation
Institution name	Uniformed Services University of the Health Sciences
Title of your work	Neutron Fading Characteristics of Copper-Doped Lithium Fluoride (LiF:MCP) Thermoluminescent Dosimeters (TLDs)
Publisher of your work	Uniformed Services University of the Health Sciences
Expected publication date	5/30/08
Permissions cost	0.00 USD
Value added tax	0.00 USD
Total	0.00 USD

OXFORD UNIVERSITY PRESS LICENSE TERMS AND CONDITIONS

May 30, 2008

This is a License Agreement between Jeffrey A Delzer ("You") and Oxford University Press ("Oxford University Press"). The license consists of your order details, the terms and conditions provided by Oxford University Press, and the payment terms and conditions.

License Number	1946621467734
License date	May 12, 2008
Licensed content publisher	Oxford University Press
Licensed content publication	Radiation Protection Dosimetry
Licensed content title	Influence of absorbed dose and deep traps on thermoluminescence response: a numerical simulation
Licensed content author	F. Mady, et. al.
Licensed content date	September 2006
Type of Use	Thesis / Dissertation
Institution name	Uniformed Services University of the Health Sciences
Title of your work	Neutron Fading Characteristics of Copper-Doped Lithium Fluoride (LiF:MCP) Thermoluminescent Dosimeters (TLDs)
Publisher of your work	Uniformed Services University of the Health Sciences
Expected publication date	5/30/08
Permissions cost	0.00 USD
Value added tax	0.00 USD
Total	0.00 USD

OXFORD UNIVERSITY PRESS LICENSE TERMS AND CONDITIONS

May 30, 2008

This is a License Agreement between Jeffrey A Delzer ("You") and Oxford University Press ("Oxford University Press"). The license consists of your order details, the terms and conditions provided by Oxford University Press, and the payment terms and conditions.

License Number	1946620682703
License date	May 12, 2008
Licensed content publisher	Oxford University Press
Licensed content publication	Radiation Protection Dosimetry
Licensed content title	Individual and collective doses from cosmic radiation in Ireland
Licensed content author	P. A. Colgan, et. al.
Licensed content date	March 2007
Type of Use	Thesis / Dissertation
Institution name	Uniformed Services University of the Health Sciences
Title of your work	Neutron Fading Characteristics of Copper-Doped Lithium Fluoride (LiF:MCP) Thermoluminescent Dosimeters (TLDs)
Publisher of your work	Uniformed Services University of the Health Sciences
Expected publication date	5/30/08
Permissions cost	0.00 USD
Value added tax	0.00 USD
Total	0.00 USD

OXFORD UNIVERSITY PRESS LICENSE TERMS AND CONDITIONS

May 30, 2008

This is a License Agreement between Jeffrey A Delzer ("You") and Oxford University Press ("Oxford University Press"). The license consists of your order details, the terms and conditions provided by Oxford University Press, and the payment terms and conditions.

License Number	1946620439516
License date	May 12, 2008
Licensed content publisher	Oxford University Press
Licensed content publication	Radiation Protection Dosimetry
Licensed content title	Dependence of LiF:Mg,Cu,P (MCP-N) Glow-Curve Structure on Dopant Composition and Thermal Treatment
Licensed content author	P. Bilski, et. al.
Licensed content date	February 1, 1997
Type of Use	Thesis / Dissertation
Institution name	Uniformed Services University of the Health Sciences
Title of your work	Neutron Fading Characteristics of Copper-Doped Lithium Fluoride (LiF:MCP) Thermoluminescent Dosimeters (TLDs)
Publisher of your work	Uniformed Services University of the Health Sciences
Expected publication date	5/30/2008
Permissions cost	0.00 USD
Value added tax	0.00 USD
Total	0.00 USD

Concerning figures used from Reference 2, permission was granted from the authors via email.

McKeever, Stephen [stephen.mckeever@okstate.edu]

Sent on 12 May 2008 6:43 PM

Jeff,

The publisher has gone out of business and the business was sold to Oxford University Press. I do not know if the copyright of the books was also transferred at the time of the sale, but you can contact them and ask. For my part, you are most welcome to use the figures. Best wishes, Steve

Sent on 13 May 2008 8:17 PM

Marko Moscovitch {moscovim@georgetown.edu}

Jeff.

Sure, you have my permission to use figures from our book. Good luck.
MM

BIBLIOGRAPHY

1. Naval Dosimetry Center, N., *Historical Records of the United States Naval Dosimetry Center*. 2005.

2. McKeever, S.W.S., M. Moscovitch, and P.D. Townsend, *Thermoluminescence Dosimetry Materials: Properties and Uses*. 1995: Nuclear Technology Publishing.

3. Kortov, V., *Materials for thermoluminescent dosimetry: Current status and future trends*. Radiat. Meas., 2007. doi: 10.1016/j.radmeas.2007.02.067.

4. Moscovitch, M., et al., *The application of LiF:Mg,Cu,P to large scale personnel dosimetry: current status and future directions*. Radiat Prot Dosimetry, 2006. 119(1-4): p. 248-254.

5. Jones, L.A. and R.P. Stokes, *Pre-Irradiation and Post-Irradiation Fading of the Harshaw 8841 TLD in Different Environmental Conditions*. Radiat Prot Dosimetry, 2006: p. ncl133.

6. Kathren, R.L., *Health Physics: A Backward Glance*. 1980: Elsevier Science Ltd.

7. Cassata, J.R., et al., *A New Paradigm in Personal Dosimetry Using LiF: Mg,Cu,P*. Radiation Protection Dosimetry, 2002. 101(1): p. 27-42.

8. Schulman, J.H., *Radiophotoluminescence Dosimetry System of the U.S. Navy*. Nucleonics, 1953. 11(10): p. 52-56.

9. Bos, A.J.J., *Theory of Thermoluminescence*. Radiation Measurements, 2007. 41: p. S45-S56.

10. Bartlett, D.T., R.J. Tanner, and D.J. Thomas, *Active Neutron Personal Dosemeters - A Review of Current Status*. 1999. p. 107-122.

11. Spurný, F., *Individual Dosimetry for High Energy Radiation Fields*. Radiat Prot Dosimetry, 1999. 85(1-4): p. 15-20.

12. Olko, P., et al., *Dosimetry of heavy charged particles with thermoluminescence detectors--models and applications*. Radiat Prot Dosimetry, 2004. 110(1-4): p. 315-318.

13. Daniels, F., C.A. Boyd, and D.F. Saunders, *Thermoluminescence as a Research Tool*. Science, 1953. 117.

14. Blase, E.F., R.E. Lagerquist, and R.C. Palmer, *A Thermoluminescent Personnel Dosimeter System*, in *Eigth Annual Meeting of the Health Physics Society*. 1963.

15. Cameron, J.R., *Radiation Dosimeter Utilizing The Thermoluminescence of Lithium Fluoride.* Science, 1961.

16. Niewiadomski, T., *25 Years of TL Dosimetry at the Institute of Nuclear Physics, Kraków.* 1996. p. 1-6.

17. Nash, A.E. and F.H. Attix, *Test Results for Harshaw Model 2271 TLD System at NRL.* 1973: Washington DC.

18. Devine, R.T., M. Moscovitch, and P.K. Blake, *The US Naval Dosimetry Centre Thermoluminescence Dosimetry System.* 1990. p. 231-236.

19. Velbeck, K.J., K.L. Streetz, and J.E. Rotunda, *Next Generation Model 8800 Automatic TLD Reader.* 1999. p. 381-386.

20. Moscovitch, M., et al., *A TLD System Based on Gas Heating with Linear Time-Temperature Profile.* Radiat Prot Dosimetry, 1990. 34(1-4): p. 361-364.

21. Sáez-Vergara, J.C. and A.M. Romero, *The Influence of the Heating System on the Hypersensitive Thermoluminescent Material LiF:Mg,Cu,P (GR-200).* Radiat Prot Dosimetry, 1996. 66(1-4): p. 431-436.

22. Doremus, S.W. and G.A. Higgins, *Pre-Irradiation Fade and Post-Irradiation Fade for LiF:Mg,Ti, TLD-600, and TLD-700, as a Function of Time.* 1994. p. 119-125.

23. Daniels, R.D., T.D. Taulbee, and P. Chen, *Radiation exposure assessment for portsmouth naval shipyard health studies.* Radiat Prot Dosimetry, 2004. 111(2): p. 139-150.

24. Nakajima, T., *Development of a new highly sensitive LiF thermoluminescence dosimeter and its applications.* Nucl. Instrum. Methods, 1978. 157: p. 155-162.

25. Wu, D.-K., *A High Sensitivity LiF Thermoluminescent Dosimeter-LiF(Mg, Cu, P).* Health Physics, 1984. 46(5): p. 1063-1067.

26. Moscovitch, M., *Personnel Dosimetry Using LiF:Mg,Cu,P.* Radiat Prot Dosimetry, 1999. 85(1-4): p. 49-56.

27. Alves, J.G., et al., *Long-term stability of a TLD-based individual monitoring system.* Radiation Protection Dosimetry, 2006. 120(1-4): p. 289-292.

28. Horowitz, A. and Y.S. Horowitz, *Elimination of the Residual Signal in LiF:Cu,Mg,P.* 1992. p. 265-269.

29. Lupke, M., et al., *Sensitivity loss of Lif:Mg,Cu,P thermoluminescence*

dosemeters caused by oven annealing. 2006. p. 195-201.

30. Horowitz, A. and Y.S. Horowitz, *Elimination of the High Temperature Glow Peak in LiF:Cu,Mg,P.* 1993. p. 69-72.

31. Ben-Amar, G., et al., *Investigation of the Glow Peak Parameters, Reusability and Dosimetric Precision of LiF:Mg,Cu,P at High Heating Rates up to 20Ks-1.* Radiat Prot Dosimetry, 1999. 84(1-4): p. 235-238.

32. Budzanowski, M., *The Influence of Post-exposure Heating on the Stability of MCP-N (LiF:Mg,Cu,P) TL Detectors.* Radiat Prot Dosimetry, 2002. 101(1-4): p. 257-260.

33. Tang, K., et al., *Influence of Readout Parameters on TL Response, Re-usability and Residual Signal in LiF:Mg,Cu,P.* Radiat Prot Dosimetry, 2002. 100(1-4): p. 353-356.

34. Zha, Z., et al., *Preparation and Characteristics of LiF:Mg,Cu,P Thermoluminescent Material.* Radiat Prot Dosimetry, 1993. 47(1-4): p. 111-118.

35. Cai, G.G., et al., *Thermoluminescence of LiF:Mg,Cu,P (GR-200A) TLD After Annealing Between 200 and 400 oC.* Radiat Prot Dosimetry, 1996. 65(1-4): p. 163-166.

36. Baker, S.T. and P.J. Gilvin, *Comparison of the Effects of Exposure to Light in Harshaw LiF:Mg, Ti AND LiF:Mg, Cu, P.* 2006. p. ncl119.

37. Jones, A.R., A.H. Ohno, and W.F. Richter, *A Personal Dosemeter Using LiF(Mg,Cu.P) Thermoluminescent Material.* Radiat Prot Dosimetry, 1989. 27(4): p. 261-266.

38. Yuen, P.S., W.F. Richter, and M.S. Aikens, *Study of GR200F LiF:Mg,Cu,P Detectors for Extremity Dosimetry.* Radiat Prot Dosimetry, 1993. 47(1-4): p. 341-346.

39. Shen, W., et al., *New Advances in LiF:Mg,Cu,P TLD (GR-200A).* Radiat Prot Dosimetry, 2002. 100(1-4): p. 357-360.

40. Gilvin, P.J., et al., *Type Testing Of A New TLD For The UK Health Protection Agency.* Radiat Prot Dosimetry, 2007: p. ncm239.

41. Ranogajec-Komor, M., et al., *Investigation of the Performance of 7LiF:Mg,Cu,P Under Environmental Conditions.* Radiat Prot Dosimetry, 1999. 85(1-4): p. 217-221.

42. Olko, P., et al., *Microdosimetric Interpretation of the Anomalous Photon Energy Response of Ultra-Sensitive LiF:Mg,Cu,P TL Dosemeters.* Radiat Prot Dosimetry, 1993. 47(1-4): p. 31-35.

43. Olko, P., et al., *On the relationship between dose-, energy- and LET-response of thermoluminescent detectors.* Radiat Prot Dosimetry, 2006. 119(1-4): p. 15-22.

44. Olko, P., et al., *Modelling of the Thermoluminescence Response of LiF:Mg,Cu,P (MCP-N) Detectors after Doses of Low-Energy Photons.* Radiat Prot Dosimetry, 1999. 84(1-4): p. 103-107.

45. Olko, P., et al., *Microdosimetric modelling of the response of thermoluminescence detectors to low- and high-LET ionising radiation.* Radiat Prot Dosimetry, 2006. 122(1-4): p. 378-381.

46. Olko, P., *Microdosimetric Interpretation of Thermoluminescence Efficiency of LiF:Mg,Cu,P (MCP-N) Detectors for Weakly and Densely Ionising Radiations.* Radiat Prot Dosimetry, 1996. 65(1-4): p. 151-158.

47. Duggan, L. and T. Kron, *Glow Curve Analysis of Long-term Stability of LiF:Mg,Cu,P as Compared to LiF:Mg,Ti.* Radiat Prot Dosimetry, 1999. 85(1-4): p. 213-216.

48. Gilvin, P.J., *Comparison of Time Effects, Decision Limit And Residual Signal In Harshaw LiF:Mg,Ti and LiF:Mg,Cu,P.* 2007. p. ncl118.

49. Perry, O.R., et al., *LiF:Mg,Cu,P Based Environmental Dosemeter and Dose Calculation Algorithm.* Radiat Prot Dosimetry, 1999. 85(1-4): p. 273-281.

50. Sáez-Vergara, J.C., et al., *Thermally Induced Fading of Individual Glow Peaks in LiF:Mg,Cu,P at Different Storage Temperatures.* 1999. p. 269-272.

51. Sáez-Vergara, J.C., et al., *Thermally Induced Fading of Individual Glow Peaks in LiF:Mg,Cu,P at Different Storage Temperatures.* Radiat Prot Dosimetry, 1999. 85(1-4): p. 269-272.

52. Naval Dosimetry Center, N., *Standard Organization and Regulations Manual.* 2005. p. 313.

53. Ramlo, M., M. Moscovitch, and J.E. Rotunda, *Further Studies in the Reduction of Residual in Harshaw TLD-100H (LiF:Mg,Cu,P).* Radiat Prot Dosimetry, 2007: p. ncl115.

54. Alves, J.G., J.L. Muñiz, and A. Delgado, *On the Thermal Stability of LiF GR-200 in Environmental Exposures.* Radiat Prot Dosimetry, 1998. 78(2): p. 107-111.

55. Taylor, J.R., *An Introduction to Error Analysis.* 1997, Sausolito, California: University Science Books.

56. Knoll, G.F., *Radiation Detection and Measurement.* Third ed. 2000: John Wiley & Sons, Inc.

57. Systat, *SigmaPlot for Windows.* 2006.

58. Systat, *SigmaStat for Windows.* 2004.

59. Eisenbud, M. and T. Gesell, *Environmental Radioactivity.* Fourth ed. 1997: Academic Press.

60. Medicine, I.o., *Committee for the Study of the Future of Public Health.* 1988, Washington, DC: National Academy Press.

61. Chen, T.C. and T. G. Stoebe, *Role of Impurities in the Thermoluminescence of LiF:Mg,Cu,P.* Radiat Prot Dosimetry, 2002. 100(1-4): p. 243-246.

62. Chen, T.C. and T.G. Stoebe, *Role of Copper in LiF:Mg,Cu,P Thermoluminescent Phosphors.* Radiat Prot Dosimetry, 1998. 78(2): p. 101-106.

63. Bos, A.J.J., et al., *Thermoluminescence Properties of LiF(Mg,Cu,P) with Different Cu Concentrations.* Radiat Prot Dosimetry, 1996. 65(1-4): p. 199-202.

64. Sun, F., et al., *X Ray Diffraction and ESR Studies on LiF:Mg,Cu,P Phosphor.* Radiat Prot Dosimetry, 1994. 51(3): p. 183-189.

65. Wang, S., et al., *A New TL Detector Developed for Multiple Applications.* Radiat Prot Dosimetry, 1993. 47(1-4): p. 223-225.

66. Luo, L.Z., et al., *LiF:Mg,Cu,P glow curve shape dependence on heating rate.* 2006. p. 184-190.

67. Budzanowski, M., et al., *Estimation of the Time Elapsed Between Exposure and Readout Using Peak Ratios of LiF:Mg,Cu,P (MCP-N,GR200A).* Radiat Prot Dosimetry, 1999. 85(1-4): p. 149-152.

68. Bacci, C., et al., *Comprehensive Study on LiF:Cu,Mg,P (GR-200 A).* Radiat Prot Dosimetry, 1993. 47(1-4): p. 215-218.

69. Bilski, P., M. Budzanowski, and P. Olko, *Dependence of LiF:Mg,Cu,P (MCP-N) Glow-Curve Structure on Dopant Composition and Thermal Treatment.* Radiat Prot Dosimetry, 1997. 69(3): p. 187-198.

70. Horowiz, Y.S. and A. Horowitz, *Characterisation of LiF:Cu,Mg,P (GR-200) for Personnel Thermoluminescence Dosimetry.* 1990. p. 279-282.

71. Cai, G.G., et al., *Beta Energy Dependence of LiF:Mg,Cu,P Thermoluminescent Films on Thickness of Sensitive Layer.* Radiat Prot Dosimetry, 1992. 40(1): p. 53-57.

72. Tang, K., et al., *Comparative Study of Trapping Parameters and Repeatability of LiF:Mg,Cu,P (GR-200A) from Different Production Batches.* Radiat Prot Dosimetry, 2002. 100(1-4): p. 345-348.

73. Cai, G.G., et al., *Dose Response of the Individual Peak for LiF:Mg,Ti,(TLD-100) and LiF:Mg,Cu,P (GR-200A) TL Materials at the Photon Energies of 30, 104, 1250 keV.* Radiat Prot Dosimetry, 1996. 65(1-4): p. 213-215.

74. Mahajna, S., et al., *Kinetic Trapping Parameters in LiF:Mg,Cu,P via 'Prompt' and 'Residual' Isothermal Decay.* Radiat Prot Dosimetry, 1993. 47(1-4): p. 73-77.

75. Kitis, G. and T. Otto, *Isothermal Decay Readout: Application to LiF:Mg,Cu,P and a-Al2O3:C.* Radiat Prot Dosimetry, 1999. 86(3): p. 181-190.

76. Delgado, A., et al., *Isothermal Decay of Glow Peaks in LiF:Mg,Cu,P.* Radiat Prot Dosimetry, 1993. 47(1-4): p. 49-51.

77. McKeever, J., et al., *Diffuse Reflectance and Transmission Measurements on LiF:Mg,Cu,P Powders and Single Crystals.* Radiat Prot Dosimetry, 1993. 47(1-4): p. 123-127.

78. Velbeck, K.J., et al., *The dose-response of Harshaw TLD-700H.* 2006. p. 255-258.

79. Shoushan, W., *The Dependence of Thermoluminescence Response and Glow Curve Structure of LiF(Mg,CU,P) TL Materials on Mg,Cu,P Dopants Concentration.* Radiat Prot Dosimetry, 1988. 25(2): p. 133-136.

80. McKeever, S.W.S., *Modelling Supralinearity in Gamma Irradiated TL Dosemeters.* 1990. p. 83-89.

81. Kim, J.L., et al., *Energy responses of the LiF series TL pellets to high-energy photons in the energy range from 1.25 to 21 MV.* Radiat Prot Dosimetry, 2006. 119(1-4): p. 353-356.

82. Montano-Garcia, C. and I. Gamboa-deBuen, *Measurements of the optical density and the thermoluminescent response of LiF:Mg,Ti exposed to high doses of 60Co gamma rays.* Radiat Prot Dosimetry, 2006. 119(1-4): p. 230-232.

83. Tang, K., *Thermal Loss and Recovery of Thermoluminescence Sensitivity in LiF:Mg,Cu,P.* Radiat Prot Dosimetry, 2000. 90(4): p. 449-452.

84. Mady, F., et al., *Influence of absorbed dose and deep traps on thermoluminescence response: a numerical simulation.* Radiat Prot Dosimetry, 2006. 119(1-4): p. 37-40.

85. Nagaoka, K., et al., *Measurements of neutron dose rates with a balloon in Japan.* Radiat Prot Dosimetry, 2007. 126(1-4): p. 585-589.

86. Colgan, P.A., H. Synnott, and D. Fenton, *Individual and collective doses from cosmic radiation in Ireland.* Radiat Prot Dosimetry, 2007. 123(4): p. 426-434.

87. Piesch, E. and B. Burgkhardt, *Albedo Neutron Dosimetry.* Radiat Prot Dosimetry, 1985. 10(1-4): p. 175-188.

88. Lee, Y.K., *Analysis of neutron and photon response of a TLD-ALBEDO personal dosemeter on an ISO slab phantom using TRIPOLI-4.3 Monte Carlo code.* Radiat Prot Dosimetry, 2005. 115(1-4): p. 329-333.

89. Bilski, P., et al., *Thermoluminescence Efficiency of LiF:Mg,Cu,P (MCP-N) Detectors to Photons, Beta-Electrons, Alpha Particles and Thermal Neutrons.* Radiat Prot Dosimetry, 1994. 55(1): p. 31-38.

90. Cai, G.G., et al., *Thermal Neutron and Gamma Responses of 6LiF:Mg,Cu,P and 7LiF:Mg,Cu,P TL Films.* 1991. p. 51-53.

91. Burgkhardt, B. and E. Piesch, *Field Calibration Technique for Albedo Neutron Dosemeters.* Radiat Prot Dosimetry, 1988. 23(1-4): p. 121-126.

92. Piesch, E. and B. Burgkhardt, *Albedo Dosimetry System for Routine Personnel Monitoring.* Radiat Prot Dosimetry, 1988. 23(1-4): p. 117-120.

93. Delgado, A., *Recent Improvements in LiF:Mg,Ti and LiF:Mg,Cu,P Based Environmental Dosimetry.* Radiat Prot Dosimetry, 1996. 66(1-4): p. 129-134.

94. Tanner, J.E., et al., *Dose Equivalent Response of Personal Neutron Dosemeters as a Function of Angle.* Radiat Prot Dosimetry, 1997. 70(1-4): p. 165-168.

95. St John, T.J., et al., *Technical aspects of the Naval Dosimetry Center quality assurance programme.* 2006. p. 273-277.

96. Thermo-Electron, *Model 8800 Automatic TLD Card Reader with WinREMS.* 2005: Oakwood Village, OH.

97. Tawil, R.A., et al., *A System for Environmental Monitoring.* Radiat Prot Dosimetry, 1993. 47(1-4): p. 317-321.

98. Shleien, B., *The Health Physics and Radiological Health Handbook.* 1992: Scinta, Inc.

99. Olsher, R.H., et al., *Characterization of Neutron Reference Fields at Us Department Of Energy Calibration Fields.* Radiat Prot Dosimetry, 2007: p. ncm012.